neuro UC | Centro Interdisciplinario de Neurociencia

Detection of electrophysiological patterns of declarative memory reactivations during sleep

Presented in Partial Fulfillment of
the Requirements for the Degree of

Doctor of Philosophy in Neurosciences

in the

Centro interdisciplinario de neurociencias

Pontificia Universidad Católica de Chile

by

Andrea del Pilar Sanchez Corzo

Advisor
Ranganatha Sitaram, Ph.D.

Coadvisor
Sergio Ruiz, Ph.D.

Committee
Tomás Ossandón, Ph.D.
Eugenio Rodriguez, Ph.D.
Pablo Brockman, Ph.D.

June 2021

PONTIFICIA UNIVERSIDAD CATÓLICA DE CHILE
Doctorado en Neurociencias

El Comité de Tesis, constituido por los Profesores abajo firmantes, aprueba la Defensa Pública de la Tesis Doctoral titulada:

DETECTION OF ELECTROPHYSIOLOGICAL PATTERNS OF DECLARATIVE MEMORY REACTIVATIONS DURING SLEEP

Aprobación Defensa:

ANDREA DEL PILAR SÁNCHEZ CORZO

Calificándose el trabajo realizado, el manuscrito sometido y la defensa oral, con nota

7,0 (siete coma cero)

Dr. Mauricio Cuello
Director de Investigación y Doctorado
Escuela de Medicina
Pontificia Universidad Católica de Chile

Dr. Felipe Heusser
Decano
Facultad de Medicina
Pontificia Universidad Católica de Chile

Dra. Claudia Sáez
Sub-Directora
Dirección de Investigación y Doctorado
Escuela de Medicina
Pontificia Universidad Católica de Chile

Dr. Francisco Aboitiz D.
Jefe Programa Doctorado en Neurociencias
Profesor Evaluador
Facultad de Medicina
Pontificia Universidad Católica de Chile

Dr. Ranganatha Sitaram
Director de Tesis
Escuela de Medicina
Pontificia Universidad Católica de Chile

Dr. Sergio Ruiz
Co-Director de Tesis
Escuela de Medicina
Pontificia Universidad Católica de Chile

Dr. Tomás Ossandón
Profesor Evaluador
Facultad de Medicina
Pontificia Universidad Católica de Chile

Dr. Eugenio Rodriguez
Profesor Evaluador
Escuela de Medicina
Pontificia Universidad Católica de Chile

Dr. Pablo Brockmann
Profesor Evaluador Externo
Facultad de Medicina
Pontificia Universidad Católica de Chile

Santiago, 29 de junio de 2021.-

Acknowledgements/ Agradecimientos

Quisiera agradecer a muchísimas personas que han hecho posible la realización y ahora culminación de este proyecto de doctorado, y que me han apoyado y acompañado durante estos años.

A mi director de Tesis, Dr. Ranganatha Sitaram, quien me dió la bienvenida desde un inicio a su laboratorio y me apoyado académicamente durante estos años, y quien ha confiado en mi y en mis capacidades, siendo también un apoyo en el área personal cuando los momentos han sido difíciles.

A la VRI por financiarme durante los primeros años de doctorado y apoyarme durante mi pasantía en el extranjero, así como permitirme oportunidades como el concurso de tesis en 3 minutos, permitiendome financiar una pasantía adicional y gastos relacionados a mi tesis.

A todos mis compañeros de laboratorio, especialmente al grupo conformado dentro del proyecto de sueño, y autodenominado "los sleepers", quienes han trabajado de la mano conmigo en los diferentes análisis de datos y discusiones interesantes semanalmente. Al Dr. David Baum, quien no sólo ha realizado exaustivos análisis, sino también ha trabajado conmigo haciendo los experimentos durante la noche y me ha ayudado a preparar el laboratorio de sueño. A Martin Irani, quien con su talento y crecimiento científico tan acelerado, se ha convertido en una fuente de nuevas ideas y apoyo en la programación de los análisis de datos. A Renate Reissenager, Grace Whitaker, y Daniel Solomons que nos apoyan desde su experiencia matemática, estadística y neurocientífica.

Quiero agradecer también al Profesor Dr. Jan Born, quien me dió la bienvenida en su laboratorio durante mi pasantía en Alemania, y a su grupo donde conocí a grandes personas y con quienes compartí experiencias científicas de alta calidad. Especialmente a Jens G. Klinzing, quien no solo fue mi mentor durante el tiempo que estuve en el laboratorio del Dr. Jan Born, sino también quien ha compartido conmigo todo su conocimiento, sus códigos, y los datos adquiridos, que, al ser de tan alto nivel, me han permitido realizar una tesis de buena calidad. Jens actualmente también se ha

convertido en un gran mentor y fuente de retroalimentación siendo gran conocedor de la investigación en sueño y memoria que se realiza actualmente.

Tambien quiero agradecer a mi familia, quienes siempre han estado presentes a pesar de la distancia, han confiado en mi, y me llenan de motivacion.

A Oscar Henao por que gracias a él decidí postularme al programa de doctorado y me acompañó durante la mayor parte del mismo con gran apoyo.

A Marcos Domic, Martín Irani, Ishani Tahakkar, Pamela Gonzalez, por su amistad durante estos años.

A Benja Benavides y su familia por abrirme las puertas de su casa en el ultimo año durante la pandemia.

Dedication

Dedicado a mi familia, y a mi país Colombia, que sufre momentos difíciles...

Table of Contents

List of Figures

CHAPTER 1

Theoretical Background

1.1 MEMORY

Learning and memory are related concepts and form an essential part of our lives, allowing past experiences to influence future behavior and permit organisms to adapt to the environment. While learning is the ability of the Central Nervous System (CNS) to acquire new information which is evidenced by a behavioral change as an effect of the experience (effect of the interaction with the environment), memory is the persistence of learning over time and refers to the process of how the learned information is encoded, stored, and retrieved after (Kandel *et al*. (2013)).

Memory is the basis of what living beings are, as it includes all information on the 'what', 'who', 'where', and 'when' of our life experiences (Chen and Wilson (2017)). Based on it, we act and decide because it defines our sense of self-identity. Memory is formed in a three stages process: encoding, storage/consolidation, and recall. Encoding is the initial acquisition of new information. It refers to processes that involve attention for new information learned to be elaborated in the first encounter. The extent and nature of this encoding determine how the learned material will be recalled later. For a memory to be kept and well-retained, requires attention and association with the knowledge that is already well established in memory. The storage and consolidation refer to the strengthening and stabilization of these new contents. Consolidation includes processes that alter recently stored information, still labile, to make it more stable for long-term storage, involving the expression of genes and the synthesis of new proteins, inducing structural changes that store memory in a stable way over time. Storage includes the mechanism and places where memory is preserved over time. Finally, recall refers to the processes that allow the retrieval and use of stored information. Retrieval involves gathering different types of information that are stored separately in different storage locations. It is a constructive process, and therefore subject to distortion. In this stage of memory, when a retrieval cue (a

part of the sequence) arrives, the sequences in the hippocampus related to a particular experience are activated, directing towards the neocortical assemblies that originally processed the events during perception (Kandel *et al*. (2013)). Figure 1.1 shows an example of the different stages of memory formation.

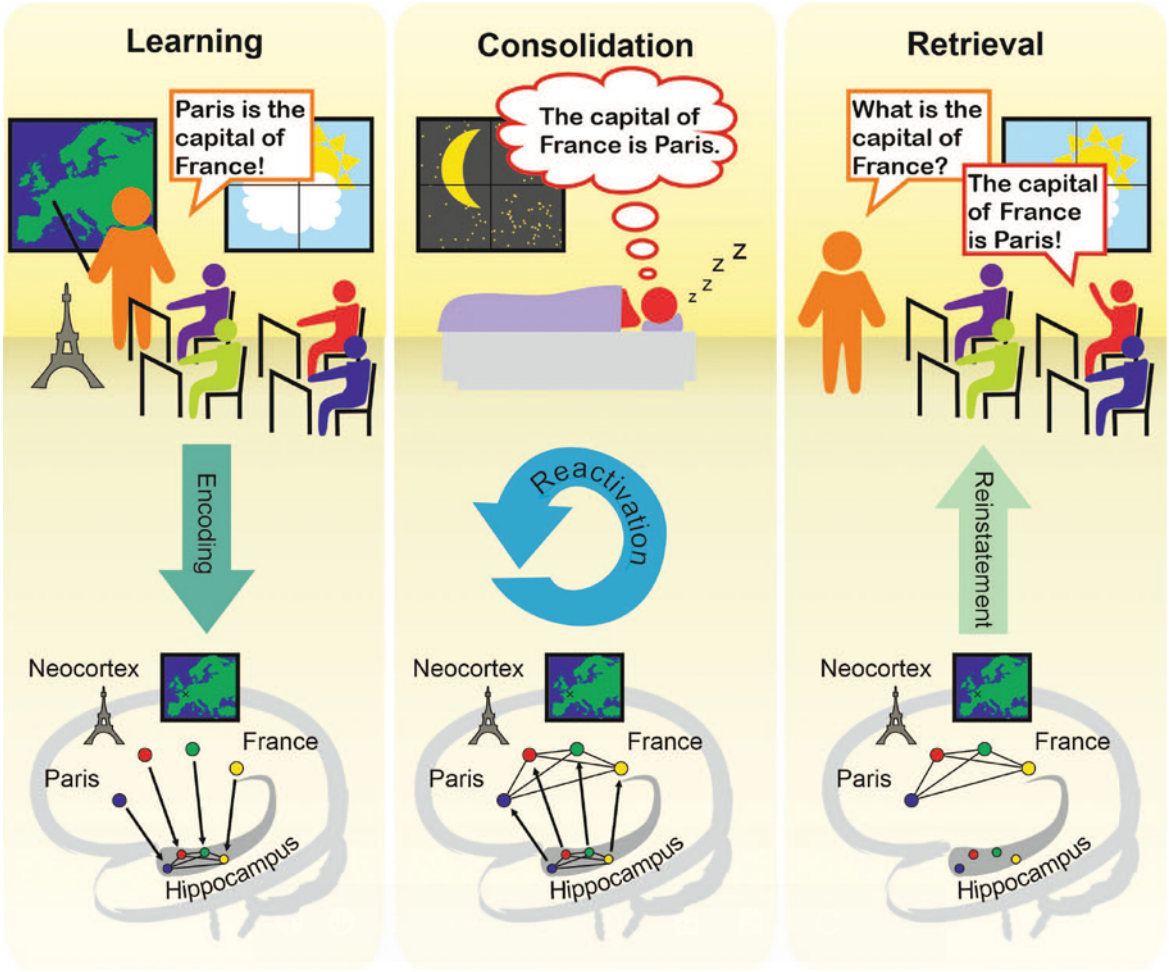

FIGURE 1.1: Taken from Feld and Diekelmann (2020)

Memory systems can be classified according to temporal, and qualitative criteria. The temporal criterion takes into account the duration or persistence of the information in time. The qualitative criteria separate memory according to the type of content of the information that is stored (see details of qualitative distinction in section 1.1.1).

The temporal criteria for separating memory recognize two main types of memory, short-term and long-term memory. Short-term memory maintains information over a short period (seconds), while long-term memory spans years and even all life, involving the unconscious repetition of past experiences between encoding and

retrieval. This is also supported by the fact that short-term memory can remain unimpaired in amnesic patients or, inversely, impaired in patients whose long-term memory functions remain intact (Brem *et al*. (2013)).

Figure 1.2 shows the temporal and qualitative divisions of memory, as well as subdivisions and associated brain regions. The sensory memory is included as well in this schematic, being the shortest type of memory maintaining information for less than 1 second. In the following section, the long-term memory is described in detail as this is the type of memory that we are mostly interested in in this project.

1.1.1 *Long-term Memory*

Long-term memory is essential for development and adaptation over time. Classical and prominent models of human long-term memory separate memory systems based on the way the retrieval occurs: consciously or unconsciously, dividing them into two broad classes. The ability to consciously recall information is known as declarative memory, while various forms of unconscious learning and memory skills are referred to as non-declarative memory (Henke (2010)). See Figure 1.2 for a detailed schematic.

Declarative Memory — The declarative (or explicit) memory system includes the memory of events, dates, and facts that can be deliberately and consciously recalled and described verbally (Kandel *et al*. (2013)). In addition, declarative memory includes the capacity to recall particular experiences and draw generalizations from a variety of experiences. A typical example of this generalization is the ability of the brain to find similar features or overlapping representations of different sea creatures seen in different experiences but still retain their specific characteristics (categorization) (Witkowski *et al*. (2020)).

Declarative memory can be divided into episodic and semantic memory. The episodic memory consists of memories of autobiographical events and personal experiences. The semantic memory consists of facts and general knowledge; it is impersonal and contains objective knowledge devoid of autobiographical context (one example of this is the type of knowledge, is the one acquired from books) (Henke (2010); Kandel *et al*. (2013)).

Non-Declarative Memory — The term 'non-declarative' (implicit) memory encompasses many memory systems which are difficult to verbalize and do not require conscious processes to evoke them. Their common characteristics are shown mainly in behavior, allowing its distinction from the declarative memory system. This type of memory includes procedural learning of sensorimotor and cognitive skills and habits; simple conditioning; priming; operant conditioning; habituation and sensitization (Henke (2010)).

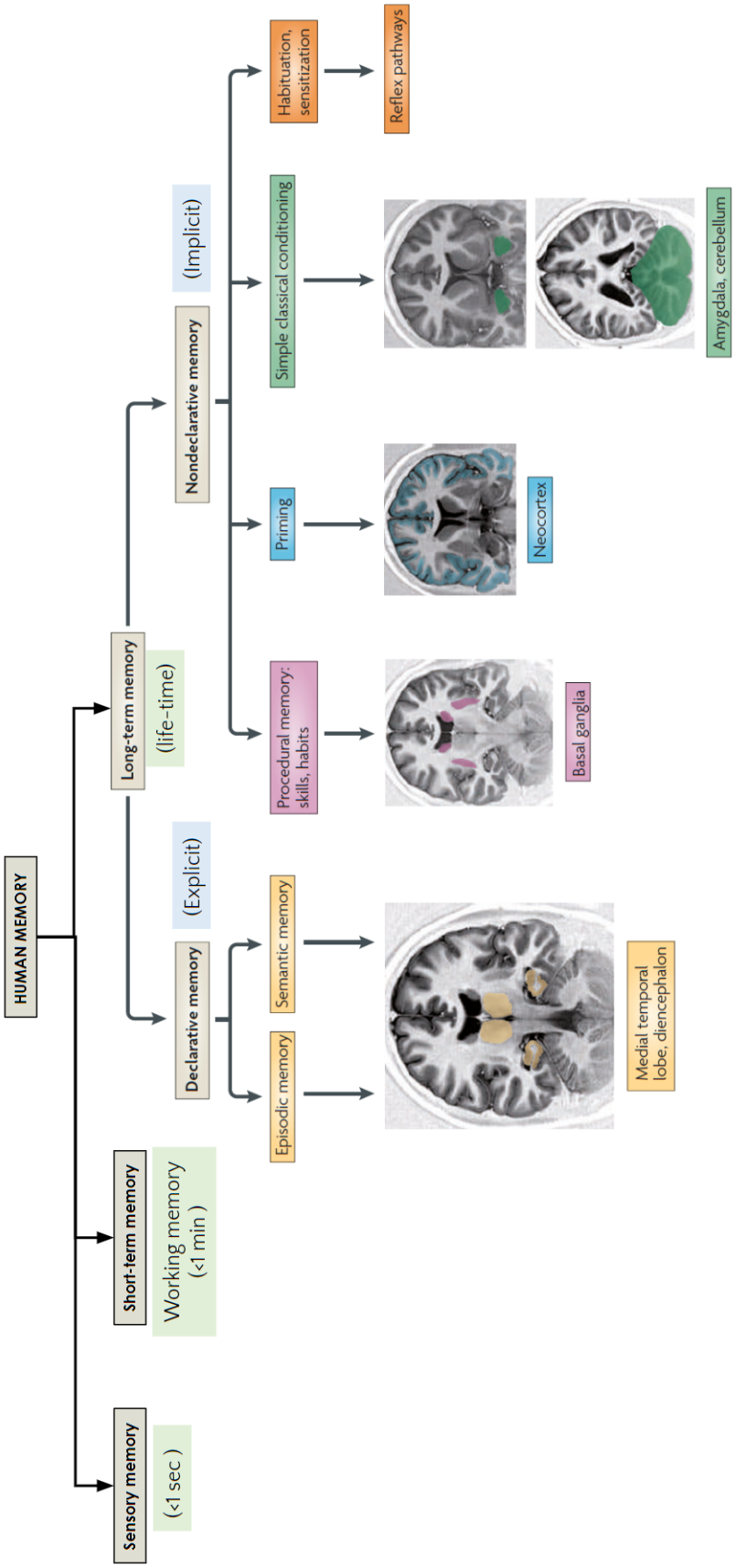

FIGURE 1.2: Adapted from Henke (2010)

1.1.2 *Role of the hippocampus in the long-term memory formation*

The first evidence that memory processes could be specific to some areas of the human brain was collected by the neurosurgeon Wilder Penfield while performing electrical stimulation of the temporal lobe showing that when stimulating regions of the temporal lobe, patients were able to evoke memories (Penfield (1952)). However, more convincing evidence emerged in the mid-1950s from the study of patients who had undergone a bilateral excision of the hippocampus and neighboring regions in the temporal lobe to treat epilepsy (Scoville and Milner (1957)). Scoville and Milner, who investigated the cognitive impairments of patients after intervention in the medial temporal lobe and showed that the medial temporal lobe is dedicated to episodic memory, independent of other cognitive functions. The best-known case is of the patient H.M. that despite having lost a large part of his temporal lobe, he could learn new motor skills at an average rate.

All patients with injury to the medial temporal lobe were unable to recall learning experiences, but when given ample training opportunities, they displayed sensori-motor learning (Scoville and Milner (1957)). Also, they preserved perceptual and conceptual priming of single items (Levy *et al*. (2004); Tulving *et al*. (1991)). They showed an intact delay in eye blinks in classical conditioning when trained with a tone presented just before the onset of an air puff (Weiskrantz and Warrington (1979)). They demonstrated sustained cognitive skill development and long-term learning of the intricacies of rule-governed stimulus sequences, both of which are used in artificial grammar learning, even in more cognitively demanding tasks (Henke (2010);Knowlton *et al*. (1992)). Since the hippocampus was recognized as an essential region for long-term memory formation, it was possible to differentiate between explicit and implicit memory (Kandel *et al*. (2013)).

All previous evidence supports that the hippocampus is vital and almost exclusive for declarative memory formation. However, Research has demonstrated that the hippocampus region's contribution to memory is temporary, even for memories of spatial environments learned in childhood. The length of the hippocampus' critical involvement may be influenced by the mediation of neighboring cortical areas, and

injury outside of the hippocampus can lead to prolonged memory loss (Eichenbaum (2000)). evidence of the hippocampus' involvement in conscious memory does not rule out its participation in types of unconscious memory (Henke (2010)). In 2015, Addante performed a study of a group of patients with evidence of damage limited to the hippocampus. He found that patients had a dramatic impairment of implicit memories compared to healthy subjects, suggesting that the hippocampus is fundamental for memory processing beyond conscious awareness (Addante (2015)).

1.2 MEMORY CONSOLIDATION

Memory consolidation refers to the process of transforming, stabilizing, and integrating new and initially labile memories acquired in the awake state within the brain, becoming part of the neocortical circuits of long-term memories (Diekelmann and Born (2010)). But, how can these physical changes emerge during wakefulness while the brain processes a continuous stream of new information? To explain this process, (Marr (1971)) proposed a model assuming two separate memory storages, each working at different learning rates. First, in this model, features from the new information are encoded by neural networks and are initially retained on the temporal lobe's fast-learning regions as shown in Figure 1.3. Then, during "offline" periods, these memory traces are gradually redistributed to the neocortical areas enhancing cortico-cortical connections where long-term storage is located. This two-stage model of memory consolidation offers a solution for dealing with the dilemma of how the hippocampal-cortical system achieves plasticity related to the acquisition of new information without affecting stability, which means no overwriting of older, pre-existing memories because memory traces are repeatedly re-activated in the fast-learning store (see Figure 1.3) driving reactivation in the slow-learning store making memories gradually redistributed and long-term store connections stronger. The active re-processing of fresh memories within the neural networks that encoded them is then involved in memory consolidation. (Diekelmann and Born (2010)) (this active re-processing is detailed in section 1.2.1). This is supported by the observation that learning experiences are strengthened during post-encoding 'offline' periods. The

first evidence on how the brain strengthens memories was seen when sequences of neuronal firing in the hippocampus during exploration of a novel environment were spontaneously reactivated during subsequent sleep in rats (shown in Figure 1.4) and the magnitude of the reactivation also predicted future memory performance (Skaggs and McNaughton (1996); Wilson and McNaughton (1994); Schreiner and Staudigl (2020)).

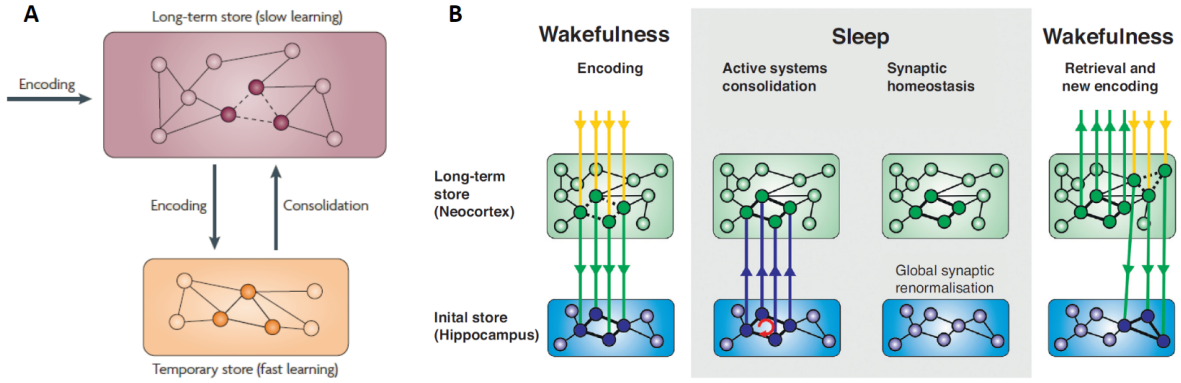

FIGURE 1.3: During wakefulness, the rapid learning mechanism of the hippocampus (shown by green arrows) in the domain of hippocampal-dependent declarative memory rapidly combines sensory information (shown as yellow arrows) from the sensory cortices into a temporary representation. The memory trace is frequently played again during subsequent sleep, especially Slow Wave Sleep (SWS), which causes it to change and integrate into the neocortex's long-term memory storage (shown by blue arrows), a process known as active systems consolidation. Sleep not only strengthens synapses, which removes useless information, but also consolidates pertinent memories. Rapid Eye Movement (REM) sleep appears to be important for the hippocampus, contrary to the synaptic homeostasis hypothesis, which emphasizes the importance of SWS for cortical renormalization. The hippocampus (shown by green upward arrows) can be accessed during wakefulness, and new knowledge can be stored into its updated stores (represented by yellow and green downward arrows).Taken from Feld and Born (2017))

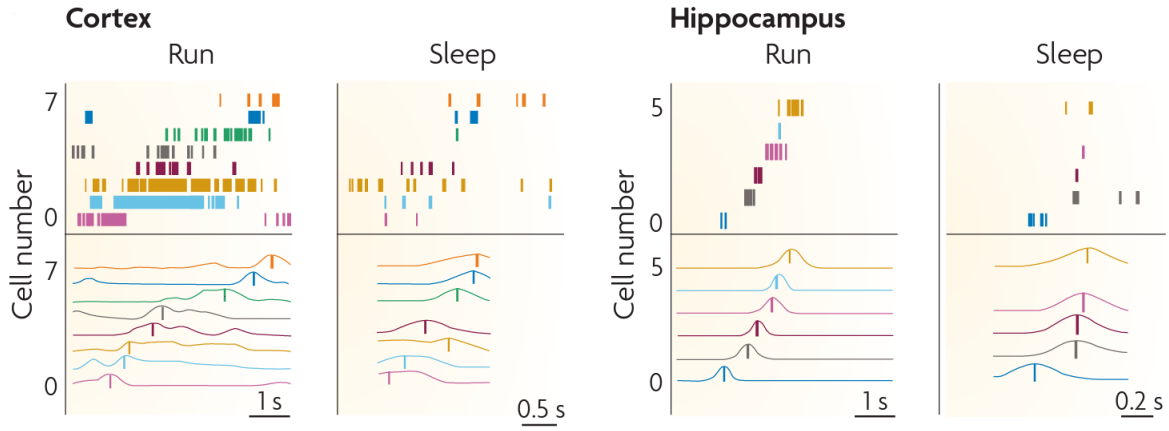

FIGURE 1.4: The sensory cortex and hippocampus' neurons fire in a distinctive pattern of sequential firing during encoding (exploring a circular track). Each row in the diagrams represents a single cell, and the marks in the upper parts indicate spikes. The curves in the lower parts show the average firing patterns of the cells. The temporal firing patterns found in the cell assemblies during running recur in the cortex and hippocampus during Slow Wave Sleep (SWS). Taken from (Diekelmann and Born (2010)), based on (Ji and Wilson (2007))

1.2.1 *Memory Reactivation*

Memory reactivation is the phenomenon in which patterns of activation of neural networks expressed during the encoding of new information are re-expressed at a later time (Favila *et al*. (2020a)). This phenomenon is observed across hippocampal and cortical areas and correlates with objective and subjective expressions of memory. It comprises reinstatement, replay, and pattern completion (Schreiner and Staudigl (2020); Vieweg *et al*. (2015)): Reinstatement refers to the reoccurrence of a neural pattern present during a past experience. Replay implies a reinstatement with temporal dynamics and order (forward versus backward replay; non-compressed or time-compressed replay). Pattern completion is a process ascribed specifically to the hippocampal CA3 region, in which the original memory trace is restored (completed) via reactivation, as a vital aspect of successful episodic memory recall as it allows for the activation of a previously formed connection. (for example an object with a certain environment) (Schreiner and Staudigl (2020); Vieweg *et al*. (2015)).

Studies in rodent models make clear that both the consolidation of memories during sleep and their retrieval during wakefulness depend on the hippocampal-triggered memory reactivation. Studying reactivation processes is essential because it enables the study of the cognitive processes connected to reactivation processes and aids in evaluating the multi-sensory components of real-life experiences and memories (Carr *et al*. (2011); Skaggs and McNaughton (1996); Schreiner and Staudigl (2020); Wilson and McNaughton (1994)).

Memory reactivation differences between the awake bran and the sleeping brain — The transfer of information is different in wakefulness compared to during sleep. In contrast with wakefulness, there is no external information during sleep, so memories go through straight-forward traces of reconsolidation without risk of being interfered with conflicting information (Rasch and Born (2007)).

In the awake brain, new information from the external world passes through the entorhinal cortex to reach the hippocampus. In this case, the hippocampus is in an aroused state associated with theta, and gamma oscillations. On the other hand, during sleep, the information flows from the hippocampus to the neocortex. In this

case, activation in the hippocampus is initiated as bursts of neuronal activity during SWS (BuzsÁk (1998)).

Whereas reactivation of memories during wakefulness induces labialization of the representation that enables its acute updating (Diekelmann and Born (2010)), reactivations during sleep, especially SWS, leads to an immediate stabilization of the memory which is assumed to be a consequence of an optimal communication between the hippocampus and the neocortex. Supporting this idea, the study of (Gais *et al*. (2007)) shows increasing functional connectivity between the medial prefrontal cortex and hippocampus during sleep after learning as compared to wakefulness. Additionally, neuronal activity in rodents suggests that newly acquired memories are reactivated during offline periods, preferentially during sleep, because of the absence of interference from external inputs. For example, studies in which recorded rat hippocampal place-cells were exposed to their individual place fields, significantly increased spiking activity was noticed in the cell that was exposed during subsequent sleeping states, which was not present in the unexposed cell (Pavlides and Winson (1989)). It has been seen that experience-dependent reactivations are also present in other brain areas such as the thalamus, putamen, ventral striatum, and neocortex (Ribeiro *et al*. (2004)), as well as in other species.

It is suggested that information is replayed during sleep at a faster time scale. In a study of memory reactivation during sleep in rats, during exploratory behavior in which encoding phases appear, the neuronal patterns were noisier, less accurate, and in general at a different firing rate than in sleep (Nádasdy *et al*. (1999)).

Rodent studies have shown that, during wakefulness, reactivations can occur in a reversed temporal order. At the termination of a run, place neurons on an elevated track fired in reverse order, but in anticipation of the run, in forward order. These bidirectional reactivations during wakefulness may help the establishment of higher-order episodic associations during learning.(Diba and Buzsáki (2007); Rasch and Born (2007)). On the other hand, (Ji and Wilson (2007)) show in rats that the temporal firing sequences observed in cell assemblies of the sensory cortex and the hippocampus during the exploration of a circular track re-appear in SWS both in the cortex and in the hippocampus in the same order as they were activated while running. Further-

more, hippocampal neuronal assemblies that are activated during maze learning are also reactivated during SWS in the same temporal order as during learning (Maquet (2000)).

Memory reactivation during wakefulness Studies indicate that memory reactivation can emerge while the animals are awake i.e. during immobility, grooming, consummatory behavior, and task engagement (Schreiner and Staudigl (2020)), but also, the reactivation of a memory trace is necessary to achieve the subjective experience of remembering, it is therefore assumed that reactivations can happen in "offline" periods during the awake state as well as during memory retrieval.

Brain activity during 'rest' is significantly affected by a prior learning episode (Vincent, 2009), and the consolidation of recently learned information is known to take place over a period of several hours after learning (Albert *et al*. (2009))

In 2012, Wimber and colleagues presented participants with flickering words at different frequencies and discovered that when participants correctly recognized a previously learnt word, the imposed frequencies reappeared (Wimber *et al*. (2012)). Later, (Linde-Domingo *et al*. (2019)) found evidence for memory reactivation of visual memories during retrieval and investigated their temporal structure. Interestingly, the order of the reactivation during retrieval was found to be reversed when compared with encoding.

Memory Reactivation During Sleep The first evidence for memory reactivation during sleep came from studies in rodents showing that the firing rates of hippocampal neurons during behavior, doing exploration of a new environment, tend to correlate with spontaneous firing rates of the same neurons during subsequent sleep (Lewis and Bendor (2019); Pavlides and Winson (1989)). Also, during sleep, hippocampal sequences spontaneously trigger memory reactivation in the neocortex. It is suggested that the repetition of memory reactivation of neuronal sequences stabilize memories to long-lasting representation, storing them permanently in neocortical networks. Moreover, fMRI and positron emission tomography investigations of memory reactivation in humans during sleep revealed that brain activation linked to acquiring different

memory contents reappears during sleep (Bergmann *et al*. (2012); Maquet (2000); Schreiner and Staudigl (2020)); for example, After navigating a virtual maze, the hippocampus region spontaneously activates again during subsequent sleep, but it has also been shown for declarative and motor learning (Peigneux *et al*. (2004)).

The advantage of sleep over wakefulness for memory reactivation to happen is that the competition from other information processing is minimal. Researchers argue that communication between the hippocampus and the neocortex has certain advantages during sleep in terms of proper decontextualization and transfer of information to extra-hippocampal regions (Witkowski *et al*. (2020)).

1.3 SLEEP AND MEMORY CONSOLIDATION

1.3.1 *Functions of Sleep*

Sleep is defined behaviorally as "the normal suspension of consciousness" (Purves (2004)) and is identified by specific patterns of brain activations. Almost one-third of our lives is spent in sleep and occurs in all mammals, and is considered to be present in all vertebrates. Sleep is so important that we crave it when deprived of it. Continued sleep deprivation can be fatal (Purves (2004)). During sleep, animals do not eat, reproduce, or forage, and are vulnerable to predation. This may lead us to think that from an evolutionary perspective, the function of sleep is of high relevance. The harmful consequences of sleep deprivation, which show that sleep serves purposes that cannot be simply circumvented, reinforce this. (Anafi *et al*. (2019)). The clinical importance of sleep is obvious from the prevalence of sleep disorders, such as insomnias (Purves (2004)). On the premise that if sleep is removed, its underlying function will also be lost, sleep deprivation experiments have been used to deduce the function of sleep. On one hand, sleep deprivation has an impact on both neural and non-neural tissues. Prolonged lack of sleep over several days can cause a hypermetabolic state, skin damage, multi-organ failure, and ultimately lead to death. Conversely, sleep is essential for memory formation, brain plasticity, maintaining neuron health, promoting insulin release and responsiveness, regulating body temperature, and supporting immune and skin function. Sleep deprivation also

has associated consequences, such as increased emotional stress, increased muscle tension, alterations in temperature and dietary changes (Anafi *et al*. (2019)).

Sleep does not imply a diminution of brain activity. On the contrary, during REM (rapid eye movement) sleep, the brain is as active as it is during wakefulness (Purves (2004)) and brain oxygen consumption during sleep can surpass the one during wakefulness. However, one main function of sleep is to isolate the brain from the body and the environment (Buzsaki (2006)). Sleep is comprised of carefully regulated brain states that are managed by a group of brainstem nuclei that have widespread connections throughout the brain and spinal cord (Purves (2004)).

Sleep architecture and its oscillatory signatures — In humans, at least four sleep stages with progressively higher wakening threshold can be distinguished (Buzsaki (2006)), but sleep consists of two main groups: Non-REM (NREM) sleep and rapid-eye-movement (REM) sleep, which alternate in a cyclic manner (Diekelmann and Born (2010)). NREM involves sleep stages 1 and 2 known as light sleep and the SWS which is the most representative period, comprising sleep stages 3 and 4. Stage 1 is the phase transition between wake and sleep. It is identified by relatively low-amplitude electroencephalography (EEG) (as compared to wakefulness) with mixed frequencies, mainly in the slow alpha and theta range. Stage 2 is marked by the emergence of k-complexes and sleep spindles. Some delta waves are seen in stage 2, but constitute less than 20%. Stages 3 and 4 are known as SWS or delta sleep. Stage 4 is characterized by the dominance of delta activity with only a few traces of spindles, whereas stage 3 is a mixture of spindles and delta waves (20 to 50%). Stage 4 only accounts for 5–15% of total sleep time and may not even exist after age 40 (Buzsaki (2006)). In clinical evaluation of sleep scoring, stage 4 of sleep is omitted and combined with stage 3 (Berry *et al*. (2017)), although some research groups consider that stage 4 has substantial differences. In human nocturnal sleep, SWS is characterized by slow, high-amplitude EEG oscillations (also known as slow-wave activity, or SWA), which are predominant in the early hours of the night and decrease in intensity and duration throughout the sleep period. In contrast, rapid-eye movement sleep (REM sleep), which occurs toward the end of the sleep period

awakeness and is characterized by fast, low-amplitude oscillations similar to those in waking, increases in intensity and extent. REM sleep is characterized by increases in blood pressure, heart rate, and metabolism to levels almost as high as those found in the awake state. Other significant characteristics of this stage of sleep include rapid eye movements, pupillary constriction, and the paralysis of numerous major muscle groups. All animals and at least some birds have been found to have REM sleep. (Purves (2004)) and composes usually 20-25 percent of total sleep time in human adults. This sleep stage is an indicator of the end of a NEM/REM sleep cycle (Buzsaki (2006)).

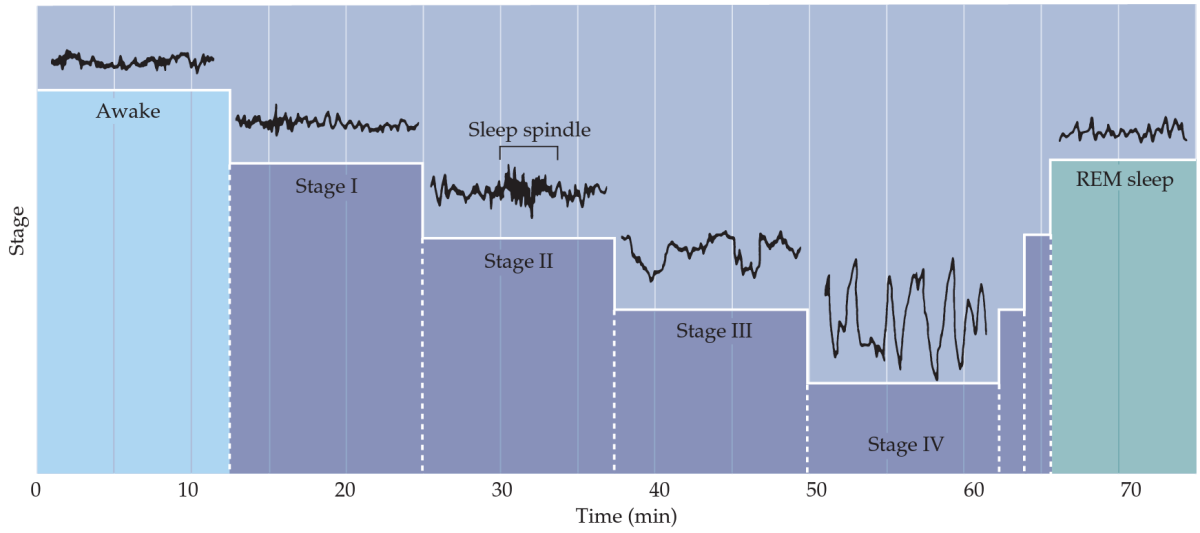

FIGURE 1.5: The waking state: high-frequency (15–60 Hz) and low-amplitude activity. Stage I: Theta and alpha activity and increasing amplitude vs awake. Stage II: sleep spindles occurring periodically. Stage III: slower waves at 2–4 Hz and higher amplitude than previous sleep stages. Stage IV: slow waves at 0.5–2 Hz and the highest amplitude. REM sleep: low-amplitude, high-frequency activity similar to the awake state. Taken from (Purves (2004)), adapted from (Hobson (1989))

In general, four or five NREM/REM cycles with a period of 70–90 minutes each occur within a night. All sleep stages occur in a periodic sequence (see Figure 1.6) (Buzsaki (2006)).

Electrophysiological signatures of NREM Sleep and their relationship with memory consolidation The periods of NREM sleep are distinguished by slow, rolling eye movements and reductions in muscle tone, physical movements, heart rate, respiration, blood pressure, metabolic rate, and temperature. All of these parameters reach their minimum levels during S4 (Purves (2004)). NREM contains sleep stages S1,

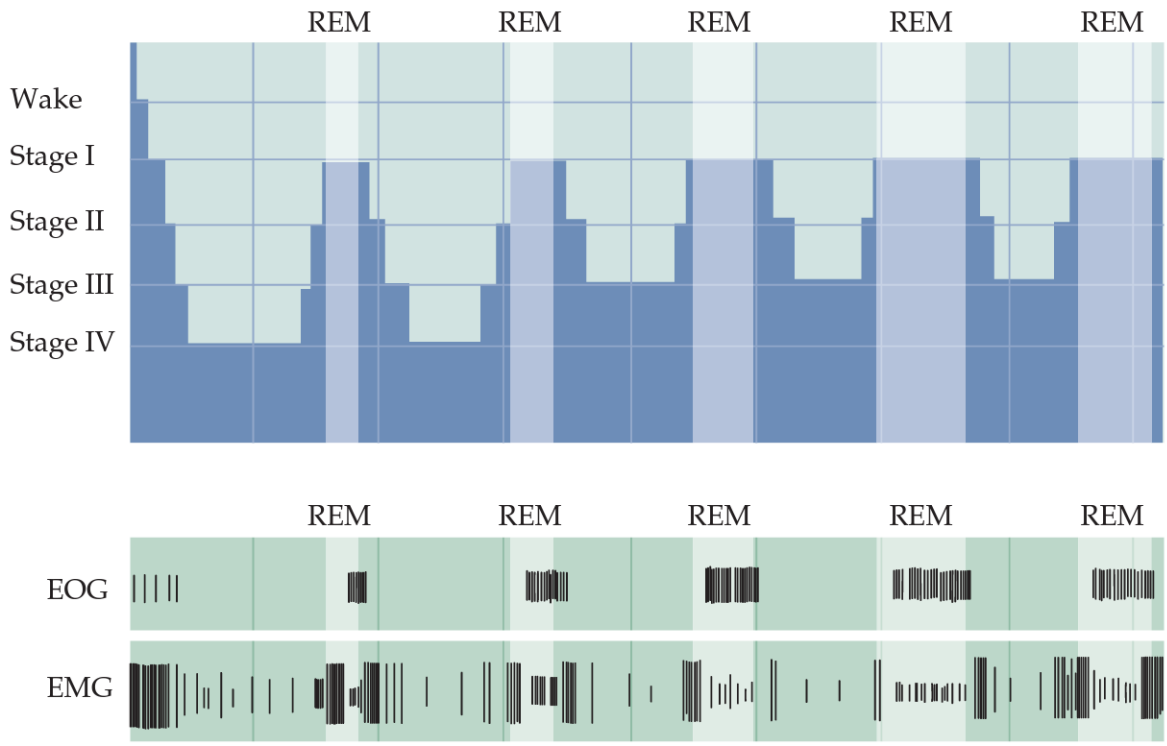

FIGURE 1.6: Physiological changes in a volunteer over time (x-axis) during the various sleep stages in a typical 8-hour sleep period. Note that stage IV is attained only in the first two cycles. electro-oculogram (EOG) and electromyogram (EMG) activity are shown in the lower panels. Most eye movements evident in the EOG occur in REM sleep and the greatest EMG activity occurs during the onset of sleep and just prior to awakening. Taken from (Purves (2004))

S2, and SWS. SWS is more prominent during the first half of the night (Diekelmann and Born (2010)). S1 is usually very short and is identified by a decrease in the amplitude of the EEG in which a combination of alpha and theta waves can happen together. S2 is characterized by sleep spindles and k-complexes. Slow oscillations (SO) (defined later) can occur as well during S2 but account for less than 20%. Finally, the SWS is mainly characterized by SO, spindles, and sharp-wave ripples, and usually is identified by high amplitude in the EEG signal due to the synchronization of large populations of neurons, and with almost complete absence of eye movements and reduced muscle tone. Differences between S3 and S4 are established according to the percentage of SO occurrence. Usually, 20% to 50% of S3 activity is composed of SO, and SO composes more than 50% of the S4 activity (Wolpert (1969)).

Sleep spindles Regular electroencephalographic oscillations between 10 and 15 Hz that typically last 0.5-2 seconds are referred to as spindle activity. Although they

are present at a similar level throughout SWS, sleep spindles are more frequently seen in human sleep stage 2 as distinct waxing and waning spindles (Diekelmann and Born (2010)) (see Figure 1.7). After their sporadic onset, the intensity of sleep spindles increases progressively with the increasing coupling to SO (Buzsaki (2006)).

Spindles are the result of the interaction between GABAergic neurons of the nucleus reticularis, and glutamatergic thalamo-cortical projections. They originate in the thalamus and are propagated to cortical regions (De Gennaro and Ferrara (2003); Steriade (2006)). Sleep spindles are located in the prefrontal cortex for learning word-pairs (Clemens *et al*. (2005); Schmidt *et al*. (2006)), in the parietal cortex after a visuospatial learning task (Clemens *et al*. (2006)), and motor cortex after motor learning (Nishida and Walker (2007)). Studies in rats and humans showed an increase in the spindle density after motor and declarative learning. Further, an increase in spindle density was correlated with improvement of memory after sleep (e.g. Gais *et al*. (2002)). The thalamo-cortical spindles seem to prepare the cortical networks for long-term storage (Diekelmann and Born (2010)) by driving synaptic Long Term Potentiation (LTP) as an underlying mechanism of memory consolidation (Rosanova and Ulrich (2005)).

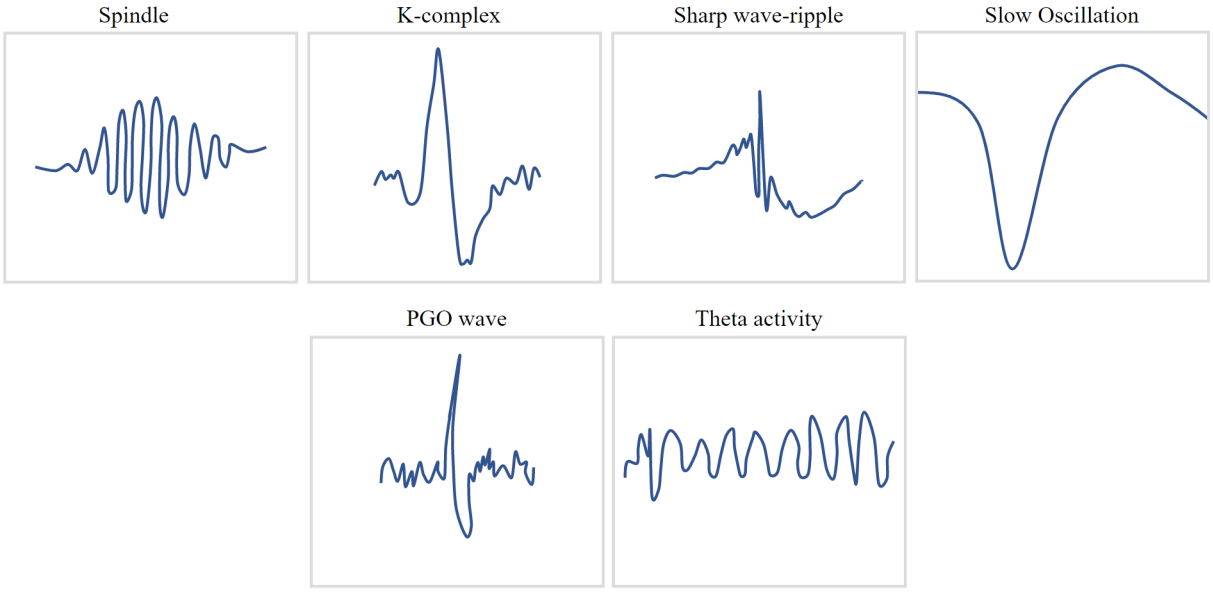

FIGURE 1.7: The spindles, k-complexes, sharp wave ripples, and SO are the most noticeable field potential oscillations during NREM sleep. Ponto-geniculo-occipital (PGO) waves and theta activity are markers of REM sleep. Adapted from (Diekelmann and Born (2010)).

K-complexes Spindles are frequently preceded by a high-amplitude wave that has a sharp component in the shape of the letter "K" which is why they are referred to as K-complexes. This pattern typically occurs during S2 and S3 sleep, periods in which the occurrence of spindles is higher. K-complexes are associated with a population burst discharge of cortical neurons projecting to the thalamus (Buzsaki (2006)). All sensory input modalities can trigger K-complexes, which accounts for the spatial heterogeneity of K-complex initiation in various cortical regions. (Buzsaki (2006)).

Sharp Wave Ripples Sharp Wave Ripples (SWR) are characteristic of SWS and consummatory behavior. They occur irregularly, and are present during immobility, drinking, eating, showering, but more frequently during SWS. It represents a spread of excitatory activity in the recurrent CA3 collateral system (Buzsaki (2006)).

SWRs are the most synchronous network pattern in the limbic system, prevalent during sleep (BuzsÁk (1998)). The hippocampal sharp-wave ripples are associated with the reactivation of neuron ensembles which were activated during learning (Buzsáki (1989); Nádasdy *et al*. (1999); Peyrache *et al*. (2009); Wilson and McNaughton (1994)). During one unique ripple, only a small subpopulation of pyramidal neurons fire (Buzsáki (1989); Csicsvari *et al*. (2000)), which suggests selectivity. In rats, odor cue learning produced a robust increase in the number and amplitude of ripple events (Eschenko *et al*. (2008)). Moreover in humans, it was possible to correlate the number of learned images with the number of SWR in the entorhinal and perientorrinal cortices, which are important output regions of the hippocampus (Axmacher *et al*. (2008a)).

Slow Oscillations The SO (<1Hz) are produced in the neocortex and have been ascribed the role of a time-giving pacemaker inducing global up and down states that synchronize with the thalamo-cortical sleep spindles and the hippocampal ripples. Detection of SO is important as they mark the SWS stages of sleep. The SWS is characterized by being the highest coherent neuronal activity (BuzsÁk (1998)).

The global up and down states induced by the SO enable, in a temporal frame, the dialogue between the neocortex and subcortical structures which is necessary for the memory redistribution (Sirota *et al*. (2003); Sirota and Buzsáki (2005)). Studies using transcranial electrical stimulation at 0.75 Hz have shown how induced SO improved the consolidation of hippocampus-dependent memories, but not those hippocampal-independent memories (Marshall *et al*. (2006)).

Coupling of spindles, SWR and SO Consistent findings in different animals and humans, show how the activity of spindles and ripples increase during the up-state and is suppressed during the down-state of the SO (Sirota *et al*. (2003); Sirota and Buzsáki (2005); Isomura *et al*. (2006); Mölle *et al*. (2002);Mölle *et al*. (2006))). SWR complexes are also temporally coupled with spindles (Siapas and Wilson (1998); Wierzynski *et al*. (2009)). Such ripple-spindle events may have a role in hippocampal-neocortical communication, as ripples and hippocampal reactivations related to memory are presented exactly into the excitatory phases of the SO cycle (BuzsÁk (1998); Mölle and Born (2009); Sirota *et al*. (2003)). Thus, the feedforward control of SO over SWR and spindles permits the transfer of information to the neocortex during the up-state, which favors the induction of persistent synaptic changes, and consequently, long-term storing the information in the cortex (Diekelmann and Born (2010)) see Figure 1.8.

Electrophysiological signatures of REM Sleep and their relationship with memory consolidation In the brain, REM sleep is recognized by ponto-geniculo-occipital (PGO) waves, theta, and gamma oscillations. Neuroimaging studies in humans have shown that REM sleep activates the pons, thalamus, limbic areas, and the temporo-occipital cortices (supporting the appearance of PGO waves), and de-activates the prefrontal areas (Sasaki, 2012). Theta and gamma oscillations appear during REM sleep and during exploratory behavior. Interneurons are in phase coupled with both oscillations (BuzsÁk (1998)).

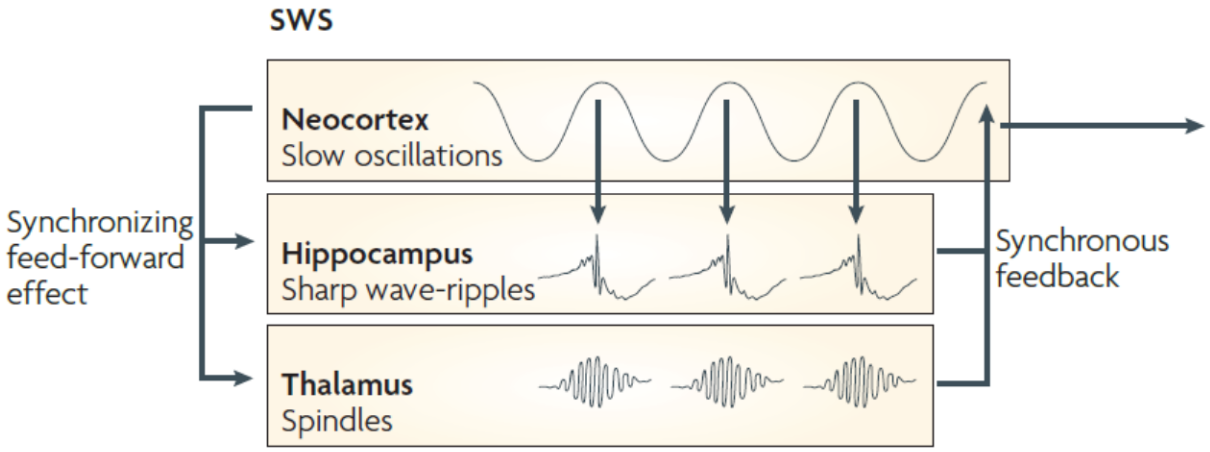

FIGURE 1.8: The active system consolidation model introduced in Figure 1.3 asserts that both neocortical and hippocampal networks encode wakefulness-related events. After Slow Wave Sleep (SWS), slow oscillations cause these representations in the hippocampus to repeatedly reactivate, synchronized with sharp wave-ripples and thalamo-cortical spindles (a result of the slow oscillation's synchronizing feed-forward effect). The slow oscillations coordinate these events, promoting the formation of ripple-spindle events, which facilitate the effective transfer of the reactivated information from the hippocampus to the neocortex. When spindle activity occurs during the depolarizing slow oscillation up-state in conjunction with the hippocampal memory output, cortical networks are more vulnerable to long-lasting synaptic plastic alterations. Taken from (Diekelmann and Born (2010))

ponto-geniculo-occipital (PGO) waves PGO waves are found during REM in animals, but they are not clearly identifiable in humans yet. They are propagated from the brainstem to the lateral geniculate nucleus and the visual cortex and are representative of bursts of synchronous activity (Diekelmann and Born (2010)). In rat studies, results show a robust increase of PGOs density in REM sleep for 3 to 4 hours after training for an avoidance task (S. Datta (2000)). An increase in PGO is associated with an increase of performance of memory post-sleep as well as an increase of expression of plasticity-related Immediate Early Gene (IEG) activity (Datta *et al*. (2008)). REM sleep-dependent consolidation processes appear to be supported by PGO waves and the theta rhythm of the EEG (Diekelmann and Born (2010)).

Theta oscillations Theta activity (4-8 Hz) is the product of hippocampal systems which generate extracellular currents. The most prominent are entorhinal afferences to granular cells and to hippocampal CA1-CA3 pyramidal cells. Theta also is a result of inhibitory currents in the perisomatic region of pyramidal neurons (Buzsáki *et al*. (1983)).

Theta activity occurs during the codification of hippocampal memories and is also related to emotional memories (Diekelmann and Born (2010)). Some studies show a

relationship between theta and the neuronal replay of memories in the hippocampus during REM (Louie and Wilson (2001); Poe *et al*. (2000)). Poe and coworkers (2000) show that the place cells which code for a known path are reactivated preferentially during the theta waves after training (Poe *et al*. (2000)). In humans, neocortical theta activity increased during REM after learning word-pairs (Fogel *et al*. (2007)). Theta is also related to emotional memories. Nishida et al showed how theta activity in the right prefrontal cortex was related to emotional memory consolidation (Nishida *et al*. (2009)). However, a decrease of REM theta activity was found in mice after fear conditioning (Hellman and Abel (2007); Nishida *et al*. (2009)). One interesting feature of theta is the reduced coherence between limbic-hippocampal and thalamo-cortical circuits compared to wakefulness and SWS (Axmacher *et al*. (2008b); Cantero *et al*. (2003)) and in a wide range of frequencies, which could be a consequence of decoupled areas and memory systems (Diekelmann and Born (2010)).

Gamma oscillations Theta usually modulates gamma activity (40-100 Hz). This activity is present in the hilus and in the vicinity of CA1 and CA3 pyramidal Cells (Buzsáki *et al*. (1983)), with a reduced coherence between these two areas (Montgomery *et al*. (2008)).

Sleep and declarative memory — There are many studies supporting the fact that the consolidation of hippocampus-dependent memories such as declarative memory, is especially characteristic of SWS. (Wilson and McNaughton (1994)) showed that neuronal assemblies activated during maze behavior are reactivated during SWS, suggesting consolidation. Moreover, hippocampal reactivations were observed in a study in humans using positron emission tomography (PET) during SWS following a period of route learning in a virtual environment (Peigneux *et al*. (2004)). Plihal and Born conducted an experiment in which subjects learned declarative memory tasks (spatial rotation task and paired-associate list) and non-declarative memory tasks (priming task, and mirror-tracing). Here, after retention intervals of early and late sleep during the night, subjects' recall was assessed and compared with the retention during wakefulness. Results showed that declarative memory was better

improved during early sleep when compared to retention during wakefulness or after late retention sleep. This result may reflect the influence of SWS on consolidation because SWS was shown to be more prominent and five times longer during early sleep than during late sleep (Plihal and Born (1997a, 1999)). Moreover, Aeschbach and colleagues evaluated the improvement in the performance of subjects in a texture discrimination task after a Slow Wave Activity (SWA) suppressed sleep. Subjects did not show improvement, as compared with the control sleep group with unsuppressed SWS (Aeschbach *et al*. (2008)).

Although most studies demonstrate the role of SWS in declarative memory consolidation, there are some studies that have shown that this phenomenon could be attributed to REM sleep as well. For example, Fogel et al. showed a significant increase in theta power after paired associate learning, this being the first evidence of REM sleep theta's role in the consolidation of declarative memory (Fogel *et al*. (2007)). Supporting this idea, in a REM sleep deprivation, in which a cognitive task was designed to evaluate factual, spatial, and temporal components of episodic memory, Supporting this idea, in a cognitive task designed to evaluate factual, spatial, and temporal components of episodic memory, REM-sleep deprived subjects showed a significantly lower recall of spatial information as compared to SWS deprived subjects. Moreover, REM-sleep deprivation caused an impairment of temporal information recall and significant impairment in true memories related to fewer R responses than SWS deprivation (Rauchs *et al*. (2004)).

Sleep and non-declarative memory — There is strong evidence supporting that REM sleep benefits non-declarative memories. Maquet and colleagues found reactivations in the cuneus and premotor cortex during REM sleep in the night following procedural learning of a motor task (Maquet *et al*. (2000a,b); Maquet (2000)). In Plihal and Born's study mentioned above, after learning a declarative memory task and a procedural memory task, retention intervals of early and late sleep during the night, subjects' recall were assessed and compared with the retention during wakefulness. Findings show that procedural memory was better improved after late retention sleep. This result may reflect the influence of REM sleep because REM

sleep was two times longer during late sleep than during early sleep (Plihal and Born (1997b)). Another similar study compared emotional memory retention using emotional text material versus neutral text material. In this case, retention improved with sleep in comparison with wakefulness, specifically for late sleep intervals in which REM sleep was three times greater than early sleep (Wagner *et al*. (2001)). In a study in rats exposed to a conditioned avoidance learning session, after learning trials, rats had 25.5% more REM sleep in comparison with control trials (Datta (2000)). Researchers calculated the P-wave density, characteristic of REM sleep, and found a significant increase in the first four periods of REM sleep after learning. Moreover, the increase between the first and the third REM periods was proportional to the better performance after sleep (Datta (2000)).

In contrast to the above results, some studies support the idea of non-declarative memory consolidation during NREM sleep. In a first study, after training visual texture discrimination, researchers compared the effects of early and late sleep intervals. Findings show that discrimination skills were improved in early sleep, but not during the late sleep interval, suggesting that SWS could drive procedural memory formation (Gais *et al*. (2006)). Similar findings are reported by Huber R. and colleagues in which an increase in SWA is reported in motor cortical areas during sleep after a motor skill learning (Huber *et al*. (2004)). Specifically. for NREM sleep Stage 2, Fogel et al. show an increase in the duration of stage 2 sleep after pursuit motor learning. Researchers also measured different spindle features as density, average duration which showed an increase after learning (Fogel *et al*. (2007)).

1.3.2 *Cues to enhance memory consolidation*

After a large variety of evidence demonstrating that cues help memory to enter into the active state from conditioning learning studies, Hars and colleagues did the first research using cues to induce memory reactivation during sleep in rats in the 1980s (Hars *et al*. (1985a); Klinzing and Diekelmann (2019)). In this study, mild non-aversive electric shocks to the ear were paired with extended aversive foot shocks, so rats learned to avoid the foot shocks when the stimulation in the ear happened. When the

shock to the ear was presented again during REM sleep, the avoidance response was enhanced (Hars *et al*. (1985b); Klinzing and Diekelmann (2019)).

Rasch and colleagues were the first ones to manipulate reactivations of memory in humans using a cue (Rasch *et al*. (2007)). In this study, subjects were presented with an odor cue while learning a 2-dimensional object location task. When memory retrieval was tested after sleep, the memory of the card locations was significantly enhanced when the odor had been presented during SWS as compared to the control condition involving the presentation of the odor alone without prior association of it to the memory content during learning as well as compared to cue presentation during REM sleep. A subsequent functional imaging investigation revealed that re-exposure to the odor cue during SWS activated the hippocampus after learning (Diekelmann *et al*. (2011)). This study shows enhancement with cue re-exposition during SWS, but not during REM sleep. It also shows a stronger activation of the hippocampus during sleep than during wakefulness, further supporting the hypothesis that cueing during SWS is specifically enhancing reactivation processes of memory contents (Rasch *et al*. (2007)).

The study of Rasch and colleagues opened a whole research field on Cued Memory Reactivation (CMR) or Targeted Memory Reactivation (TMR). The studies make use of particular cues for remembering things that have been experimentally connected to learning experiences. A common experimental paradigm is depicted in Figure 1.9 in which participants are trained on a memory task while sensory stimuli are provided. The memory task and continual cue presentation help students connect the cues to the context and learning material. The stimuli are then repeated the following night. It is assumed that the presentation of the cues induce memory reactivation, supported by the fact that individuals often display improved recall if they received the reminder signals while they were asleep compared to control (Klinzing and Diekelmann (2019)). This effectiveness can also last for over a week (Hu *et al*. (2015)).

Cued memory reactivation (CMR) can be defined as "the application of learning-associated sensory reminder cues, like odors or sounds, to manipulate memory consolidation processes during sleep" (Klinzing and Diekelmann (2019)). CMR is useful

in research to understand the effects and mechanisms of sleep-associated memory consolidation and has good potential on clinical and home settings.

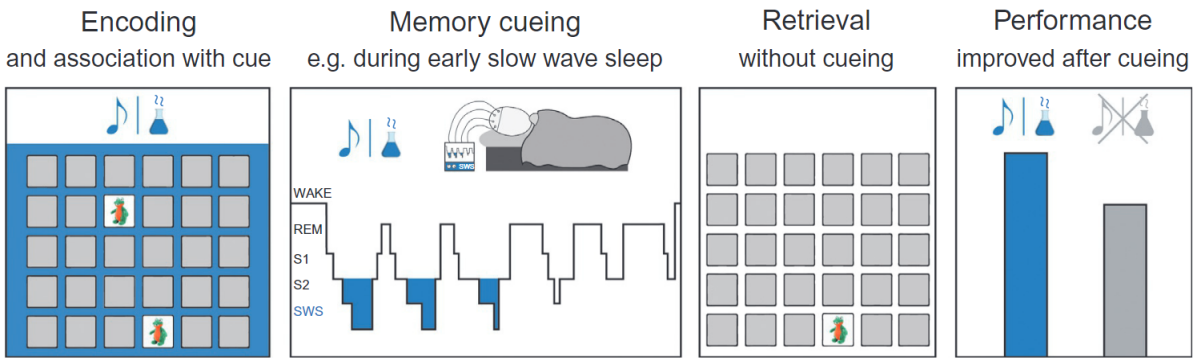

FIGURE 1.9: Participants practice a memory task while receiving sensory cues concurrently (indicated in blue). Cues become linked to the subject matter being learned. All or some of the cues are presented once more as reminders during particular sleep stages throughout subsequent sleep (e.g., during early SWS, indicated in blue). Following sleep, retrieval of the learned material is evaluated without the use of cues. Taken from (Klinzing and Diekelmann (2019))

There is another commonly used term called Targeted Memory Reactivation (TMR) which is applied in relation to the reactivation of single memory traces. TMR usually uses sounds as stimulus. The first study demonstrating that sounds can also serve as cues to enhance memory consolidation during sleep was conducted by Rudoy and colleagues (Rudoy *et al*. (2009)). In this study, auditory cues were associated with the learning of a two-dimensional object-location memory task before a nap. During NREM sleep, subjects were presented with the cue sounds of half of the objects learned during pre-nap and for the rest of sleep they presented with constant white noise. During the post-nap test, subjects had better performance at locating the cued images than locating uncued images. This finding implies that the above procedure "targets" item-specific content.

Many research conducted over the past ten years employing various learning styles, cues, subject groups, lengths of sleep, and sleep stages have demonstrated the efficiency of cued memory reactivation (Klinzing and Diekelmann (2019)). This effectiveness can last for over a week (Hu *et al*. (2015)). However, it is unclear how similar or distinct the neural activations are under different cueing modalities.

The olfactory system has the benefit of reaching the entorhinal cortex and hippocampus more immediately bypassing the thalamus (Zelano and Sobel (2005)). However, odors act slowly and have no temporal dimension, making it difficult to target

specific times. Contrarily, the temporal and spectral characteristics of the auditory system are precise. To facilitate the execution of serial procedural finger movements, ordered sequences of tones are preferable to scents, which are used as generic context cues (Klinzing and Diekelmann (2019)), as we explain in the following subsections.

Odor Cues — Most studies on humans use familiar odors for olfactory cues, such as the scent of roses, mint, orange-vanilla, citrus, or pine. On the contrary, other studies use unfamiliar odors, like isobutyraldehyde (IBA) (Klinzing and Diekelmann (2019)).

The studies that prefer olfactory cues argue that using odor as a cue is particularly advantageous because odor has a negligible impact on the sleep architecture (Badia *et al*. (1990); Carskadon and Herz (2004)). Odors do not disturb ongoing sleep processes and have been reported to not affect sleep quality either. Moreover, neural responses to odors are minimal during sleep (Rasch *et al*. (2007)). On the other hand, odor activates associated memories with strong potential, since primary olfactory processing areas project directly to higher order regions (Zelano and Sobel (2005)), without projecting to the thalamus as compared with other types of stimulus. Consequently, it enables the modulation of hippocampus-dependent declarative memories. However, none of the studies measured the effectiveness of different odors, but all of them induced consistent behavioral effects, indicating that they are equally suited for cued memory reactivation (Klinzing and Diekelmann (2019)).

The first study to use odor cues in humans was performed by Rasch and colleagues (Rasch *et al*. (2007)). In this study, they show that odor re-exposure during SWS was effective for the retention of hippocampus-dependent declarative memories but ineffective for the retention of hippocampus-independent procedural memories; this effect was not observed during REM sleep, alertness, or when the odor had been skipped during earlier learning. This result became one of the strongest evidences of memory reactivation of declarative memories preferably during SWS. Later in time, another study evaluated the stability of memories inducing reactivation on different brain states using odor cues. Induced reactivation during waking destabilized memories, but when presented during SWS, memories were immediately stabilized.

Furthermore, fMRI showed activations of the hippocampus and posterior cortical regions during reactivation in SWS, and activation of the prefrontal cortex during reactivation in wakefulness (Diekelmann *et al*. (2011)). Shanahan and colleagues used simultaneous EEG-fMRI recording in human subjects during olfactory cueing with an object-location memory task. Pattern analysis of fMRI recordings showed that presentation of the odor during sleep induced enhanced activity of the ventromedial prefrontal cortex correlated with post-sleep task performance, indicating induced reactivation (Shanahan *et al*. (2018)).

The amount of sleep and odor cue stimulations seem to have an influence on the effectiveness of odor-cued memory reactivation. (Diekelmann *et al*. (2012)) and colleagues compared the influence of the stimulation period on the consolidation of previously learned hippocampus-dependent visuospatial memories, showing that cue-induced memory reactivations during 40-min sleep enhanced memory stability in the same amount as 90 min of sleep without odor presentation. The time spent in SWS was also associated with memory enhancement, concluding that the efficacy of memory consolidation for declarative memories depends on the duration of SWS and that external cues can accelerate this consolidation process (Diekelmann *et al*. (2012)).

Along with enhancing explicit knowledge, olfactory cued memory reactivation while people sleep may also improve the ability to think creatively and solve problems in situations that are similar to those in real life. This was demonstrated in a study in which participants were given a challenge that required a creative solution while being presented with an odor before going to sleep. After cue odor presentation during sleep, participants were found to be more creative in comparison to the control groups (different odor, or no odor) (Ritter *et al*. (2012)).

Odor cues are also used in fear extinction applications. This was shown by Hauner and colleagues in 2013 where participants underwent olfactory contextual fear conditioning before sleep. Presentation of the odor during SWS helped the stimulus-specific fear extinction, reducing hippocampal activity and reorganizing the amygdala ensemble patterns (Hauner *et al*. (2013)).

Interestingly, the effect of the odor on memory reactivation is not the same for men and women. When subjects were trained on a serial reaction time task (SRTT) in the

presence of an odor, and then presented with the same odor or an odorless vehicle for the control condition during subsequent SWS, the results of the morning test on their explicit knowledge about the task showed that odor cueing did not significantly affect overall explicit knowledge. However, they showed differences when analyzing male and female participants independently (Diekelmann *et al*. (2016)).

Odors are argued to be less specific and associated with the entire learning experience triggering the reactivation of a whole set of learning contents and their associated aspects (Klinzing and Diekelmann (2019)). However, some studies have been able to describe certain local effects of the odor in the brain and specific associations with the contents to which they were associated (Bar *et al*. (2020); Rihm *et al*. (2014)). In the study of Rihm and colleagues, participants practiced a visuospatial memory exercise while an odor was present. The same odor, a new odor, or an unscented vehicle was provided during subsequent SWS. Only when the same odor was presented during sleep, there was an improvement in memory. Also, significant increases in frontal delta and parietal fast spindle power were seen with an increased negative-to-positive slope of the frontal SO for this condition (Rihm *et al*. (2014)). On the other hand, Bar and colleagues showed evidence for spatially local reactivation of memories. In this study, subjects were presented with words located in a certain visual field location, and simultaneously they were stimulated with an odor in one nostril. Presenting the odor in one nostril during sleep induced local memory reactivation specific to the hemisphere in which the words were cued (Bar *et al*. (2020)).

Auditory cues — Auditory cues are more specific than odor cues and can be linked to single learning contexts. One example of the specific use of auditory cues is the case of the association of the "meow" sound with the picture of a cat (Rudoy *et al*. (2009)). This is particularly advantageous since it enables researchers to study in more detail the memory reactivation, comparing the specific activation brain patterns during the encoding of specific memory contents during their encoding, their reactivation during sleep as well as. Furthermore, it is possible to include information of temporally ordered sequences using auditory stimulus (Klinzing and Diekelmann (2019)). It also gives greater temporal resolution allowing for more accurate time-

locked analysis of neuronal signals since auditory sensing is more controlled in time as compared to odor whose sensing might depend on ventilatory activity (Klinzing and Diekelmann (2019)). Auditory cueing seems to be more versatile in its application for different types of memory since it is possible to vary different parameters such as volume, length, sequence, and pitch in a more controlled way as compared to air-moved odors. However, auditory stimulation can have an impact on sleep architecture affecting the memory consolidation processes. This can happen because auditory stimuli evoke event related potentials in the brain that may alter sleep's ongoing oscillations (Klinzing and Diekelmann (2019)).

Several human studies used common sounds like "meow," "a dog barking," or "the clicking of an alarm clock" as auditory cues. Other research used verbal stimuli like real words, made-up words, foreign language vocabulary, or phrases in an artificial language. In several experiments, basic tones, musical notes, or tonal sequences, like melodies, were also used as memory cues. No study directly examined the efficacy of various auditory signals when it came to olfactory cues. The following is a list of the findings from these studies. It is still unclear whether some auditory cues are more effective than others, despite the fact that the majority of auditory cues produced behavioral effects (Klinzing and Diekelmann (2019)).

Rudoy and colleagues studied for the first time the effect of using auditory CMR. Auditory cues were presented to the participants during a two-dimensional object-location memory task before taking a nap. During sleep, subjects were presented with constant white noise, and during NREM sleep, they were presented with the cue sounds of half of the objects learned pre-nap. During the post-nap test, subjects had a better performance at locating the cued images than locating uncued images. Also, the mean amplitude of the EEG signal from 600ms to 1000ms after the sound onset was higher when there was less forgetting; thus, as measured by brain potentials, the degree of recall improvement or deterioration appears to have been influenced by sound-induced memory processing during sleeping. Based on this observation, the level in which cues influence the consolidation could be dependent on the level of attention on these cues. These results show that memory processing during sleep could be highly specific (Rudoy *et al*. (2009)).

Later, in 2012, Van-dongen and colleagues showed that the thalamus and medial temporal lobe are involved in the reactivation of memories triggered by associated sounds. In this study, participants learned object-location associations with object-related sounds. During subsequent SWS, a subset of the associated sound was presented while participants were recorded with fMRI. Increased right parahippocampal cortical activation was linked to related noises. The thalamus, bilateral medial temporal lobes, and cerebellar activation in response to sound during sleep were linked with behavioral outcomes. Additionally, during the retrieval of reactivated memories, it was positively linked with variations in parahippocampal-medial prefrontal connectivity (Van Dongen *et al*. (2012)).

TMR has been proven to be effective independent of the motivation of learning. In a study, participants learned object-location associations while hearing characteristic object sounds and associated with a certain reward value. Behavioral performance was reduced for low-value than high-value associations after 90 min of nap or wake interval. However, using TMR during nap time, both low and high-value related memories were "rescued" from forgetting (Oudiette *et al*. (2013)).

TMR effect during REM sleep has been studied as well for declarative memories. Revealing enhanced cortical responses during retrieval. When participants learned pictures of faces, while presented with auditory cues and the same cues were presented during REM sleep, they enhanced subsequent retrieval performance. fMRI measurements show that during retrieval, response in a visual area and in a cortical region of multisensory (auditory-visual) convergence was enhanced (Sterpenich *et al*. (2014)).

Another series of studies on declarative memory used TMR during sleep to increase vocabulary learning (Schreiner *et al*. (2015);Schreiner and Rasch (2015a);Schreiner and Rasch (2015b)). They cued prior learned Dutch words either during NREM or during waking. After TMR, Dutch words improved the memory for the German translation after being presented during sleep and not during waking. This successful verbal cueing during NREM sleep correlates with frontal negativity in ERPs, higher frequency of SO, as well as an increase in the right frontal and left parietal oscillatory theta power (Schreiner and Rasch (2015a)). Furthermore, they proved that during

sleep, memories are reactivated and more open to integrating new information after the cue. In a first study, they presented Dutch-German word pairs to the participants. During sleep memory cues were presented directly followed by either correct or conflicting auditory feedback or a pure tone. The effect of the cueing was a blocked memory benefit. This auditory stimulation also removed the characteristic increases in theta and spindle activity, markers of successful reactivation during sleep (Schreiner *et al*. (2015)).

Direct content-stimulus associations seem to be important for TMR. In a study of Cairney and colleagues, participants were presented with pictures in specific screen locations simultaneously with a semantically related sound. In a separate task, they were presented with the same pictures with no screen location association but with an unrelated word association. During SWS, half of the sounds were replayed again. TMR enhanced memory recall of picture locations (involving direct cue-memory associations) but not for picture-word pairs (indirect cue-memory associations). Additionally, a recall test was performed before sleep, and the TMR showed to benefit the low accuracy memories before sleep, but not the ones recalled with high accuracy (Cairney *et al*. (2016)), being another proof that consolidation via TMR strengthens memories. In a second experiment, they switched the gender of the verbal auditory stimuli between the one presented during encoding and the one presented during sleep. When presented during sleep, the nonidentical verbal cues reduced forgetting of both cued and uncued associations concluding that "TMR with nonidentical verbal cues may utilize linguistic decoding mechanisms, resulting in widespread reactivation across a broad category of memories"(Cairney *et al*. (2017)).

Another factor contributing to the beneficial effect of TMR is prior learning. (Groch *et al*. (2017)) used targeted memory reactivations to evaluate the influence of prior knowledge to new acquisition of information for successful reactivation and consolidation of memories during sleep. They show that cueing benefited memory retention the next morning only for stimuli related to prior knowledge but not for stimuli unrelated to prior knowledge. This effect is also seen at an oscillatory level, specifically for spindle and theta activity that is increased for the prior knowledge condition vs the non-prior knowledge.

In 2018, after decoding analysis of EEG data became a common tool, (Cairney *et al*. (2018)) introduced a novel paradigm presenting adjective-object and adjective-scene associations before sleep. Adjectives were presented in an auditory modality. Later during sleep, they presented some of the already encoded adjectives in addition to new adjectives. Those ones triggering a memory reactivation evoked an increase in fast spindles. Also, it was possible to decode the type of memory category linked to the verbal cue (object or scene) with the data during the induced spindle activity, which also correlated with the behavioral performance after sleep.

Novel experimental paradigms have been developed in the last years using auditory TMR as a tool. On one hand, TMR with auditory stimulation has been explored in real-time closed-loop setups. (Shimizu *et al*. (2018)) developed an EEG-based closed-loop system to precisely deliver auditory stimulation at the time of down-state to up-state transitions during NREM sleep. This technique improved significantly spatial navigation efficiency after sleep that is accompanied by increases in the power of the fast spindle band. On the other hand, (Simon *et al*. (2018)) innovated using a paradigm of forgetting, training participants first to associate the act of forgetting with an auditory tone (2-s auditory synthesized sound). In a separate task, subjects learned object-sound location pairings. During SWS, participants were presented with a subset of the cue sounds paired with the "forgetting tone". Behavioral results show an impairment in the recall of the location of the reactivated objects. This approach, after further validation, could be used in the therapy of phobias in the future.

Other cues — Only one study attempted CMR with tactile cues, in which participants were trained on a finger-sequence tapping task using their non-dominant hand. Later during sleep, subjects were presented with mechanical fingertip stimulation in the same sequence that was presented during learning. Control condition included an untrained sequence. However, this tactile cueing did not affect motor skill performance after sleep (Klinzing and Diekelmann (2019); Pereira *et al*. (2017)).

1.3.3 *Electrophysiological signatures of memory reactivations*

Many attempts have been made to describe the way the brain consolidates memory by memory reactivations. In this section, I describe oscillatory signatures, temporal signatures, and the localization in the brain mainly by lateralization paradigms of memory reactivation that are reported in the literature.

Memory reactivations can be described by correlating activity during learning with the activity either during the retrieval of the same content previously learned, or during sleep when memory reactivation is occurring (most of the time, triggered by a cue). Approaches of univariate and multivariate pattern analysis have been used in order to describe the memory reactivation signatures. In univariate analysis, the variation of neural activity between conditions is identified in specific brain regions: electrodes (in the case of EEG), or voxels (in the case of fMRI). In multivariate analysis, patterns of activity are identified involving different brain regions. In the case of multivariate analysis, different approaches were used to describe memory reactivations. Among them, we have pattern similarity analysis, decoding models, and encoding models. In Pattern similarity analysis, activity across voxels or sensors is correlated between conditions (learning vs reactivation); reactivation is detected when the correlation surpasses the one between non-corresponding patterns. In decoding models, supervised models are trained on the neural activity recorded during learning and then tested on neural activity recorded during memory reactivation states; reactivation is identified when classification accuracy increases. Finally, for encoding models, mathematical models are fit to neural data recorded during learning, and reactivation is detected when the model parameters generalize from learning to reactivation (Favila *et al*. (2020b)).

Oscillatory signatures of memory reactivation — Most of the oscillatory signatures of memory reactivation are described in sleep studies. The most relevant oscillatory rhythms appearing during memory reactivation in sleep are slow waves, delta, theta, and fast spindles.

The relevance of delta is confirmed by the study of (Oudiette *et al*. (2013)) described in section 1.3.2, which showed a correlation between memory accuracy for low-value

objects and frontopolar midline delta power during SWS (See Figure 1A). The relevance of spindles is confirmed by (Antony *et al*. (2012)) who conducted a study in which participants learned to play two melodies by pressing four keys in time with sequences of visual symbols. After a nap, they enhanced relative performance in one melody, when when it was presented during sleep as compared to the uncued melody. They only addressed the effectiveness of cueing during SWS recognizing it as critical for systems memory consolidation. EEG recordings showed a correlation between reactivation advantage and the percentage time of SWS, as well as with the number of spindle events at electrode F_4. The authors report that, in general, the effect of spindles was largest over cortical regions contralateral to the hand used to perform the melodies.

Interestingly, one study showed the need for a silent period after spindle activity to facilitate memory reactivation. (Farthouat *et al*. (2017)), studied the effects of auditory presentations of previously learned material during wakefulness or non-rapid eye movement (NREM) sleep on memory consolidation. A list of word pairings that were presented to participants both visually and audibly was learned. Half of the pairs' first words were delivered as sounds during the consolidation period (whether the learner was awake or asleep), followed by either the right pair or the wrong connection. TMR had beneficial effects on the correct pair cueing but not for the incorrect one only during wakefulness. Time-frequency analyses showed an early rise of power in the theta band and a few hundred milliseconds later in the fast spindle band after cue presentation. The increase in sigma activity (spindle-related) suggests an association with memory reactivation. However, when presenting the second word immediately after (either correct or incorrect), the sigma activity is extinguished, suggesting a necessity for a period of no stimulation after the cue presentation.

Following studies have reproduced the role of both delta and spindles for memory reactivation. The study of (Rihm *et al*. (2014)), described in section 1.3.2, showed an increase in slow oscillation slopes, frontal delta, and parietal spindle power during the first 10s of an odor cue during SWS. Later, Creery and colleagues conducted a study in which participants learned to associate each of the images of common objects with a unique screen location, paired with a characteristic sound. During SWS, half of the

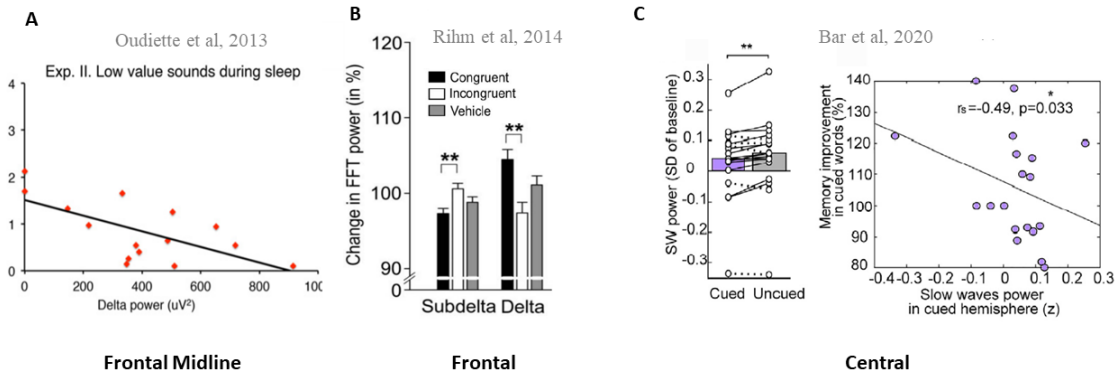

FIGURE 1.10: A Shows the correlation between memory accuracy for low-value objects with delta power at frontopolar midline EEG during SWS in (Oudiette *et al*. (2013)). B shows the variations in relative EEG power during the last 10 seconds of baseline and the first 10 seconds of odor-on. Subdelta (0.5–1.5 Hz) and delta (1.5–4.5 Hz) power were calculated in frontal electrodes (*p < .05, **p < .01). Taken from (Rihm *et al*. (2014)). C left displays the difference in Slow Wave (SW) power between the cued (purple, left) and uncued hemisphere on average (gray, right). Lower/higher power in the hemisphere with the cue is indicated by solid/dashed lines, respectively. **p < 0.01. The scatterplot in C right displays the relationship between the SW power in the cued hemisphere during odor cueing and post-sleep recall for cued words as a percentage of pre-sleep baseline (as SD of baseline) (*p < 0.05) Taken from (Bar *et al*. (2020)).

sounds were presented. EEG analyses revealed that the cueing benefit correlated with delta power and fast spindle density. Specifically, relative delta power values were highest for the frontal electrode cluster, and spindle density values were highest for the parietal cluster (Creery *et al*. (2015)).

Furthermore, the phase of the SO is important for the reactivation of memory to happen. In (Batterink *et al*. (2016)) study, participants learned arbitrary spatial locations for objects, each one paired with a characteristic sound. Then, during SWS, half of the sounds were presented. This study was the first to prove that the memory benefit was predicted by the slow-wave phase in which the stimulation was presented. Specifically, they show that cueing is most effective during the first half of the downstate of the SO. Additionally, in another series of studies, using closed-loop TMR to stimulate during a specific phase of the SO, participants first learned foreign vocabulary, while presented with a sound. Later during sleep, the sound was presented during up- and down-states of slow oscillations, respectively, in a within-subject design. The presentation of cues during the up-states improved recall performance, which was not the case for the down-states. Electrophysiologically, the memory reactivation was associated with a characteristic power increase in the theta and sleep spindle band. The event-related potential associated with TMR in upstate

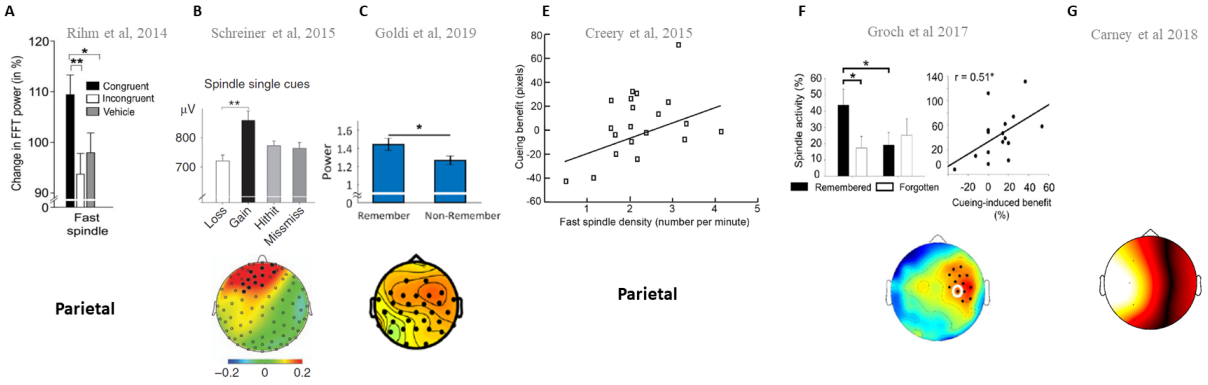

FIGURE 1.11: A. Shows the changes in relative EEG power during the first 10 s of odor cue presentation compared with the last 10 s of baseline. Fast spindle power (13.0–15.0 Hz) is retrieved from parietal electrodes. Taken from (Rihm *et al*. (2014)). B. shows the correlation between successful cueing of dutch words and enhanced power in the spindle band **p<.01. Taken from (Schreiner *et al*. (2015)). C top shows mean spindle power for SO upstate cueing within the significant clusters shown as filled black dots in the bottom topoplot comparing remembered vs not-remembered words. Taken from (Göldi *et al*. (2019)). E. shows the relationship between spindle density and the cueing benefit. Fast spindle density was averaged over parietal locations. Taken from (Creery *et al*. (2015)). F. shows average fast spindle activity in response to later remembered and later forgotten cues indicated for stimuli related and stimuli not related to prior knowledge. The topographical distribution of the difference in the Standard error of the mean (SEM) is shown for mean activity in the fast spindle band for a time interval between 1100–1300 ms after cue onset. Scatterplots indicate the correlation between fast spindle response to remembered cues and the cueing-induced benefit for stimuli related to prior knowledge. Fast spindle activity was significantly correlated with the cueing-induced benefit. *p<.05. Taken from (Groch *et al*. (2017)). G. shows the topography of the resulting cluster of significant spindle power increase, revealing left-hemisphere specificity of the effect of auditory cueing. Taken from (Cairney *et al*. (2018))

showed 1 Hz oscillation after cue onset, while down-state TMR seemed to disrupt the ongoing SO (Göldi *et al*. (2017, 2019)).

The coupling between SO and spindles is also considered an important signature of memory reactivations as well. (Bar *et al*. (2020)) showed that, the cued hemisphere's local TMR enhanced the phase-amplitude coupling (PAC) between the SO and sleep spindles. There was a noticeable difference in the favored phases specifically: in the cued hemisphere, the chosen phase occurred later than in the uncued hemisphere (See Figure 3C). More recently, Shreiner and colleagues have explored the role of the SO phase in memory reactivation using machine learning. In this study, authors didn't use TMR, but on the contrary, studied endogenous memory reactivation. For this, participants acquired associative memories (images with words) before sleep while recorded with surface EEG. Later, multivariate decoding was used in EEG data acquired during NREM sleep to capture endogenous memory reactivation. Results show an increase in decoding AUC during SO-spindle complexes with the precision of SO-spindle coupling predicting reactivation strength, which also correlated with memory performance after sleep (Schreiner *et al*. (2021))(See Figure 3A).

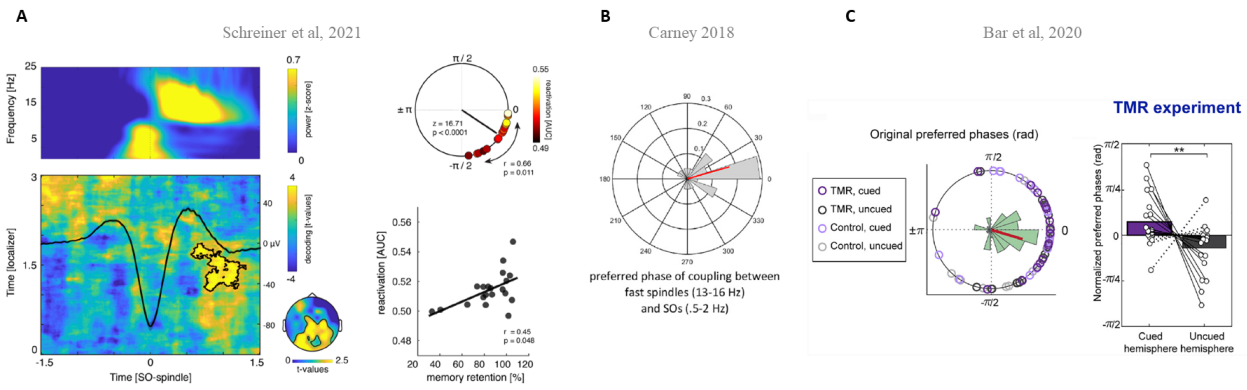

FIGURE 1.12: A. the top left figure shows the time-frequency representation of all SO-spindle segments (z-scored across time and the bottom left shows that learning-related brain patterns (objects vs. scenes) were decodable during SO-spindle complexes (contour lines indicate the extent of the significant cluster, p = 0.016; color range (blue to yellow) represents t-values against surrogate decoding performance. The topographical figure illustrates the results of a 'searchlight decoding procedure', indicating that bilateral parietal and occipital areas exhibited stimulus category related effects. Top right shows the phases of the SO-spindle modulation derived from channel Cz, illustrating the clustering of spindle power toward the SO up-state (rad = 0). Circular-linear correlation analysis between the individual mean SO-spindle coupling phase (circles) and the mean reactivation strength (area under the curve [AUC] scores; white indicates high classification performance and black indicates low classification performance) revealed a positive association (r = 0.66; p = 0.011). Bottom right shows reactivation strength correlated positively with behavioral levels of associative memory consolidation. Taken from (Schreiner *et al*. (2021)). B. shows a histogram of participants' corresponding SO-spindle modulation phases (mean direction = 15°, shown in red). Taken from (Cairney *et al*. (2018)). C. depicts phase-amplitude coupling during unilateral odor stimulation in sleep taken from (Bar *et al*. (2020)). The left figure displays the hemisphere- and experiment-specific locking of spindle amplitude peaks at SO up-state phases in frontal EEG electrodes (TMR experiment, black circles; control experiment, light circles; cued hemisphere, purple circles; uncued hemisphere, gray circles). The preferred phases for each subject are indicated by circles. The preferred phases histogram for all experiments and hemispheres is represented by green bars. The grand average phase (angle) and vector are indicated by a red line (radius). The mean normalized preferred phases for the TMR experiment are displayed on the right for the cued (purple) and uncued (gray) hemispheres. Participants are represented by circles with lines connecting them. In the cued hemisphere compared to the uncued hemisphere, full/dashed lines denote a later/earlier preferred phase, respectively. The sleep spindle amplitude in the cued hemisphere peaks later than in the uncued hemisphere in the majority of participants (15/19) (**p 0.01).

From 2015, a series of experiments showed that auditory cues consistently generate an ERP resembling a slow oscillation (SO)/k-complex potential. They also reported an increase in theta power a few hundred milliseconds after auditory cues during sleep, followed by an increase in the fast spindle band (in the upstate of the evoked SO) (Schreiner *et al*. (2015); Schreiner and Rasch (2015b); Cairney *et al*. (2018))(studies described in section 1.3.2). From this moment, theta has been included as a marker of memory reactivation (see Figure 4).

Since 2017 different studies have confirmed the relevance of theta for memory reactivation. In the study of (Groch *et al*. (2017)) described in section 1.3.2, authors show increases in theta and fast spindle power after the cue, for successful cues (stimulus paired with successfully recalled information). Later, in (Schreiner *et al*. (2018)) study, participants performed a vocabulary-learning task in the evening learning to associate Dutch words (cues) with German words (targets). During NREM sleep, the

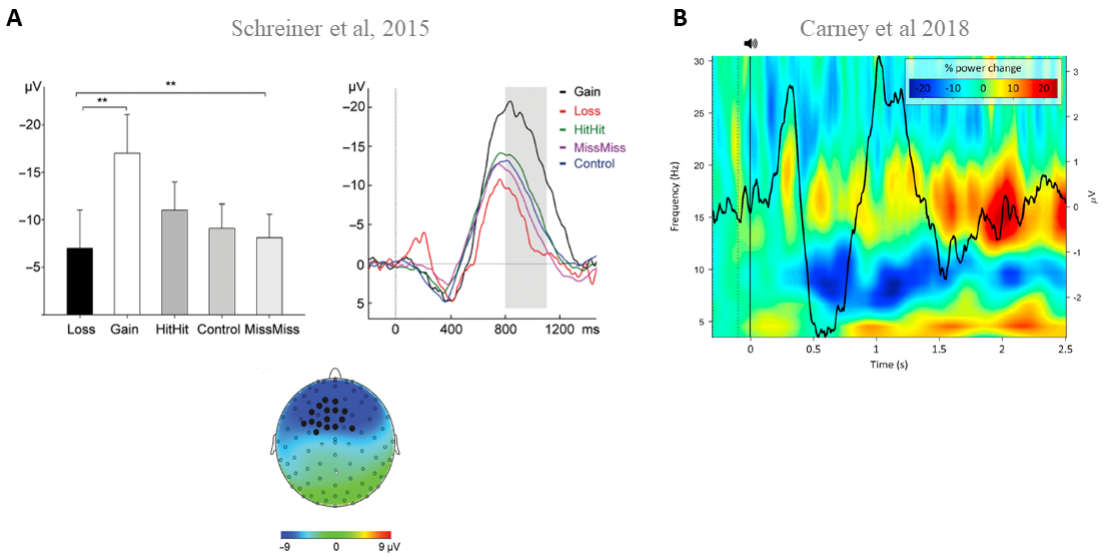

FIGURE 1.13: A. shows that successful cueing was associated with a more pronounced negativity EEG activity at frontal electrode sites (representative electrode Fz). The bar plot shows the difference in amplitude of the signal for Losses (words that were not remembered in the test post-sleep that were in the pre-sleep baseline), Gains (words that were remembered in the test post-sleep that were not in the pre-sleep baseline), HitHits (words that were remembered in both the test post-sleep and the pre-sleep baseline), and Missmisses (words that were not remembered at all). On the right, the Event-Related Potential (ERP) is shown. The waveform quantization time window is represented by the rectangle. The frontal distribution is clearly visible in the scalp map, which depicts the topographical distribution of the difference between Gains and Losses in the time window between 800 and 1100 ms. Taken from (Schreiner and Rasch (2015b)) B. shows the time-frequency representation difference map of responses elicited by old memory cues versus new control adjectives, with the corresponding ERP for old cues superimposed. Taken from (Cairney *et al*. (2018))

Dutch words were repeatedly presented and the memory performance was assessed after sleep. The results show that theta oscillations orchestrate the reactivation of memories during both wakefulness and sleep following a phase similarity approach. Specifically, the 5 Hz frequency is an oscillation that reappeared in response to TMR reminders fluctuating in power at a rate of 1 Hz indicating coordination by slow oscillations.

The study of (Antony *et al*. (2018)) described in section 1.3.2, demonstrated novel rhythmicity to spindles, such that a spindle is more likely to occur about 3-6 seconds after a previous spindle, and cueing is less effective 3-6 seconds after the occurrence of a sleep spindle, indicating that there may be a refractory period after sleep spindles during which the brain is not receptive to outside memory cueing.

In the awake brain, the oscillatory signatures of memory reactivation reinforce the role of theta in the memory reactivation process. Kerrén and colleagues demonstrate that the phase of a theta oscillation influences neuronal markers of memory reactivation in humans. They trained pattern classifiers to detect brain reactivation of previ-

ously learned word-object correlations. Classifier fidelity fluctuated regularly at 7 or 8 Hz and was modulated by theta phase. Surprisingly, the best classification phase was moved 180° between encoding and retrieval. There was also high theta phase consistency approximately 300 ms before the classifier-identified time periods of maximal brain memory reactivation (Kerrén *et al*. (2018)). On another hand, (Staudigl and Hanslmayr (2019)) conducted a sensory match/mismatch memory paradigm using temporal pattern analysis in MEG and discovered that neural pattern reinstatement of MEG activity at 6–8 Hz only improved memory in the match condition and impaired memory in the mismatch condition for the auditory but not for the visual encoded words. Michelman and colleagues have also shown an effect in theta. However, in their case, memory reinstatement was accompanied by a decrease of low-frequency (8 Hz) power and the effects were evident in the visual and auditory domains localized in their sensory-specific regions. This signature of memory reactivation was observed early in the first 500 ms after cue onset (Michelmann *et al*. (2016, 2018)).

Temporal signatures of memory reactivation — Several studies mentioned above have a temporal component of the specific signature described. In Figure 5, a compilation of different studies with a similar results is presented. In general, it is possible to observe that, in the auditory modality, the cues evoke a low-frequency response similar to a SO or a k-complex, with a theta power increase around the downstate (500 milliseconds after the cue onset), and a sigma power increase (related to spindle events) around the upstate (1000 milliseconds after the cue onset), being consistent across all studies.

Accordingly, (Göldi *et al*. (2017, 2019)) focused on the time-frequency analysis between the time points of 0 ms and 2000 ms after stimulus onset. For memory cues played during the up-state, they observed a significant increase in theta power for cued words that were remembered vs the non-remembered ones in a topographical right central distribution. Spindles also revealed a significant increase between 830 and 1770 ms involving all electrodes. In line with these findings, the study of Schreiner and colleagues in 2021 that identified endogenous memory reactivations showed that the above-chance classification occurred from 800 to 1200 ms relative to

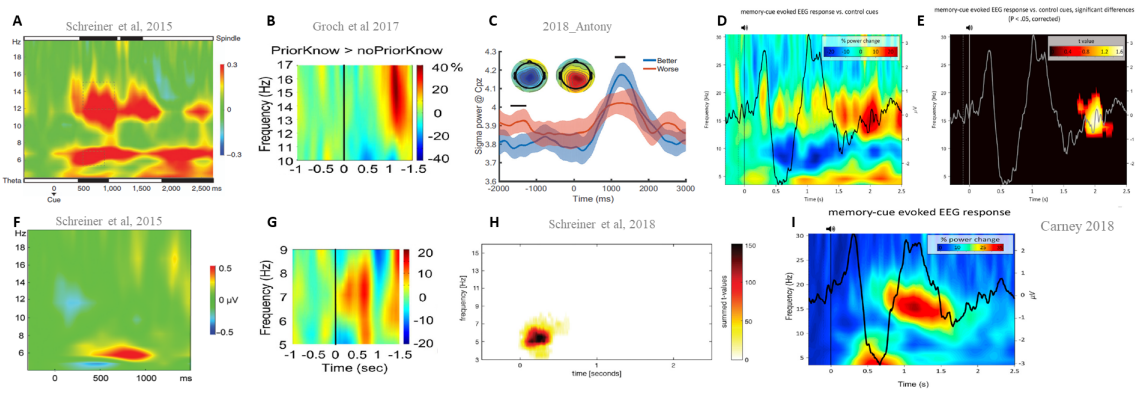

FIGURE 1.14: (A) displays a depiction of the electrode F3's time-frequency. Verbal cues were given at time 0 milliseconds. Post hoc t-test results (in black) comparing "gains" and "losses" in spindle and theta power are shown in the top and bottom panels, respectively. Taken from (Schreiner *et al*. (2015)S). (B,G) In the fast spindle frequency range, time-frequency charts show the difference between the subsequent memory effect (later remembered stimuli minus later forgotten stimuli) for stimuli linked to prior knowledge ("priorKnow") and stimuli unrelated to prior knowledge ("noPriorKnow") (B), and in the theta frequency range (G). Taken from (Groch *et al*. (2017)). (C) Items that were more easily recalled had spindle powers that were higher post-cue but lower pre-cue. Significant time intervals (p 0.05) are indicated by horizontal bars. Taken from (Antony *et al*. (2018)). Using the corresponding ERP for the old memory cues as a superimposition, (D) displays the time-frequency representation difference map of responses triggered by old memory cues vs new control adjectives. (E) is identical to (D) After statistical thresholding ($p<0.05$, corrected). Take note of the notable rise in fast spindle power (13-16 Hz) between 1.7 and 2.3 s after cue onset. Taken from (Cairney *et al*. (2018)). (F) The difference between "Gains" and "Losses" is shown by induced theta power (electrode FC6), which clearly increases in response to successful cueing. Taken from (Schreiner and Rasch (2015b)). (H) displays the wake retrieval word-specific phase similarity. Early after cue initiation (t = 0 s), a considerably improved phase similarity during successful subsequent retrieval was seen in the theta range. The significant cluster's electrodes' t-values were added together. Taken from (Schreiner *et al*. (2018)). (I) displays the time-frequency representation and ERP that are triggered by the appearance of auditory memory cues. The unthresholded time-frequency and grand average ERP are shown in the figure (both collapsed across all channels and then averaged across participants), and they show a significant increase in theta/slow spindle power in the evoked SO down-state followed by an increase in fast spindle power in the subsequent SO up-state. Taken from (Cairney *et al*. (2018)

the SO down-state coinciding with the presence of coupled sleep spindles and that the stronger the fidelity of the accompanying reactivation signal, the closer the spindles were nested towards the SO-upstate (Schreiner *et al*. (2021)).

Despite the specific signatures observed after the onset of cues in TMR, a study by Schönauer and colleagues in 2017, the first study to use multivariate pattern classification to decode the type of content that subjects viewed before sleep from the electrical brain activity during sleep, described global temporal patterns in which memory reactivations are more likely to happen. They discovered significant, subject-generalizable patterns in both REM and non-REM sleep. It's interesting to note that this processing happens in cycles, and NREM and REM sleep have different topographical distributions throughout the scalp and relevant frequency ranges. Only the SWS prediction accuracy, showed a link with memory function (Schönauer *et al*. (2017)). Figure 6 depicts the nighttime time history of categorization accuracy.

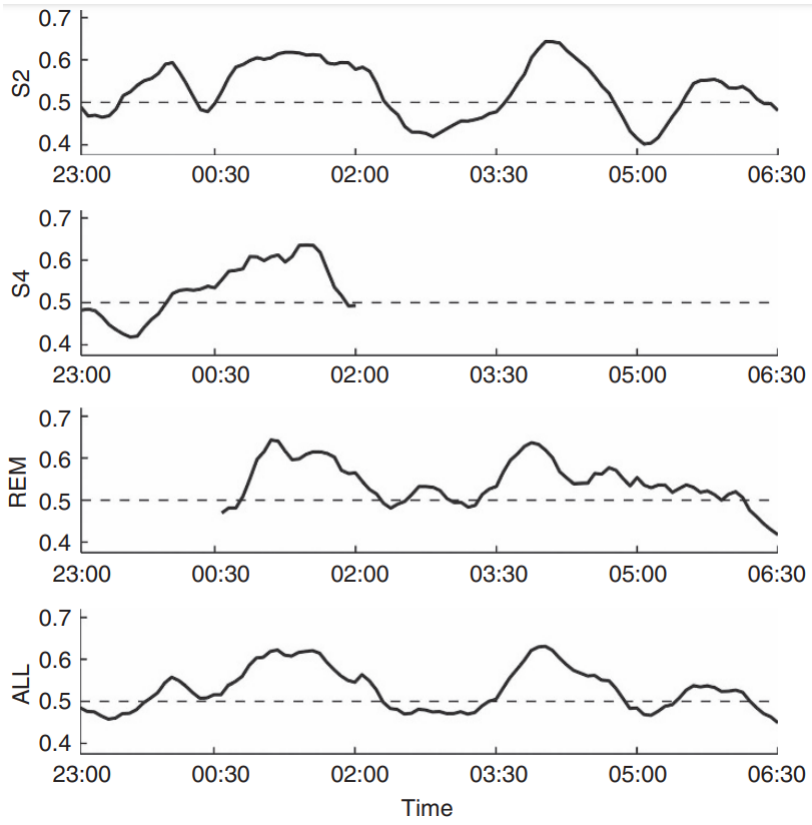

FIGURE 1.15: S2, S4, and REM sleep stages all underwent separate analyses. Performance on classification tasks oscillates and peaks between 3 and 6 hours after learning in all stages. Taken from (Schönauer *et al*. (2017)).

Apart from the mentioned studies observing temporal patterns of memory reactivation during sleep, most of the studies that focus on temporal patterns of memory reactivation are described in wakefulness during retrieval. In a study by Wimber et al, participants were presented with words on flickering backgrounds inducing a brain response at either 6 or 10 Hz. Later, during a memory test, when successfully recognizing a word, these frequency signatures emerged in the brain. These early signatures of memory reactivation happened in the first 500 ms after cue onset (Wimber *et al*. (2012)). Later, in 2014, Jafarpour and colleagues showed that MEG brain patterns appearing during encoding were later replayed during recall. Using CMR (words associated with pictures), and machine learning classification, they showed that recollection of images is associated with a replay of brain patterns happening early (180 ms) during encoding. On the other hand, this replay occurs 500 ms after the onset of the cue (Jafarpour *et al*. (2014)). In line with the previous findings, (Johnson *et al*. (2015)) performed EEG-based pattern-classification analyses using the Multi-Voxel Pattern

Analysis toolbox to apply multivariate analyses of the EEG, using neural networks with 2 layers, showed early reactivation of category-specific encoding activity during cued recall; the incidence of reactivations during a specific retrieval trial seemed to rise from the pre-stimulus phase to roughly 500 ms after the beginning of the stimulus, and they then persisted throughout the recording epoch.

Earlier memory reactivation signatures have been shown in 2016, in a study where participants performed a novel non-spatial reasoning task while being recorded using MEG. The task required selecting paths through a set of six visual objects. They trained pattern classifiers on the data recorded during the presentation of visual objects alone and tested the classifiers on data recorded during periods when no object was presented (offline periods). In the object-free periods, spontaneously happening brain patterns in fast sequences lasting on the order of 120 ms were detected (showing compressed replay) similar to the representations of encoding (Kurth-Nelson *et al*. (2016)).

Recently, in 2019, a couple of studies have shown more complex temporal signatures of memory reactivations. In one study, participants were recorded with EEG while being asked to create word-object associations and later reconstruct the object as vividly as possible when cued with the word. Once they considered having a vivid image in mind, they had to press a key. Later, authors used classification to decode at which time the model is most likely to categorize perceptual and semantic features correctly. Results show that low-level perceptual features are decoded earlier than high-level conceptual features from brain activity, but interestingly, this pattern is reversed during recall, as shown in Figure 7 (Linde-Domingo *et al*. (2019)). On another hand, in a series of studies, Liu and colleagues trained participants on a rule describing object ordering and then presented a new set of objects in randomized order to evaluate reactivation in a subsequent period of rest. The patterns of reactivation occurred in sequences accelerated in time and reversed their direction after a reward (Liu *et al*. (2019)).

Intracranial EEG-based studies evaluating the memory reactivation features during recall have provided detailed temporal signatures. Similar results to the study of Liu et al. were found earlier in 2017 where authors tested the hypothesis of a faster

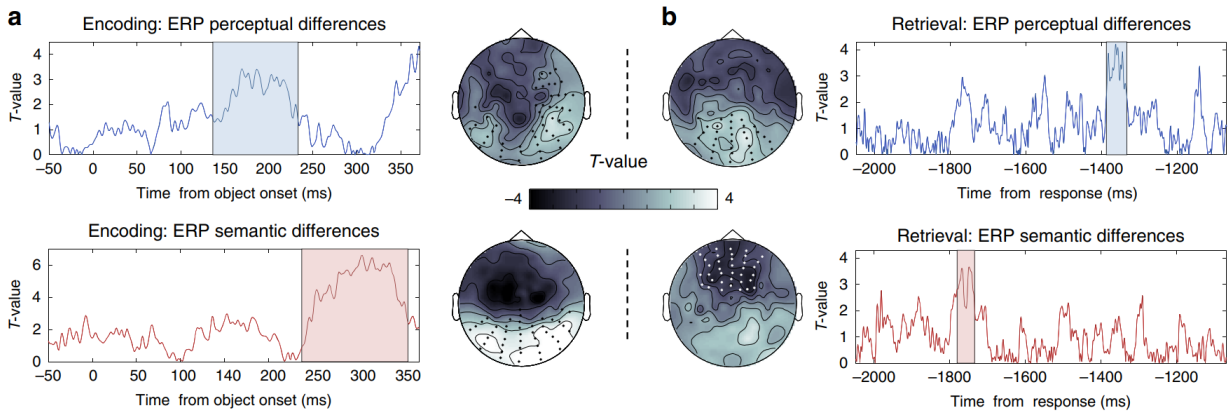

FIGURE 1.16: (a) Left panels show variations in ERP group activity (T values) over time in electrodes that formed a significant cluster when an item was presented, locked to the stimulus's onset. Line drawings versus pictures are contrasted in the top left panel, and animate versus lifeless things are contrasted in the bottom left panel. All relevant electrodes in a cluster are shown with an asterisk in the scale figures that are placed next to each contrast to show the topography of the maximal cluster as averaged across the significant time window. (b) The right panels, which are time-locked to participant answers, display ERP group differences (T values) across time in those electrodes that are contained in the most significant clusters during memory retrieval. The bottom right panel displays the semantic contrast, and the top right panel displays the perceptual contrast.Each panel has a cluster topography for each comparison, and the temporal extent of important clusters is colored-shaded.

timescale for reinstatement in the human cortex as compared to encodings. Patients were recorded with implanted electrodes (for seizure monitoring) while performing a verbal episodic memory task. During reinstatement, they observed that high gamma activity occurs faster than during encoding using a time-warping algorithm (Liu *et al*. (2019)).

In 2011, in a study using intracranial recordings conducted by Manning and colleagues, a contiguity effect during free recall is shown. Patients first learned a list of words. Later, when recalling, the authors identified similar patterns of brain activity observed during the encoding of the same item, but they were also similar to the patterns observed during the learning of neighboring list items. This similarity decreased with positional temporal distance from the learned item. On another hand, the correlation with behavioral results shows that the individual tendency to recall list items in temporal proximity relates to this neural signature of context reinstatement. These effects were particularly strong in temporal lobe recordings (Manning *et al*. (2011)). In a similar fashion, in the study of (Folkerts *et al*. (2018)), epilepsy patients performed an item recognition task. Authors calculated similarity of neural activity as a function of lag between items, and also as a function of recency of the items presented. Results evidenced that only well-remembered items show a

neural contiguity effect as compared to the not well-remembered ones which showed an anti-contiguity effect.

Local signatures of memory reactivation — Different experiments consistently showed that the memory reactivation signatures can happen locally in the brain depending on the location of the neural networks that are activated during encoding. More specifically, these studies are focused on the lateralization of memory reactivation. This is the case for the study of (Cousins *et al*. (2014)), in which authors subtracted spindle density in left (non-learning) from the right (learning) hemispheres, to explore regional spindle effects. Results show differences in spindle density between left and right electrodes as shown in Figure 8. In line with these findings, Cox and colleagues put participants to learn word-location associations (left and right) paired with different odors. During sleep, they presented a single odor in order to selectively reactivate a subset of word locations. The authors found higher amplitude and number of fast spindle events over posterior brain areas involved in visuospatial processing, contralateral to the visual field being cued showing hemisphere-specific changes in neuronal oscillations (Cox *et al*. (2014)).

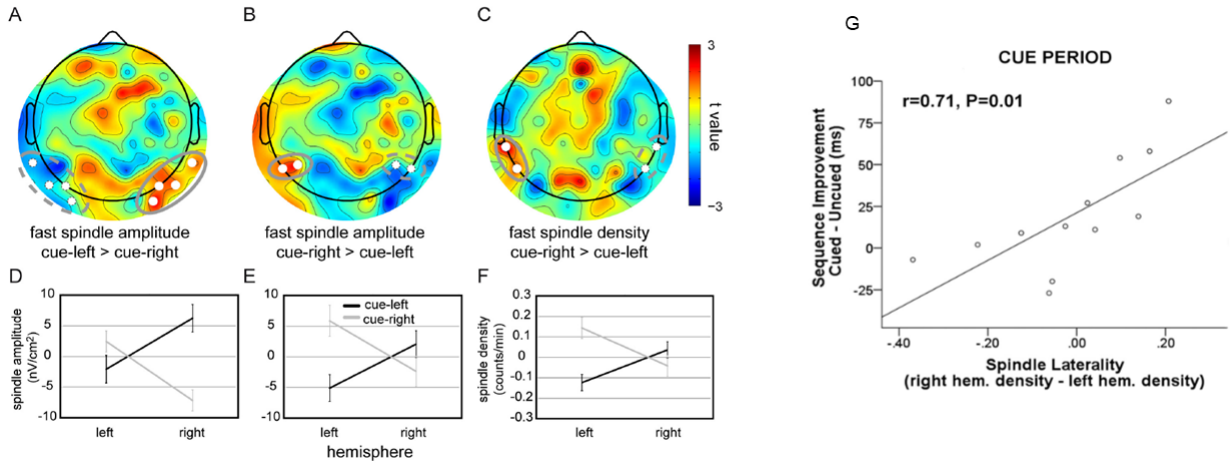

Figure 1.17: T maps (A–C) illustrating the strong cueing side effects. Significant clusters are denoted by gray solid ovals, and the significant electrodes within each cluster are denoted by white dots. Contralateral "mirror" clusters are shown in gray dashed ovals, which are utilized to examine the hemisphere-dependence of cueing side effects in (D–F). (A) In the cue-left condition, a right parieto-occipital area responded with greater spindle amplitude than in the cue-right condition. (B) The cue-right group's spindle amplitude was higher than the cue-left group's at a left parietal location. (C) More spindle density in the cue-right group compared to the cue-left group in a left parietal area. (D-F) For each cluster, there are significant crossover interactions between the cueing side and the hemisphere, indicating that spindle modulations in response to memory cues are bilaterally symmetrical. Taken from (Cox *et al*. (2014)). (G) The procedural cueing effect in an experimental group during CUE and NO-CUE was predicted by the spindle laterality at the central electrodes. Taken from (Cousins *et al*. (2014))

In 2016, in a study done by Waldhauser and colleagues, participants were presented with stimuli to the left or right of fixation at encoding. Later, they performed an episodic memory test with retrieval cues centered on the screen. Successful retrieval showed reactivation at 100-200ms characterized by a lateralized alpha/beta (10 – 25 Hz) power decrease in the visual cortex contralateral to the visual field activated at encoding (Waldhauser *et al*. (2016)).

Recently in 2019, researchers attempted to decode the content of retrieved memories in the EEG during sleep. For this, participants learned to associate spatial locations of visual objects using their left or right hand while presented with cue sounds. Later, during sleep, subjects were presented with half of the sounds associated during learning. Then authors trained a classifier using the sleep EEG data to predict learning content (focusing on lateralization). Results show a significant above-chance performance of the classifier and predicted memory performance of the participants. Specifically, they observed lateralized increased spindle power after cue presentation of successfully remembered items (Wang *et al*. (2019)).

More recently, the study of (Bar *et al*. (2020)), in which volunteers learned to associate words with left or right visual field locations cued while presented with an odor and later during sleep were presented with the odor to one nostril only, showed a local modulation of local (hemispheric) features of memory reactivation. For example, the EEG showed earlier lateralized activity. Overall, the results show robust lateralization in the EEG during the task that increases with a learning progression, supporting unihemispheric memory processes.

CHAPTER 2

Objectives

2.1 General objective

To provide a deeper understanding of the role of specific Spatio-temporal patterns of brain states of memory reactivations in the consolidation of declarative memories in wakefulness and sleep.

2.2 Specific objectives

- To characterize experimentally and computationally the spatio-temporal patterns of declarative memory reactivations in SWS sleep stages by odor cues, and to determine the relation between specific reactivation patterns and the subsequent performance of declarative memory recall in wakefulness.
- To develop a pattern classifier based on EEG signals that would be designed to identify brain states of memory reactivations during sleep.
- To identify the correlation between the spatio-temporal brain patterns of memory reactivation and the classifier performance with the consolidation effect during sleep measured by the post sleep memory performance.

CHAPTER 3

Hypotheses

- Brain activation patterns corresponding to declarative memory encoding during wakefulness, in the presence of a discriminating cue, are reactivated in SWS when the discriminating cue is presented again in sleep evidenced in memory improvement after sleep.
- It is expected that the memory representation of the declarative memory reactivations in SWS relate to ongoing EEG activity in terms of reactivation-contingent neural spindles (11-15 Hz) and slow waves (0.5 - 4 Hz).
- Specific temporal and oscillatory features selection can help improve the pattern classifier accuracy to identify memory reactivations.
- The classifier accuracy to detect memory reactivations will correlate with the post sleep memory performance.

CHAPTER 4

Methodology

4.1 EXPERIMENTAL DESIGN

The recordings have been done under Prof. Jan Born and Dr. Susanne Diekelmann at the Department of Medical Psychology and Behavioral Neurobiology at the University of Tübingen, Germany. The experimental design was developed by Dr. Jens G. Klinzing. Data were collected by Dr. med. Svenja Hinrichs. The study was approved by the ethics committee of the medical faculty and the University Clinic Tübingen (project no .: 072 / 2015BO2).

4.1.1 *Experimental paradigm*

Figure 4.1 shows a scheme of the general experimental design. Selected participants were invited for three overnight sessions (Night 0, Night 1, and Night 2) and an MRI scan session. Night 0 and 1 were separated by 1-14 nights at their home, Night 1 and 2 by 14-28 days. Night 0 was used as a conditioning night in order to allow the subject to get familiar with sleeping using the entire equipment. Participants did not perform any tasks and were not presented with an odor during Night 0. They merely wore the mask and the EEG system to habituate to the laboratory setting.

After the subjects completed both acclimatization night (Night 0) and MRI scan session, they participated in the two experimental nights. During Nights 1 and 2, participants first performed a finger-tapping Random Reaction Time Task (RRTT) while being stimulated with an odor fragrance defined as the "Motor task associated odor" or “Odor M”. Two hours after the RRTT, participants learned a declarative memory task while being intermittently stimulated with an odor fragrance defined as the "Declarative task associahttps://www.overleaf.com/project/629201a2886fed0d63c33570ted odor" or “Odor D” via a face mask allowing controlled delivery of fragrances. Resting-state electroencephalographic recordings (EEG) of 10 minutes were performed before and after the learning. After the second resting-state recording, participants went to

sleep and were presented with either of the two previously presented odors during Slow Wave Sleep (SWS). The presentation of Odor D and Odor M was randomized, such that half of the subjects received odor M on the first night and odor D on the second night and vice versa (balanced crossover design). Once participants had slept for a maximum of 100 minutes and received the minimum number of stimulations (80 stimulations), the subjects were woken up. After waking up, a film was shown during a 30-minute break interval to shake off sleep inertia before the subjects learned an interference task (without odor). This was followed by another 45-minute break interval with film before the recall test of the declarative memory task. Finally, a last resting-state recording was performed.

The study began at 7:30 p.m. with an odor familiarization phase in a separate room, followed by the RRTT. Around 8:15 p.m., the EEG cap was put on. Around 10:30 p.m. the first resting state was performed. The subjects went to bed around 11:30 p.m. The experiment ended between 2:00 and 4:00 am. The subjects slept for the remaining hours without EEG monitoring and without further tests.

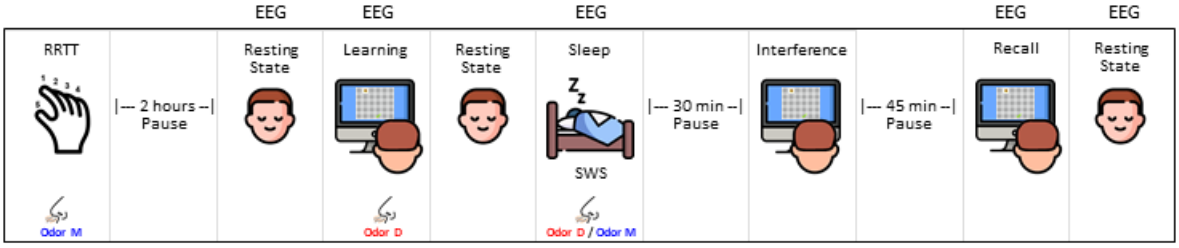

FIGURE 4.1: After the preparatory phase, a two-dimensional object localization task was learned with an olfactory presentation. In the subsequent sleep phase, in SWS (S3/4), stimulation was again carried out with odor (condition Odor D: Declarative task associated odor; condition Odor M: motor task associated odor). The subsequent break interval was followed by learning an interference task and a final test without any further odor presentation.

4.1.2 *Participants*

Participants between 19 and 25 years of age were recruited on a voluntary basis, based on their health history and sleep habits. Exclusion criteria of the former were smoking, a diagnosed psychiatric disorder, ongoing medication, and a body-mass index (BMI) lower than 25. Exclusion criteria in relation to sleep habits were a normal sleep-wake rhythm (going to bed between 22:00 and 1:00 a.m. and getting up between 6:00 a.m.

and 9:00 a.m.) as well as the waiver of shift work. On the days of the experiment, naps, alcohol, excessive exercise, or extreme stress, as well as caffeine after 2 p.m. were forbidden. After drop out due to poor sleep quality, a total of 23 subjects were taken into account for data analysis (11 men and 12 women) aged 19 to 25 years (22.17 ± 0.41 years; mean ± standard error (SEM)). In the beginning, all subjects were informed in detail and consented in writing to take part in the study. Each participant also received compensation of up to 170 euros. A total of 52 subjects participated in the study. The reasons for exclusion of recorded subjects (n = 29) were: Not enough deep sleep (n = 14), termination of the experiment for personal or temporal reasons in the MRI recording (n = 4), sleepless acclimatization night (n = 3), illness (n = 3), insufficient learning performance (at least 60 % correctly reproduced positions) in the learning test after 5 repetitions (n = 2), exceeding the maximum sleep time of 60 minutes (n = 1), technical problems (n = 2).

4.1.3 *Random Reaction Time Task RRTT*

The "Random Reaction Time Task" is a reaction and attention task in which the displayed key must be pressed as quickly as possible. The task is similar to the classic "Serial Reaction Time Task", but without repeated patterns, (ie the order of the keys to be pressed was random). A kind of piano keyboard appeared on the computer monitor with four keys that alternately turned black. The subjects placed the four fingers of their leading hand (thumb excluded) on the appropriate keys on the computer keyboard and were asked to press the correct displayed key as quickly as possible. When defective pressing the subject was given feedback in the form of red illuminated keys. The test lasted five minutes twice, with a short break of a self-selected length. During the entire test, all six keystrokes were stimulated with the motor-associated odor. There were no learnable sequences in the key sequences. The goal of the RRTT was only the familiarization of the participants with the motor-associated odor that is then presented during SWS (if applying for that night) to avoid a nuisance by an unknown stimulus.

4.1.4 *Declarative memory task*

The memory task consisted of an object-localization memory task adapted from the social game "Concentration" or "Memory". The task involved 15 card pairs for a total of 30 cards being hidden at first as gray squares in a 5 x 6 matrix defined as the "default game state".

Two sets of cards were used for the task with different images but the same type of content (which showed colorful everyday motifs such as animals or cars). In the two experimental nights, different pictures, motives and positions were used. Card positions inside each version were the same for all participants. In a randomized way, one of the versions was presented to the participants on Night 1 while the other was presented on Night 2. In the interference version of the task, the second card of each pair was located at a different position than in the main version of the task. Comparable tasks: (Diekelmann *et al*. (2012); Rasch and Born (2007); Klinzing *et al*. (2016))

Learning — Before going to sleep in Nights 1 and 2, participants learned one version of the task. For this, in two sequences of 15 card pair presentations, after the default game state, one card turned face up showing the image for 1 second before the corresponding card turned up for 3 additional seconds. Afterward, cards were turned over, and after another 3 seconds, the next card pair was presented in the same way. Each pair of cards was presented twice (see Figure 4.2A).

Right after observing the location of each pair of images twice, subjects performed the task themselves. For this, after the default game state, one card was turned up and the subject had to locate and click on the back of the second corresponding card. Upon correct selection of the card, a green tick image appeared on the back of the corresponding image for 1 second. Upon a wrong answer, a red cross appeared on the back of the selected card for 1 second. Regardless of the correctness of the clicked card, both cards (the second one being the correct corresponding card) were turned up for 3 additional seconds after the red cross or green check appeared before returning to the default game position (see 4.2B). During one run of the task, each type of image has been presented once. The run was repeated when after 15 trials, the subject had

a score of correct answers below 60% (learn test). After achieving more than 60% of correct responses, subjects are considered to have learned the task and were allowed to go to sleep.

FIGURE 4.2: **Memory task.**

Interference task — The interference task was intended to test the stability of the memory of the learning task, which is why the same memory structure was used with the same 15 pairs of images. This time, however, the position of the second card of a pair was changed according to the interference scheme AB, AC (A, B, C correspond to spatial localization) see (Diekelmann *et al*. (2012)). Again, the test subjects had two learning rounds, but this time the learning was only followed by one direct round of questions (regardless of the performance). During the interference memory, the subjects wore the odor mask, but no odor was applied.

Post-sleep performance measurement (recall test) — 45 minutes after interference, participants performed once again a unique run of the original task learned before sleep, but without repetitions of the run based on correct and wrong answers and without the feedback of correct and wrong answers for each trial. In the end only the total accuracy was displayed

4.1.5 *Odor delivery*

Two odors were used: Citral (C83007, Merck Sigma Aldrich) and Isobutyraldehyde (abbrev. IBA, 240788, Merck Sigma Aldrich). The odors were neutral, in that they do not have any reported psychotropic effect and had been assessed with intermediate valence ratings.

Odors were delivered through PTFE Teflon tubes of >4 mm of inner diameter (ID). Tubes were connected on one end to an air pump and on the other end to a 12-channel olfactometer. The olfactometer was built by Dr. Christine Barner based on Rasch *et al*. (2007) and instructions found in Lorig (2000). It allowed controlling airflow through different outlets that could be opened and closed via E-prime software. Each outlet was connected to a tube of 4 mm ID. Each tube on the other end reached into a bottle (Duran, 218012417) via a cap with a GL45 aperture and a gas washing system (Duran, 292271007) containing IBA or Citral diluted in Propanediol (134368, Merck Sigma Aldrich) to a final concentration of 12 L/mL and 24 L/mL, respectively. For a negative control condition called “vehicle”, a bottle containing Propanediol alone was prepared as well. Lastly, a bottle without liquid (referring to the "air bottle") was

prepared to allow continuous airflow outside of odor stimulation sequences. Outlets of bottles then converged into one tube reaching a nasal mask (ComfortGel Blue, Philips). The distance between bottles and the nasal mask was kept at 1.5 m in order to minimize the travel time of the odors to the participant. All important event time points were registered in the EEG recordings.

Each type of task (declarative and motor) and each version of the task has been paired to one odor in a randomized way. The pairing was achieved during the learning of the tasks by presenting odors in an event-locked manner: When the first card was faced up, the outlet opening on the olfactometer was switched to odor and switched back to air when the first and second card was turning down again as shown in Figure 4.2.

4.1.6 *Overnight odor stimulation*

During sleep, participants received a constant airflow of 6.7 NL/min of air. Upon Slow Wave Sleep (SWS) detection, participants were presented with one odor in alternating windows of 15s of air and vehicle presentation as shown in Box 1. Odor stimulation commenced after the detection of the initialization of the stable SWS period (specified as > 20% of slow waves in a 30s time window for at least 2 min) and stopped when participants shifted from SWS to another sleep stage or woke up.

...→Odor → Air→ Vehicle → Air → ... 15s 15s 15s 15s
Box 1. The sequence of stimulation during SWS. This sequence is repeated in a cyclic way until the subject switches to a different sleep stage. Once SWS appears again, the stimulation is repeated.

4.1.7 *Electrophysiological recordings*

The EEG data was acquired with a 128-electrode high-density EEG (Electrical Geodesics Inc., Eugene, United States) with a sampling rate of 1000 Hz and referenced to the mastoids (mean value from both mastoids). In addition, an electromyogram (EMG) and an electrooculogram (EOG) with a bipolar lead were recorded. For the

polysomnography evaluation, C3 and C4 (according to the international 10-20 system, filtered between 0.3 and 35 Hz and with a reduced sampling rate of 200 Hz), as well as the EMG and EOG were used.

4.1.8 *Brain anatomy recordings*

Anatomies have been acquired in a MAGNETOM prism shape scanner (Siemens Healthcare GmbH, Erlangen, Germany), with a 20- channel head coil, and MPRAGE GRAPPA sequence (176 layers; voxel size: 1.0 x 1.0 x 1.0 mm3 ; Field of view (FoV / read) = 256 mm; Repetition time (TR) = 2.3 s; Echo time (TE) = 4.18 ms; Inversion time (Engl. Inversion time (TI)) = 900ms) used. For this purpose, the test subjects were again informed in detail orally and in writing form about the risks and side effects. They were asked explicitly about possible metal in the body and it was ensured that all answered negatively.

Anatomies were recorded as DICOM files. and transformed into NIfTI using the Matlab function 'dicm2nii (xiangruili/dicm2nii - File Exchange - MATLAB Central, 2021). Afterward, the NIfTI images were bias-corrected using SPM12's segmentation function and a custom MATLAB script. These bias-corrected anatomies were used for electrode localization and for creating individual forward models for source reconstruction.

4.2 DATA ANALYSIS

4.2.1 *Sleep scoring*

Offline Sleep Scoring was evaluated in SchlafAUS software (Unpublished, non-commercial software programmed by Dr. Steffen Gais), According to the standard criteria of Rechtschaffen and Kales (1968). Each 30-s epoch was labeled with one of the following labels: Awake (W), Stage 1, 2, 3, or 4 (S1-S4), REM (rapid eye movement) sleep (R), Movement Time (MT). "Awake" was marked when more than 50% activity corresponded to alpha or mixed frequencies in low amplitudes, plus high EMG / EOG activity. S1 was marked when less than 50% activity corresponded to alpha, and no spindles or K complexes were seen. S2 was marked once spindles or K complexes

are seen and/or slow waves with amplitudes higher than 75 V and longer than 0.5s. S3 was marked when slow waves are seen from 20% to 50% of the 30-sec epoch. S4 was marked when more than 50% of activity corresponded to slow waves. REM was marked in epochs with low EMG, no slow waves, rapid eye movements. MT was marked in epochs with more than 50% movement (noise) and was marked only between two sleep epochs; otherwise, it was marked as awake. The hypnograms were generated with SchlafAUS and exported from .sls to .txt.

4.2.2 *Behavioral data*

During the learning period and after images were presented twice, subjects completed the encoding of images location by "playing" the game. Each run was repeated until after 15 trials, the subject had a score of correct answers below 60%. The number of correct responses was identified per run, per subject. After achieving more than 60% of correct responses, subjects are considered to have learned the task and were allowed to go to sleep. The percentage of correct responses in the last run represents the accuracy of learned paired locations before going to sleep. After sleep, participants were tested in a unique run of the task, without repetitions of the run, as explained in section 1.1.3. The percentage of correct responses represents the accuracy of recalled paired locations after sleep. The performance of the subjects was measured by comparing the accuracy of recalled paired locations (recall test) versus the accuracy of learned paired locations before going to sleep (learn lest) as a percentage: Recall Test / Learn Test *100.

4.2.3 *Pre-processing of EEG recordings*

For all EEG analyses, custom MATLAB scripts were combined with functions from the EEGLAB toolbox (version 2019.1). As a first step, to remove noise for power analysis, the EEG signal was filtered with EEGLAB's bandpass FIR filter with inbuilt phase-shift correction between 0.1 and 45 Hz. Then, we selected only the time periods scored as NREM sleep excluding stage 1 of sleep. Noisy channels and artifact periods were removed (6.88 ± 6.15%); the electrodes located in the face were removed as

well. In the next step, data were re-referenced to the mastoids. Noisy channels were recreated by spherical interpolation of neighboring channels. The signal was down-sampled to 200Hz and finally divided into epochs. All the ensuing EEG analyses were conducted on the resulting data after these pre-processing steps.

4.2.4 *Definition of clusters of channels*

For the analysis of activity by brain cortical regions, clusters of channels were predefined as shown in Figure 4.3.

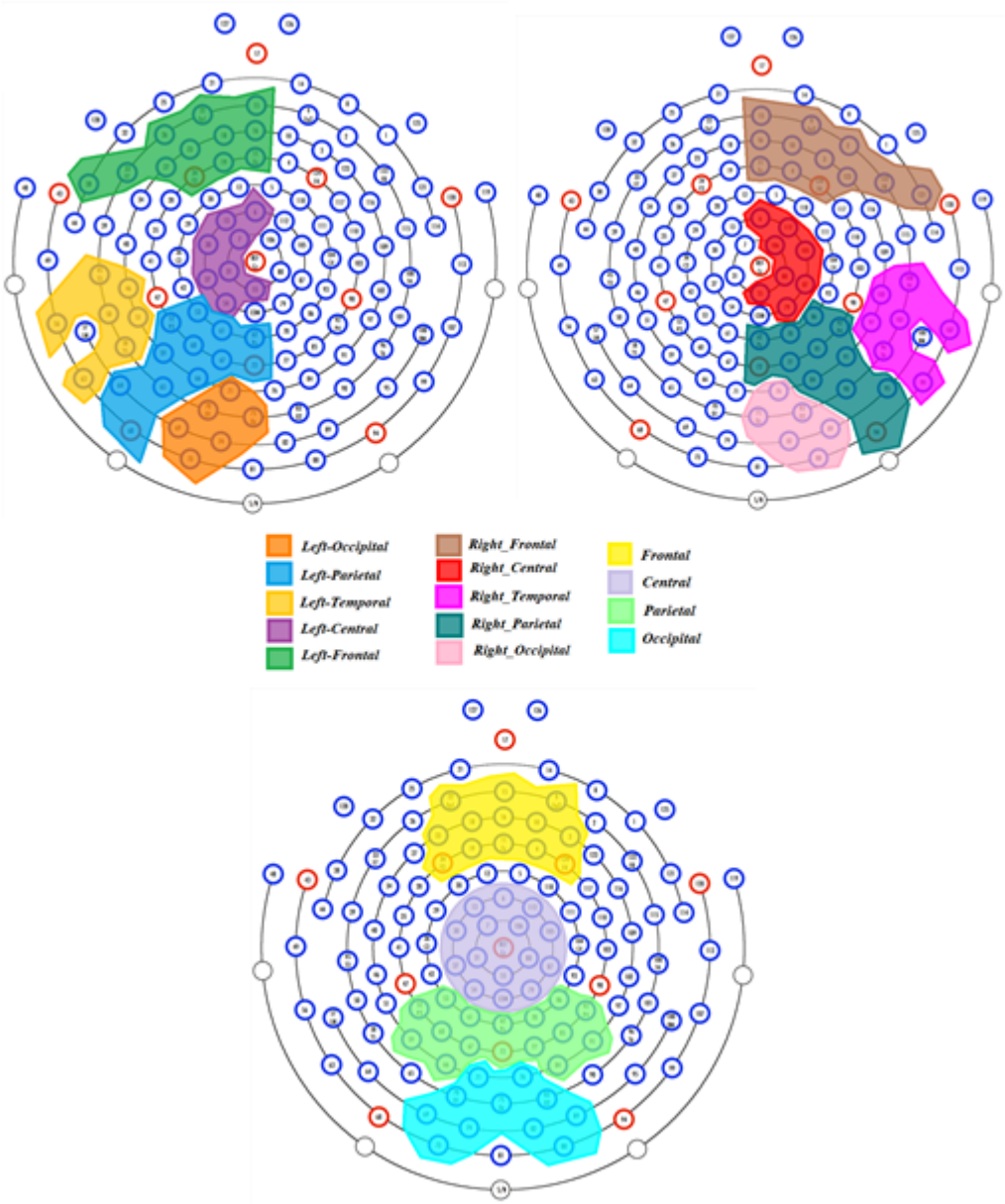

FIGURE 4.3: **Defined clusters of channels**

4.2.5 *Events detection*

SLOW OSCILLATIONS (SO) — Individual SO events were detected automatically using a custom script based on the spectral content and duration of delta oscillations and using an established detection algorithm based on (Klinzing *et al*. (2016)). In each channel separately, the EEG signal was band-pass filtered to the delta frequency range (0.5 - 4 Hz) using a zero-phase filter (an example of a resulting filtered signal is shown

in Figure 4.4). Negative and positive signal domains were identified by detection of zero-crossings on the mean amplitude of negative throws as well as the mean peak-to-peak amplitudes between negative and positive signal half-waves. We defined SO as oscillations two subsequent positive-to-negative zero-crossings and overpassing two amplitude-based thresholds: Negative half-waves with negative throws 1.1 times larger than the mean negative throw amplitude as well as oscillations with a peak-to-peak amplitude of at least 1.1 times the mean peak-to-peak amplitude were defined as SO candidates. The selected periods were later evaluated for the duration criteria. Only SO candidates with consecutive positive-to-negative zero-crossings separated by 0.8 to 2 seconds were considered Slow Oscillations (as marked in green in Figure 4.4).

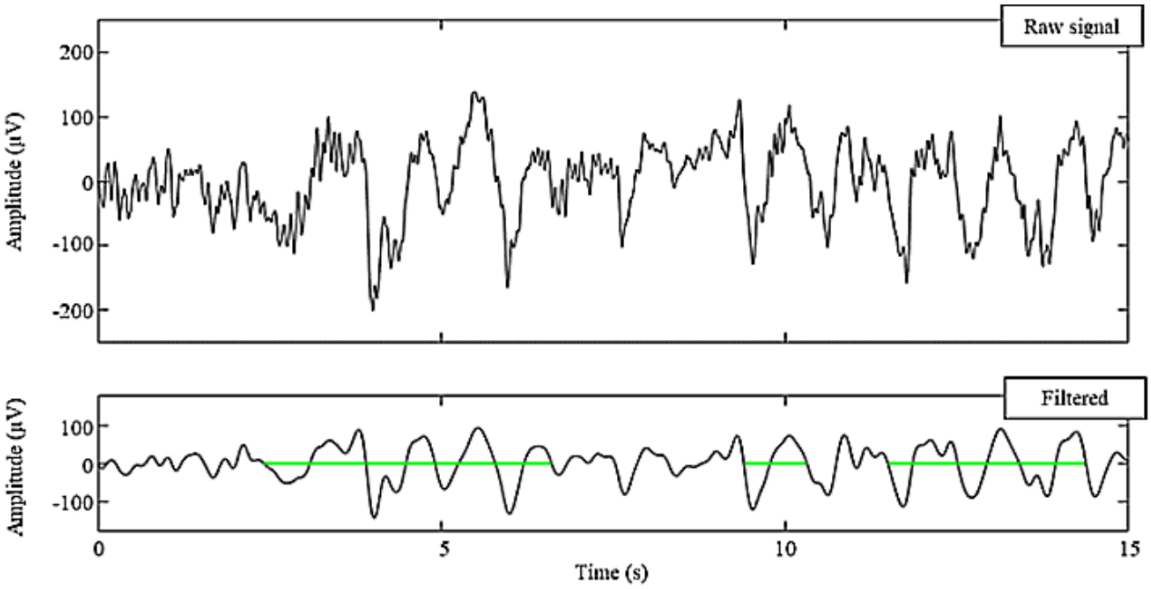

FIGURE 4.4: The top image shows an example of an epoched raw signal. The bottom plot shows the same piece of the signal filtered in the delta frequency range (0.5 - 4 Hz). Detected periods of SO are marked in green

SLEEP SPINDLES — Sleep spindles were identified from subjects' individual beta band peaks (Purcell *et al*. (2017)). Fast spindle peaks (mean = 13.79 Hz, std = 0.38 Hz, across all subjects) were calculated in the central electrodes for each subject separating fractal and oscillatory components of the whole pre-processed signal (NREM excluding S1) using Irregular Resampling Auto-Spectral Analysis (IRASA) (Wen and Liu (2016)) implemented in Fieldtrip Toolbox (Oostenveld *et al*. (2011)). Figure 4.5 shows an example of sleep spindle peaks for central (usually located in the fast spindle

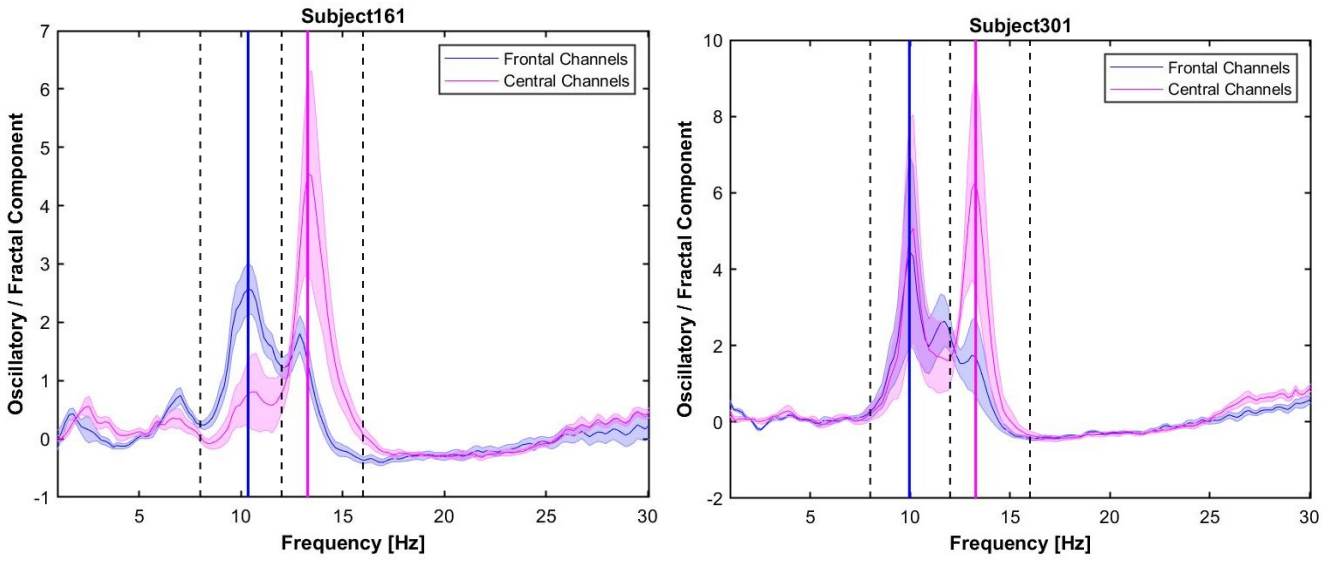

FIGURE 4.5: **Example of individual peak calculation using IRASA**

range) and frontal (usually located in the slow spindle range) electrodes. Discrete fast spindles were detected channel by channel automatically using a MATLAB custom script based on methods described in (Klinzing *et al*. (2016)). First, the EEG signal was filtered with a band-pass width of 3 Hz centered around the detected individual peak frequency (±1.5Hz). The signal envelope was calculated with a root-mean-square (RMS) representation of the filtered signal using a sliding window of 0.2 s with a step size of one sample. Additional smoothing was performed with a sliding-window average of the same 0.2s size. Time frames were considered as spindle intervals if the RMS signal exceeded a threshold set at mean + std of the RMS signal of the whole pre-processed data. Events with a duration between 0.5 s and 3 s were considered for further analysis (i.e. events marked in red/green in Figure 4.6). Final spindle event detection was performed using second amplitude thresholding, assuring that selected events were following bell-like shapes (as shown in Figure 4.6, marked in green), established at 2.5 standard deviations from the mean RMS signal. Only waves surpassing the second threshold were considered spindles. See Figure 4.6.

EVENTS' FEATURE EXTRACTION AND VALIDATION — For SO and spindles we extracted different features per event, such as: Start time: first up-down zero crossing Middle time: down-up zero crossing End time: spindle: negative zero crossing Dura-

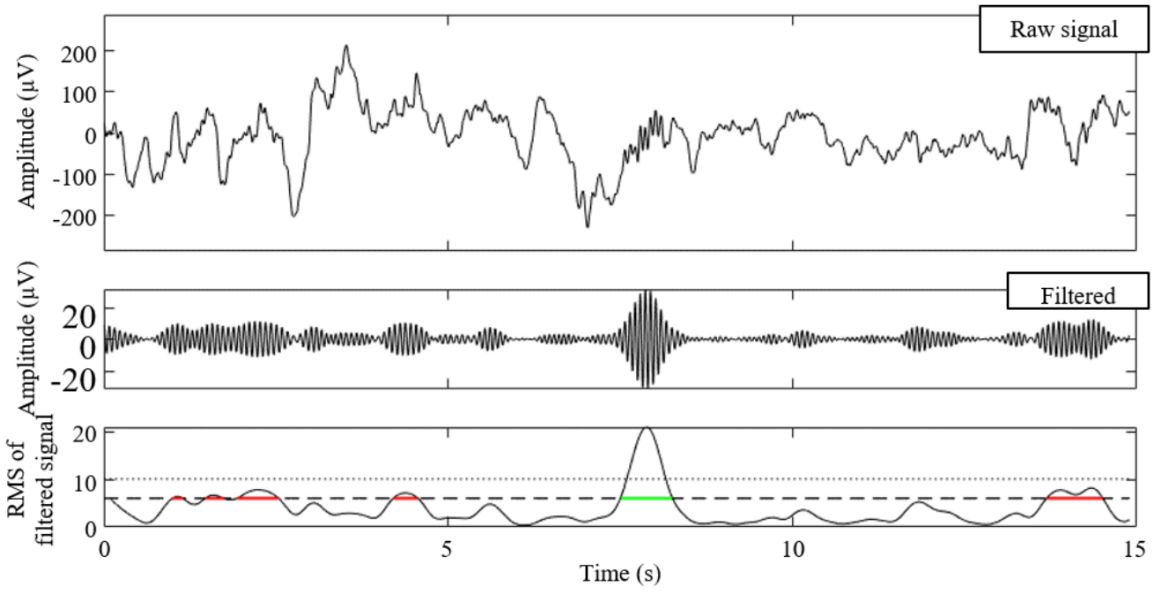

FIGURE 4.6: **Spindle detection example**

tion: duration from start to end in seconds Maximum time: time of maximum peak (upstate) Minimum time: time of minimum peak (downstate) Minimum amplitude: amplitude of minimum (upstate) in uV Maximum amplitude: amplitude of maximum (downstate) in uV Peak to peak amplitude Peak to peak time: time in seconds from peak-to-peak.

Overall, spindles and slow oscillations were evaluated in a seven-step and six-step process respectively. 1. Topographic distribution of the density of detected events, 2. Occurrence of events along hypnogram to see a general trend of sleep/wake-dependent detection by the algorithm as well as the trend in the power of the events during recording, 3. Average waveform 4. Time-frequency decomposition of the raw signal during S2-S4, 5. A number of events per time spent in each sleep/wake stage, 6. Occurrence of spindles in concert with slow oscillations (phase-coupling according to the maximum peak of their RMS representation) in S2-S4 sleep and 7. The symmetry of detected events of S2-S4 stages in order to assure that detected spindles follows a bell-like shape with the maximum peak of their RMS representation located around the event's midpoint. Slow oscillations were evaluated the same way except for symmetry.

4.2.6 *Events-coupling: spindles and SO*

For detecting the SO phase at which sleep spindles occur, we used the subset of SO events detected. For each channel, we band-pass filtered (using a zero-phase filter between 0.5 and 2Hz) the signal, computed then the Hilbert transformation, and extracted the phase angle at each point in time of SO events. Sleep spindles that occur during SO were identified in the next step. For this, we coupled the timestamp of the maximum amplitude of the spindle RMS signal, to the phase of the SO they correspond to.

We used the circ_stat toolbox from (Berens (2009)) to determine the preferred phase of occurrence of spindles during slow oscillations in Odor and Vehicle conditions. We then determined the shift in the SO phase at which spindles occur by taking the difference between the condition's preferred phase from the mean of preferred phases over conditions.

4.2.7 *Spectral analysis of spindles around SO*

Spectral analysis has been performed on 4s time windows of SO events centered around SO inflection phase time point using Morlet wavelets of 12 cycles. The range of frequencies to analyze was centered around each individual fast-spindle peak using a bandwidth of 10Hz (±5Hz) in steps of 0.05 Hz and including all time points. The corresponding time-frequency response was normalized to the complete event using z-score approximation. Events spectrum was averaged across events for each channel and for each condition (odor and vehicle) per subject and finally, a cluster permutation-based analysis was performed to identify differences in the spectrum for SO-spindles complexes at each condition (see statistical analysis section).

4.2.8 *Time-frequency analysis*

Time-frequency analysis applying Morlet wavelets was implemented in a customized script using functions of Fieldtrip toolbox (Oostenveld *et al*. (2011)) as follows: For each channel separately, we extracted the epochs of Odor and vehicle presentation (Sequence of one complete epoch corresponds to Off (Air) - Odor On - Off (Air) -

Vehicle On - Off (Air)). Wavelet analysis was performed using steps of 0.1 seconds and frequency intervals of 0.5 to 30 Hz in steps of 0.15 Hz (196 bins) and 12 cycles. For each frequency bin, we normalized the data epoch by epoch using Z-scores in relation to the complete epoch to reduce artifact effects on the results as suggested in (Grandchamp and Delorme (2011)). Time-frequency response was then epoched around odor and around the vehicle separately (5 seconds Off (Air) before odor/vehicle onset and 25sec after odor/vehicle onset: 15 sec "On" and 10 sec Off (Air)). We included the period after the odor/vehicle is switched off to incorporate possible lasting effects of the odor when switched off. Then, for each channel separately, we took the mean normalized power across all epochs (odor and vehicle independently). To further quantify the modulation in power as a result of odor cues and to compare this modulation between conditions, we evaluated the power in the frequency bands of interest: SW range (0.5-2Hz), delta (1-4Hz), theta (4-8Hz) and fast spindle range (12-16Hz).

4.2.9 *Multivariate Pattern analysis: Machine learning classification for multidimensional data*

Classification using "Raw" signal — Multivariate Pattern analysis was performed using classification to compare conditions with a customized MATLAB script and the MPVA-light toolbox functions (Treder (2020)). For this purpose, kernel SVM, k-fold cross-validation (k=5), 10 cross-validations, and z-score preprocessing were performed on different classification approaches using "Raw" signal (preprocessed data obtained as described in the pre-processing section):

- Subject-dependent (individual accuracies per subject) and subject independent (one global accuracy based on the combined data of all subjects).
- Classification either using all channels as features or individual classification channel by channel, obtaining a topographical distribution of accuracies.
- Classification by time segments after odor stimulation onset, to identify if a specific period of time in the epoch predicts for differences given by declarative memory consolidation.

- Classification around SO, spindles, and SO-spindle complexes, to restrict the information given to the classifier according to the specific events shown to be relevant to memory reactivation.

Classification using Filter Bank Common Spatial Pattern (FBCSP) — Filter Bank Common Spatial Pattern (FBCSP) based on (Ray *et al*. (2015)) was applied to the preprocessed EEG data, in order to perform classification to automatic feature extraction from the data separating conditions based on their frequency and spatial behavior. Subject-dependent classification was performed, for complete Odor/Vehicle periods, for time segments, as well as for SO events, spindle events, and SO-spindle complexes, extracting not only the accuracy but also relevant features in frequency and topography that facilitate discrimination between conditions.

Decoding relevant frequency bands discriminating for declarative memory reactivation — For decoding the relevant frequency bands discriminating for declarative memory reactivation, we used a customized MATLAB script and the functions of the MPVA-light toolbox (Treder (2020)) to perform time-frequency classification that allowed us to answer the question: is the discriminative information of Odor D vs Vehicle confined to specific oscillatory frequencies and times? In this regard, we used the time-frequency spectra calculated for single epochs, and classification was performed at each time-frequency bin separately using kernel SVM, k-fold cross-validation (k=5), and 2 repetitions.

A generalization analysis was performed to answer the question: are representations shared across time, frequency, or channel locations? To answer this, time generalization (time x time classification), frequency generalization (frequency x frequency classification), and channel generalization (channel x channel classification) were applied to the time-frequency response at each channel. In the generalization analysis, a model is trained for each generalization element and then tested at each other element. For example, classification across time does not give insight into whether information is shared across different time points. In time generalization, this question is answered by training the classifier at a certain time point t. The classifier

is then tested at the same time point t but it is also tested at all other time points in the epoch. The same happens with the frequency dimension and with the channel dimension. The result is a 2D matrix of classification performance, with performance calculated for each combination of training points and testing points.

4.2.10 *Statistical analysis*

Sleep architecture — In order to evaluate differences in sleep architecture comparing both nights, and make sure this is not a factor affecting behavioral or electrophysiological responses, we calculated the number of epochs scored, labeled, or assigned to each sleep stage and performed a nonparametric t-test comparing the percentage of epochs in each sleep stage for Night 1 vs Night 2. Other variables compared statistically between both nights were: Sleep onset (in minutes), wake after sleep onset, arousals, and sleep efficiency, defined as the percentage of sleep after lights out. Furthermore, Pearson's r and linear regression were performed for the determination of the highest impacting factors comparing the different sleep architecture measurements mentioned, as well as the number of odor stimulations during the night to the memory performance.

Memory performance — A nonparametric t-test was used to measure the memory retention for each night, with the hypothesis of obtaining better memory performance after the night of sleep in which participants were stimulated with the declarative memory associated odor (Odor D) than the control odor (Odor M).

Event detection validation — Analysis of variance (1 way ANOVA) was performed, to compare the number of events detected per sleep stage in NREM sleep. This analysis allowed us to make sure that the spindle density is higher for sleep stage 2 and then decreases as sleep goes deeper to sleep stage 4. On the other hand, SO should increase as sleep goes deeper from S2 to S3.

Events features — Event features were compared between odor and vehicle (when switched on) periods and the significance of differences was determined using

cluster-based permutation analysis over the scalp electrodes or by parametric t-tests of event features averaged over pre-defined electrode clusters.

Time-frequency of events — We performed analyses such as time-frequency comparing stimulation with vehicle and odor ("on") periods for SO-spindle complexes. For this, we used cluster-based permutation analysis on time-frequency matrices across the scalp. Thresholds for cluster data point inclusion were set at 0.05.

Correlation of detected events and memory performance — To identify the relationship between the detected events and the memory performance, we calculated Pearson's correlation between the different features of the detected events for each condition odor conditions (odor "on", vehicle "on") and the subjects' memory performance. Furthermore, Stepwise multiple linear regression analysis was performed to answer the question of which of the variables best predict performance.

Time-Frequency — In order to identify time-frequency patterns associated with declarative memory reactivation during sleep, we compared the time-series for Odor D vs vehicle using a nonparametric bootstrap (permutation-based test) with 10000 permutations for each frequency band, and nonparametric false discovery rate correction, with an established alpha value being 0.05. This statistical analysis was calculated as well for the M night, to control for statistical differences as well between Odor M and vehicle. Finally the same was applied to compare both odor conditions directly (Odor D vs Odor M)

Correlation of classification accuracy and memory performance — Subject-dependent classification accuracy has been compared with each subject's memory performance using Pearson's correlation, in order to identify if the capacity of the classifier to identify electrophysiological differences gives also information about the behavioral outcome.

CHAPTER 5

Results

5.1 Sleep architecture and sleep quality

5.1.1 *No significant differences in sleep architecture between Cue Odor D and Cue Odor M presentation during sleep*

Figure 5.1 shows the general sleep architecture for both nights representing the percentage of time in each sleep stage according to the total time of sleep. No significant differences were observed for the general sleep architecture, especially in the SWS. S1 is the only sleep staFge reporting a significant difference between both nights, being shorter for the M Night, although this period has minimal influence on cued memory reactivation effects.

	D Night	M Night	p values
Sleep onset (min)	12.17 ± 5.84	11.89 ± 5.96	0.843
TST (min)	57.46 ± 15.79	57.41 ± 16.15	0.930
REM (%)	0 ± 0	0.41 ± 1.98	0.339
S1 (%)	6.61 ± 4.19	3.92 ± 2.36	**0.015**
S2 (%)	29.23 ± 15.00	30.36 ± 17.04	0.913
S3 (%)	26.53 ± 12.45	23.65 ± 11.95	0.442
S4 (%)	17.42 ± 15.50	22.59 ± 16.79	0.362
SWS (%)	43.95 ± 14.92	46.24 ± 14.74	0.684
WASO (%)	3.74 ± 3.45	2.35 ± 2.19	0.231
Arousals (#)	5.70 ± 5.64	6.61 ± 7.52	0.903
SE	79.80 ± 8.73	80.94 ± 9.27	0.583

FIGURE 5.1: List of sleep characteristics during TMR. NREM1-4, Non-Rapid Eye Movement sleep stages 1 to 4; REM, Rapid Eye Movement sleep; SE, Sleep efficiency; Sleep onset, the latency of first sleep score after lights out; SWS, Slow-wave sleep; TST, total sleep time; WASO, wake after sleep onset. Sleep efficiency is defined as the percentage of sleep after lights out. Values are expressed as mean ± standard deviation. Statistics were performed using a non-parametric t-test.

5.2 BEHAVIORAL DATA RESULTS

5.2.1 *No significant differences in memory performance between Cue Odor D and Cue Odor M presentation during sleep.*

We found no significant differences in memory performance for D Night as compared to M Night, which means that participants obtained the same benefit in memory consolidation either if presented with the cue odor associated with the declarative memory task (Odor D), or if presented with the non associated odor (cue odor associated with the motor task, Odor M). Figure 5.2 shows the general memory performance for both nights and the detailed performance according to memory gains or losses.

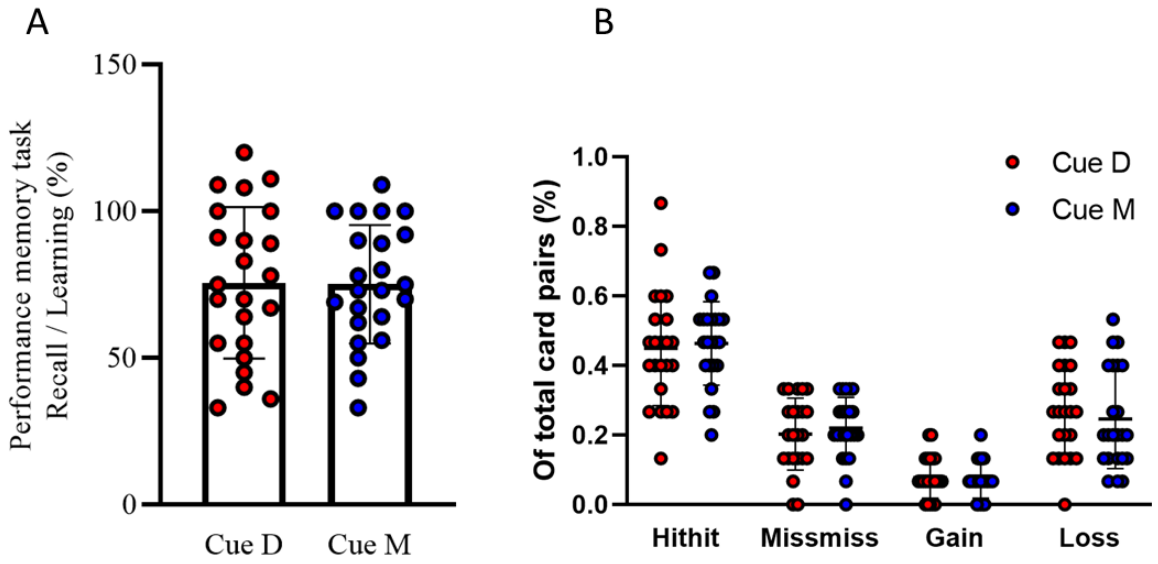

FIGURE 5.2: (A) Bar plots represent the general mean and standard deviation performance on the memory task as a measure of the percentage of the accuracy in the post-sleep test according to the subject's accuracy achieved during the learning session. Red dots indicate individual performance in D Night and blue dots indicate individual performance in M Night. Performance higher than 100% means that subjects' accuracy after sleep is higher than the accuracy before sleep. (B) Specifies in more detail the percentage of correct cards located before and after sleep (Hithit), the percentage of missing card locations before and after sleep (Missmiss), the percentage of cards that were properly located after sleep and were not correct before sleep (Gain), and the percentage of incorrect card locations after sleep that were correctly located before sleep (Loss). Dots represent individual performances for D Night (Red), and M Night (Blue).

5.2.2 *Memory performance is correlated with the number of stimulation presented during the night when presenting cue odor M, but not when presenting cue odor D.*

In Figure 5.3, the correlation between memory performance and stimulation amount is presented. We observe a significant correlation between the number of total stimulations and the memory performance for M Night, but not for D Night. Similar is

seen when calculating this correlation with the total amount of time in which subjects are stimulated with Odor. Significance improves for D Night when correlating only with valid stimulations. Odor stimulations are considered valid stimulations if they belong to a complete sequence of Odor - Vehicle trials without interruption. However, p values don't reach values below 0.05 for just valid stimulations.

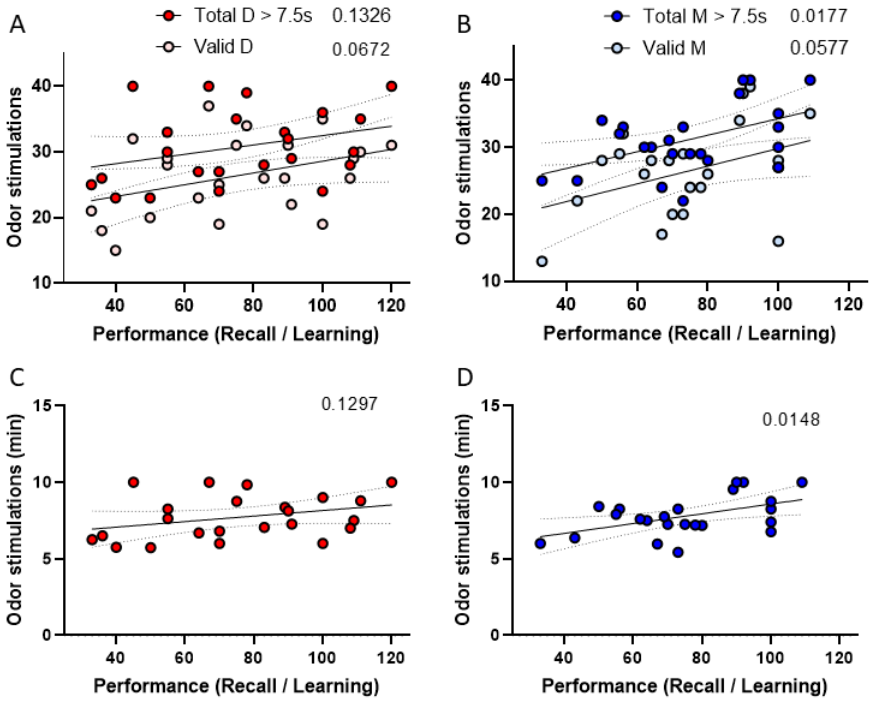

FIGURE 5.3: (A, B) shows the correlation between memory performance and the number of odor stimulations for D Night (A, red) and M Night (B, blue). Darker colors represent the total number of odor stimulations, regardless of completed sequences of odor-vehicle. Lighter colors represent the valid odor stimulations that are considered for further analysis. (C, D) show the correlation between memory performance and the total time of odor stimulation in minutes for D Night (A, red) and M Night (B, blue). Each dot indicates individual subject values for all graphs.

5.2.3 *Cue odor M can contribute to memory strength, but cue odor D stabilizes memories and prevents them from being lost or interfered with.*

When separating memory performance by Gains (Cards that were correctly located in the test post-sleep that were not in the pre-sleep learning), Losses (Cards that were correctly located during learning but were not in the post-sleep test), hithit(Cards that were correctly located during learning and in the post-sleep test), and miss miss (Cards that were never located correctly), we observe an inverse correlation between the percentage of losses and the number of stimulation for D Night that is not seen in

the M Night. On another hand, we observe a direct correlation between the number of stimulation and the percentage of hithit cards for D Night that is not occurring for M Night. M night, however, exhibits a direct correlation in the percentage of gains versus the number of odor stimulations.

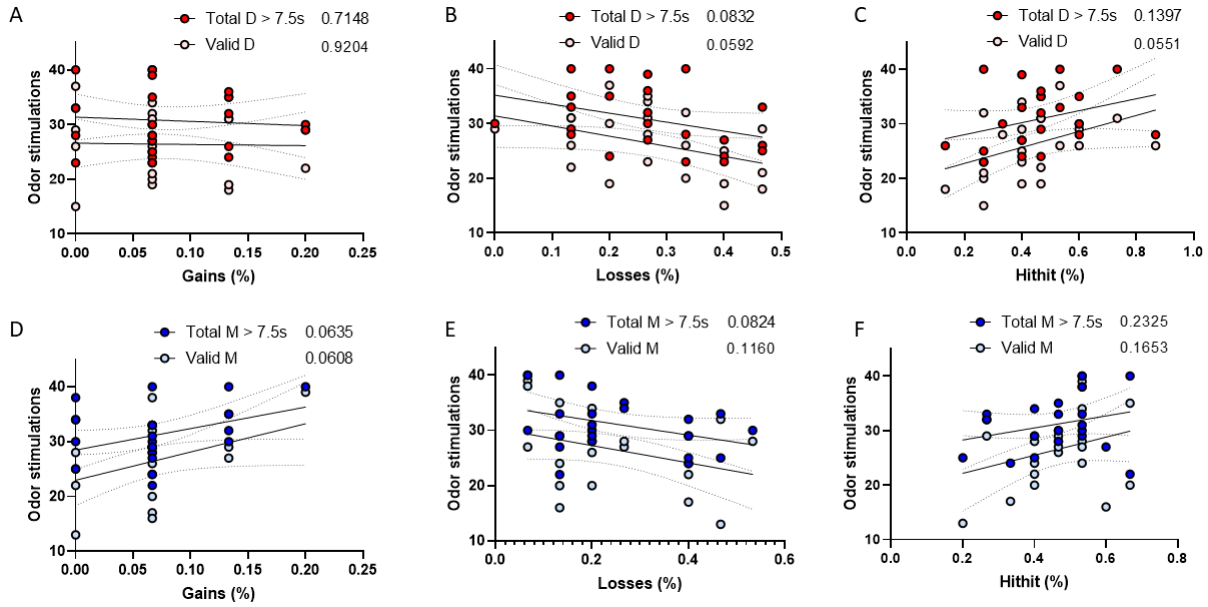

FIGURE 5.4: (A, B, C) show the correlation in D night between the number of odor stimulations and the percentage of Gains (A), Losses (B), and Hihit (C) of paired card locations. (D, E, F) show the correlation in M night between the number of odor stimulations and the percentage of Gains (D), Losses (E), and Hihit (F) of paired card locations. Darker colors represent the total number of odor stimulations, regardless of completed sequences of odor-vehicle. Lighter colors represent the valid odor stimulations that are considered for further analysis. Each dot indicates individual subject values for all graphs.

5.3 EVENT-DETECTION VALIDATION

5.3.1 *Detected SO are predominant in frontal areas, and increase in density as subjects transit to deeper NREM sleep stages*

The topographical distribution of the detected SO events shows a predominance of the events in the frontal area, being consistent with the literature. Also, the mean of the EEG data around the SO evidences a clear symmetrical oscillation. Moreover, the density of detected SO increases significantly as NREM sleep stages increase, as expected.

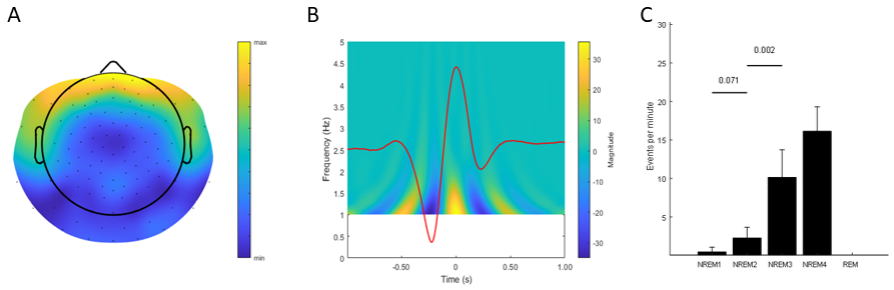

FIGURE 5.5: (A) Shows the topographical distribution of SO density over the night. (B) shows the average of all SO events detected (C) shows the mean number of detected events per minute for each sleep stage.

5.3.2 *Detected Spindles are predominant in central areas and decrease in density as subjects transit from sleep stage S2 to S4*

The topographical distribution of the detected spindle events (fast spindle) shows a predominance of the events in the central area, being consistent with the literature. Also, the mean of the EEG data around the spindle evidences a clear symmetrical oscillation. Moreover, as expected, the density of detected spindles decreases significantly as NREM sleep stages progress. Finally, Evaluation of symmetry of individual events verifies that detected spindles follow a bell-like shape with the maximum power located towards the midpoint of the events.

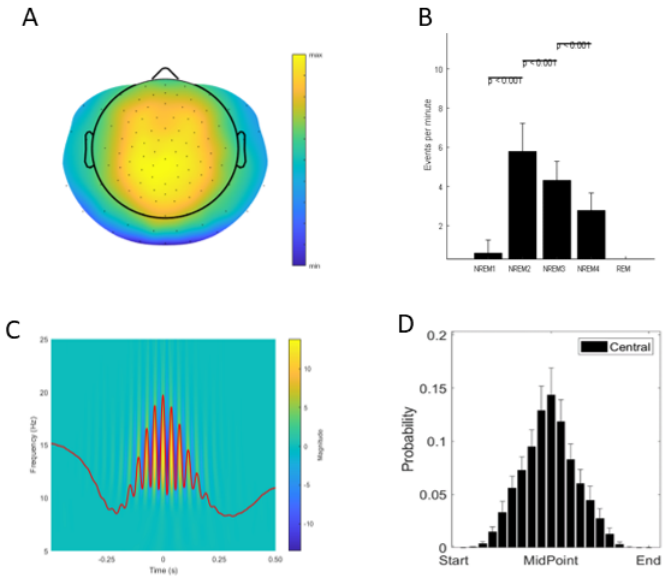

FIGURE 5.6: (A) Shows the topographical distribution of spindle density over the night. (B) Shows the average of all spindle events detected (C) Shows the mean number of detected events per minute for each sleep stage. (D) Evaluation of symmetry of individual events in order to assure they follow a bell-like shape with the maximum power located towards the midpoint of events.

5.4 EVENT COMPARISON BETWEEN CONDITIONS

5.4.1 *Significant differences for detected SO between conditions occur only for the first 7.5 seconds of odor presentation and show an increase in strength of SO for cue Odor D presentation.*

After calculating all the features for each SO detected, and comparing between odor and vehicle periods, we identified differences between the conditions only if considering the first half of the stimulation period (0 to 7.5 seconds after the odor onset). Differences were seen in the occipital lobe with a significant increase in the SO density, peak to peak amplitude, and slope for odor D presentation as compared to the vehicle condition. Moreover, the central, temporal, and parietal regions present also a significant increase in the SO peak to peak amplitude for odor D presentation. These differences are not evidenced in the odor M condition. Figure 5.7A shows the mean SO density in the right occipital region showing a significant difference for D night, but not for M night with an increase in the odor D condition. This increase happens as well in the occipital and left occipital regions (occipital: p = 0.0763 for D night, p = 0.4198 for M night. Left occipital: p = 0.0741 for D night, p = 0.4072 for M night). Figure 5.7B shows the mean SO peak to peak amplitude in the occipital region showing a significant difference for D night, but not for M night. This increase happens as well in the left and right occipital regions (left occipital: p = 0.0721 for D night, p = 0.8805 for M night. Right occipital: p = 0.0229* for D night, p = 0.5855 for M night). Figure 5.7C shows the mean SO slope in the occipital region showing a significant difference for D night, but not for M night.

Figure 5.7B shows the mean SO peak to peak amplitude in the left central, left parietal, and left temporal regions showing a significant difference for D night, but not for M night with an increase in the odor D condition. This increase happens as well in the central, parietal, and right parietal regions (central: p = 0.0798 for D night, p = 0.3246 for M night. Parietal: p = 0.0381* for D night, p = 0.5526 for M night. Right parietal: p = 0.0576 for D night, p = 0.3644 for M night).

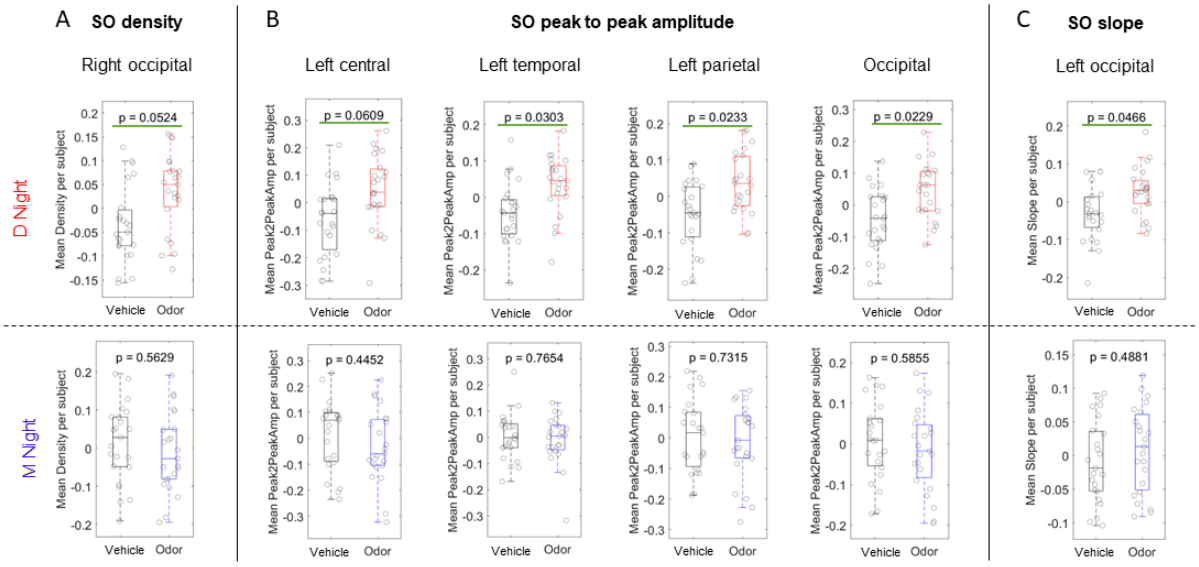

FIGURE 5.7: Changes in SO features are shown for D Night (top figures, red) and M Night (bottom figures, blue) between vehicle stimulation periods (black) and odor stimulation periods (red/blue), taking only the first 7.5 seconds of stimulation (first half). In green, periods of a significant trend are marked. Main effects were observed in SO density (A), SO peak to peak amplitude (B), and SO slope (C).

5.4.2 *Significant differences for detected Spindles between conditions occur mainly for the first 7.5 seconds of odor presentation and show an increase in strength of spindles for cue Odor D presentation*

After calculating all the features for each spindle detected, and comparing between odor and vehicle periods, we identified differences between the conditions mostly if considering the first half of the stimulation period (0 to 7.5 seconds after the odor onset). Differences were seen in the parieto-occipital region with a significant increase in the spindle density, and in the frontotemporal region with a significant increase in the spindle peak to peak amplitude. Additionally, the frontal region presents a difference in the spindle duration with a significant increase for the odor D condition. These differences are not evidenced in the odor M condition. The only significant difference observed in the complete stimulation period (0 to 15 seconds after odor onset) occurs in the left temporal region with a significant decrease in spindle peak to peak amplitude for the odor M condition in M night.

Figure 5.8A shows the mean spindle density in the right parietal and left occipital regions showing a difference for D night, but not for M night with an increase in the odor D condition. This increase trend happens as well in the left parietal and parietal

regions (left parietal: p = 0.0695 for D night, p = 0.2087 for M night. Parietal: p = 0.0229* for D night, p = 0.5855 for M night). Figure 5.8B shows the mean spindle duration in the frontal region showing a significant difference for D night, but not for M night with an increase in the odor D. This increase happens as well in the left and right frontal regions (left frontal: p = 0.0521 for D night, p = 0.0664 for M night. Right frontal: p = 0.0743 for D night, p = 0.4552 for M night). Figure 5.8C shows the mean spindle peak to peak amplitude in the frontal and left temporal regions showing a significant difference for D night, but not for M night with an increase in the odor D. This increase happens as well in the right frontal region (p = 0.0493* for D night, p = 0.7799 for M night).

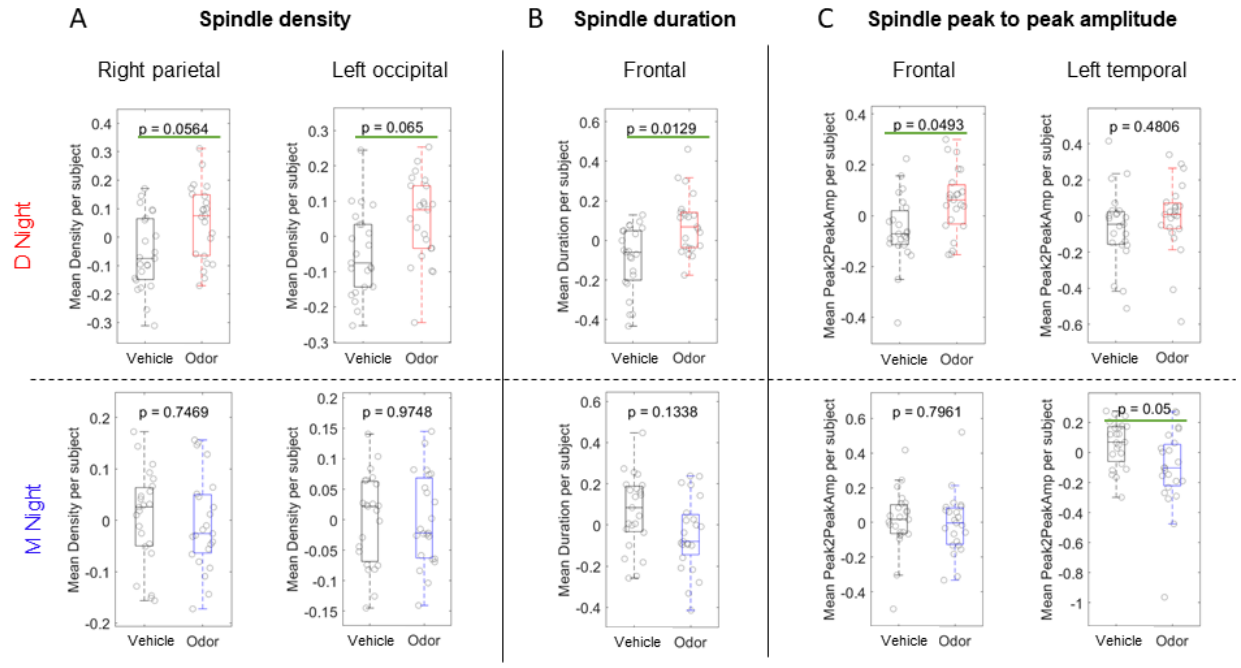

FIGURE 5.8: Changes in Spindle features are shown for D Night (top figures, red) and M Night (bottom figures, blue) between vehicle stimulation periods (black) and odor stimulation periods (red, blue), taking only the first 7.5 seconds of stimulation (first half). In green, periods of a significant trend are marked. Main effects were observed in Spindle density (A), spindle duration (B), and Spindle peak-to-peak amplitude (C).

5.4.3 *Cluster permutation-based statistics reveal a significant decrease in SO duration for right-frontal electrodes and a significant increase in SO amplitude in parieto-occipital channels during the first 7.5 seconds of odor presentation for cue odor D*

Cluster permutation-based statistics reveal a significant decrease in SO duration for right-frontal electrodes. However when calculating for the second half of odor stimulation (7.5 to 15 seconds after odor onset) there is an inverse effect in SO duration showing an increase for odor D in frontal electrodes with a p-value of 0.0608. This SO behavior occurs in D night, but not in M night.

Results also show a significant increase in SO peak to peak amplitude in parieto-occipital channels during the first 7.5 seconds of odor presentation for cue odor D. This increase is not evidenced in M Night. Finally, spindles only show a close to a significant increase in right frontocentral electrodes with a p-value of 0.0548 for odor D condition in the first 7.5 seconds of stimulation, an effect that is not evidenced in the odor M condition.

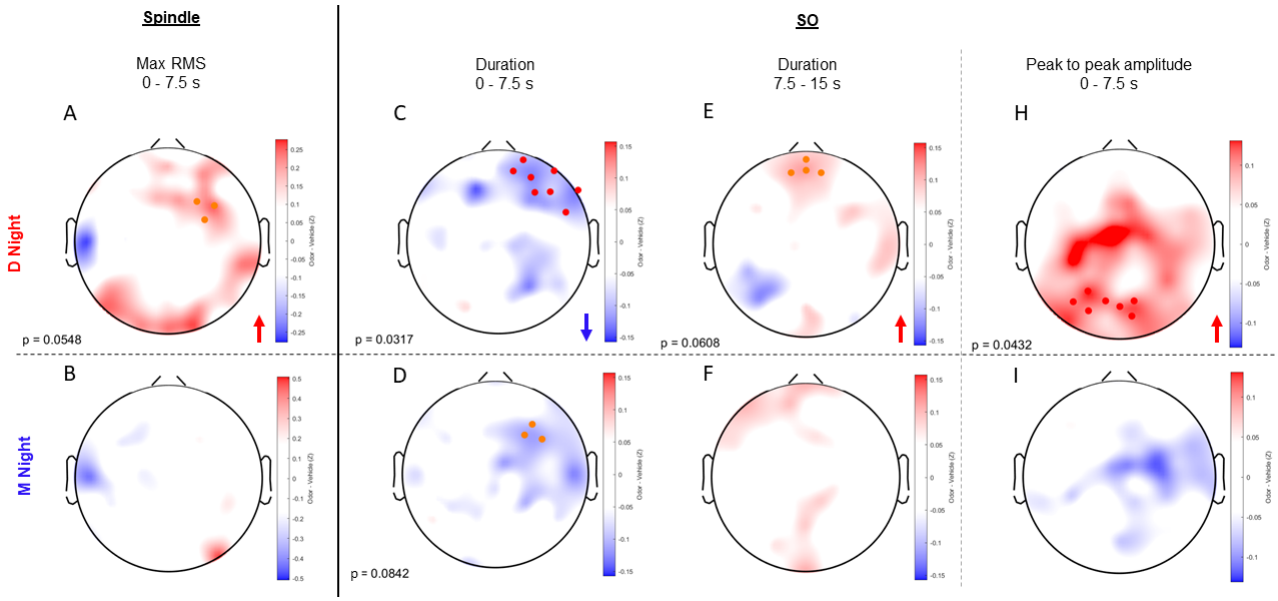

FIGURE 5.9: Topographical maps represent the difference in event features between Odor and Vehicle (Odor - Vehicle). Red dots mark clusters of channels with $p < 0.05$. Orange dots mark clusters of channels with $0.05 < p < 0.1$. Only features showing significant clusters of channels are shown.

5.5 EVENT COUPLING COMPARISON BETWEEN CONDITIONS

5.5.1 *Spindles coupled with SO present a significant shift in the preferred phase of occurrence closer to the upstate of the SO for cue Odor D in central and occipital regions as compared to the Vehicle*

Analyzing the typical phase of SOs at which sleep spindles preferentially occurred during odor-on intervals, we observed tight locking of spindles around SO up-states that are significant in central and occipital regions. In Figure 5.10 it is possible to observe the mean and standard deviation preferred SOs phase at which spindles occur.

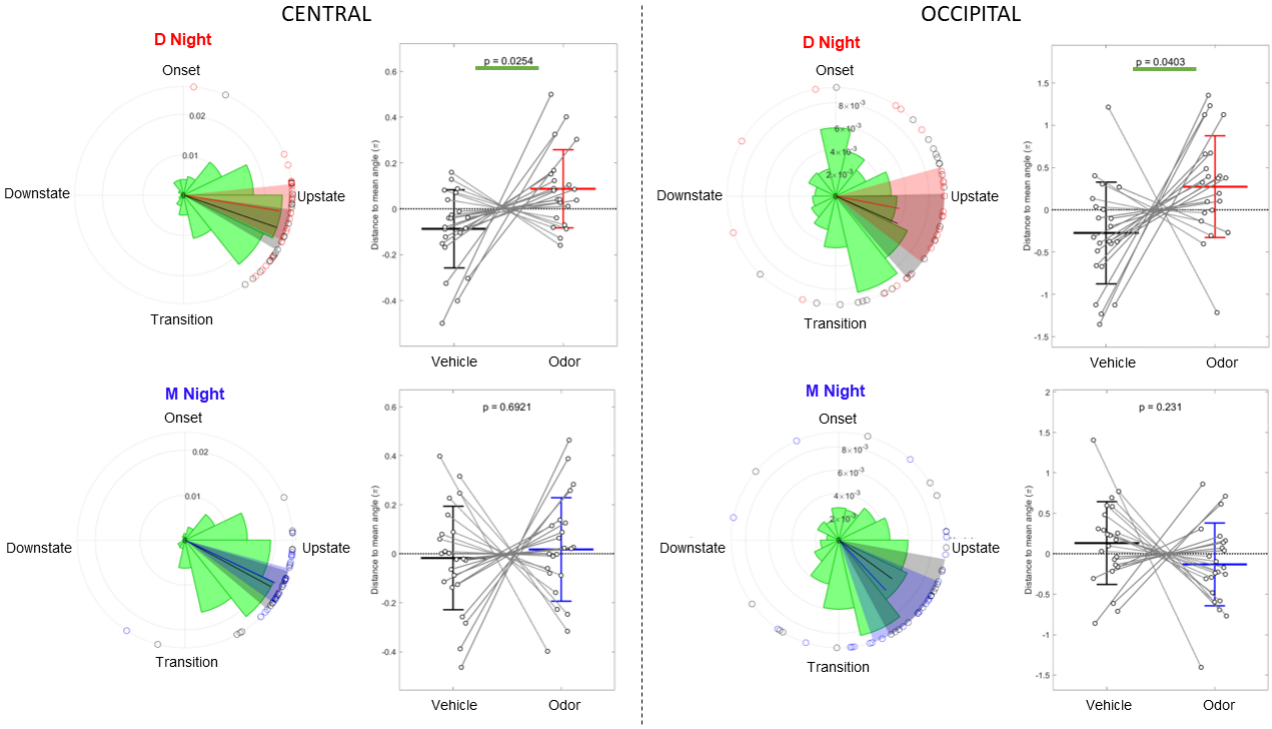

FIGURE 5.10: The coupling of spindles with SO is shown for D night (top figures, red) and M night (bottom figures, blue). Polar plots show the density of spindles occurring at each SO phase (green bars). Long lines indicate the mean of the phase at which spindles occur (preferred phase) and std is represented as the shaded area. Next to each polar plot, the mean and standard deviation of the distance to the mean angle is shown comparing the vehicle (black) and odor (red, blue) conditions. In green, p values below 0.05 are marked. Only brain cortical areas showing significant differences in the preferred phase are shown.

5.6 TIME-FREQUENCY RESPONSE

5.6.1 *The average time-frequency response shows a significant difference in spindle power after 2.5 seconds of odor onset and in the SW frequencies between 10-12 seconds and between 15-20 seconds when comparing odor versus vehicle for D night and not for M night.*

The average time-frequency response observed in Figure 5.11 shows the highest significant increase in the spindle frequency band 2.5 seconds after the odor onset versus the vehicle onset. The SW frequencies, on the other hand, show a significant decrease in power around 10 seconds after the odor onset. Furthermore, once the odor stimulation is interrupted, the vehicle (control) condition shows an increase in power for the SW band maintaining a significant difference with the Odor D condition that is decreased. All mentioned significant differences are not observed for the M night when comparing odor M vs vehicle.

It is also important to mention the increase in the SW, delta, and theta power just right after the odor onset in the odor D condition; a response that is not observed for any other condition, although for this case, it does not fulfill the significance criteria.

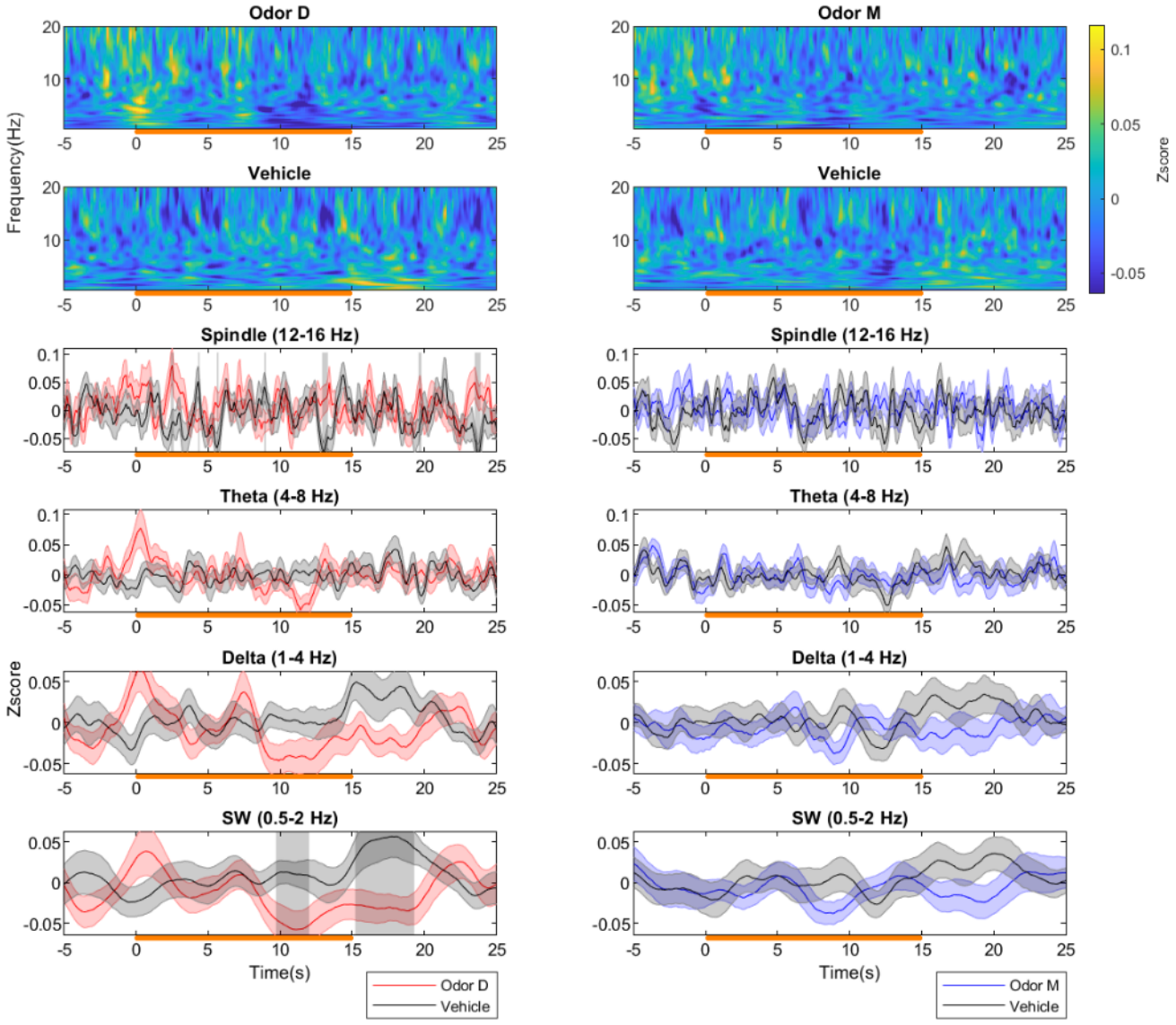

FIGURE 5.11: Time-frequency responses are shown for D night (left) and M Night (Right). TF for odor and vehicle periods are shown on top and z-scored time series of power at selected frequency bands are shown below (red for Odor D, blue for Odor M, and black for Vehicle), represented by the mean across subjects (continuous line) and SEM (shaded areas). Significant differences after a nonparametric permutation-based test and FDR correction are shown as gray transparent bars. The orange lines in the x-axis indicate the stimulation period in which the odor is released, outside this area, valves are closed allowing airflow only.

5.6.2 *The average time-frequency response by regions of interest, evidence different timing of CMR effect in different cortical areas*

When averaging the time-frequency response by clusters of channels, we evidence different timing of significant differences between conditions.

The SW frequency band shows a significant difference between odor D and vehicle first in the occipital region with a decrease in power for the odor D condition around

10 seconds until 12.5 seconds after odor onset. This significant difference is also observed in the right temporal region with a shorter duration. Moving to the parietal region, it is possible to see the same significant difference after 10 seconds, which reappears around 17 seconds with an increase in power for the vehicle condition. The frontal, central and left-temporal regions, on the other hand, show a significant difference later than the posterior region, between 15 and 20 seconds after odor onset (just right after odor termination). In this case, the increase in power for the vehicle condition is more pronounced.

The delta frequency band shows no significant difference in the occipital region, nor in the right temporal region. The left temporal, parietal, and central regions exhibit a significant difference between 15 and 20 seconds after odor onset (just right after odor termination) with an increase in power for the vehicle conditions and a decrease in power for the odor D condition. Furthermore, a significant increase around odor onset is observed very short in the left temporal and parietal regions, but more robust in the central region. Finally, the frontal area shows a significant difference in delta power for multiple time points, first at 4 seconds, then around 10 seconds, and finally around 15 seconds after odor onset.

The theta and spindle frequency bands present more confounding results, but in general perspective, we observe a significant increase in theta power around the odor onset in the central, and occipital regions for the odor D condition, and a decrease in the right temporal region around 12 seconds after odor onset for the same condition. The spindle frequency band shows a significant increase for the odor D condition at 2.5 seconds after odor onset only in the occipital region.

Importantly, the time-frequency analysis for M night has no significant differences in the time series for the different frequency bands at any region of interest when comparing odor M vs vehicle (results not shown).

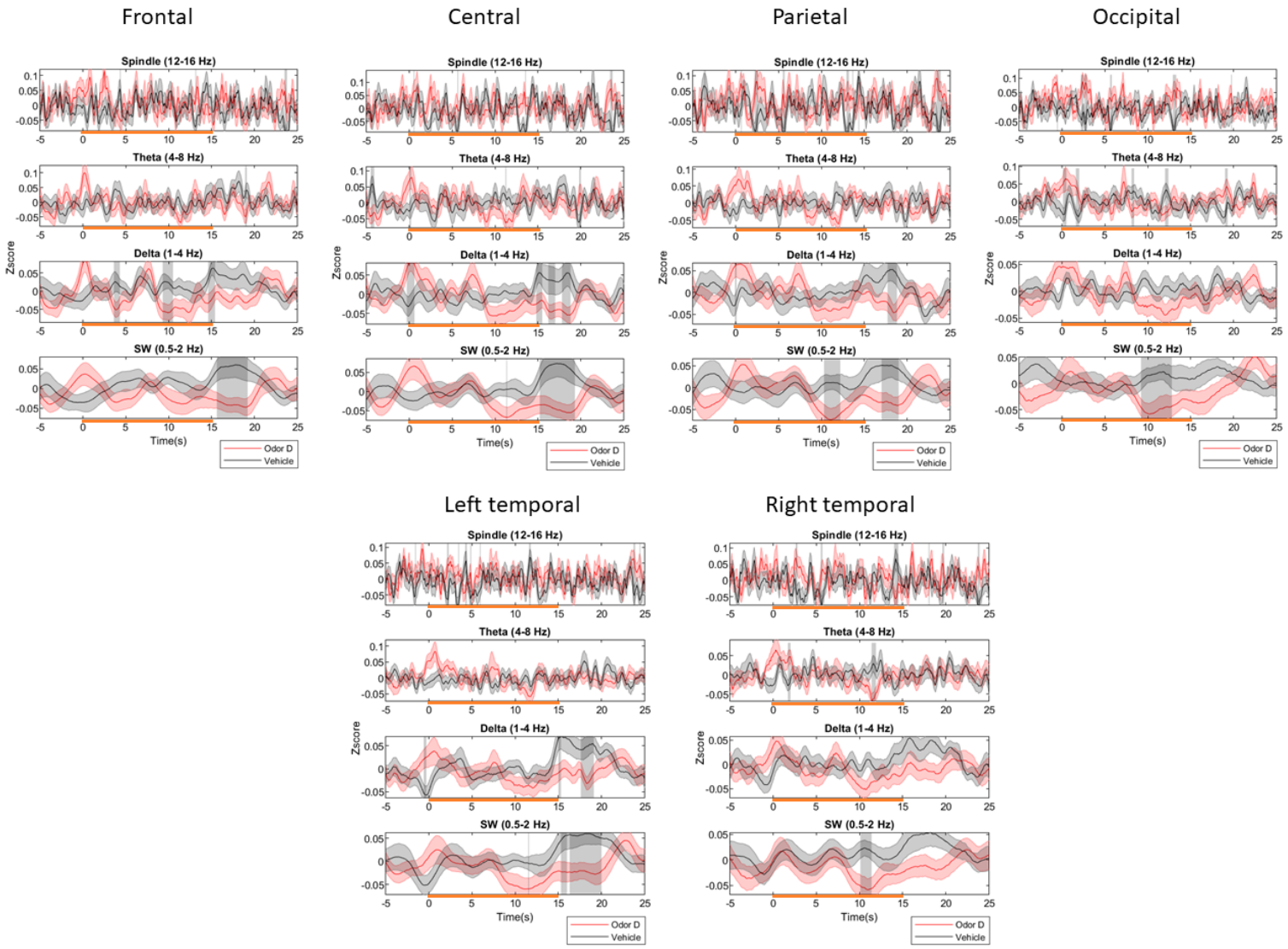

FIGURE 5.12: Time series of z-scored power at selected frequency bands are shown for D night in different regions of interest for Odor D (red), and Vehicle (black). Time series represents the mean across subjects (continuous line) and SEM (shaded areas). Significant differences after a nonparametric permutation-based test and FDR correction are shown as gray transparent bars. The orange lines in the x-axis, indicate the stimulation period in which the odor is released, outside this area, valves are closed allowing airflow only. Time series for Odor M Night don't show significant differences between Odor and Vehicle.

5.6.3 *The average time-frequency response when comparing odor D versus odor M shows significant differences in theta power around the odor onset, and 4 seconds previous to the odor onset, with an inverse response*

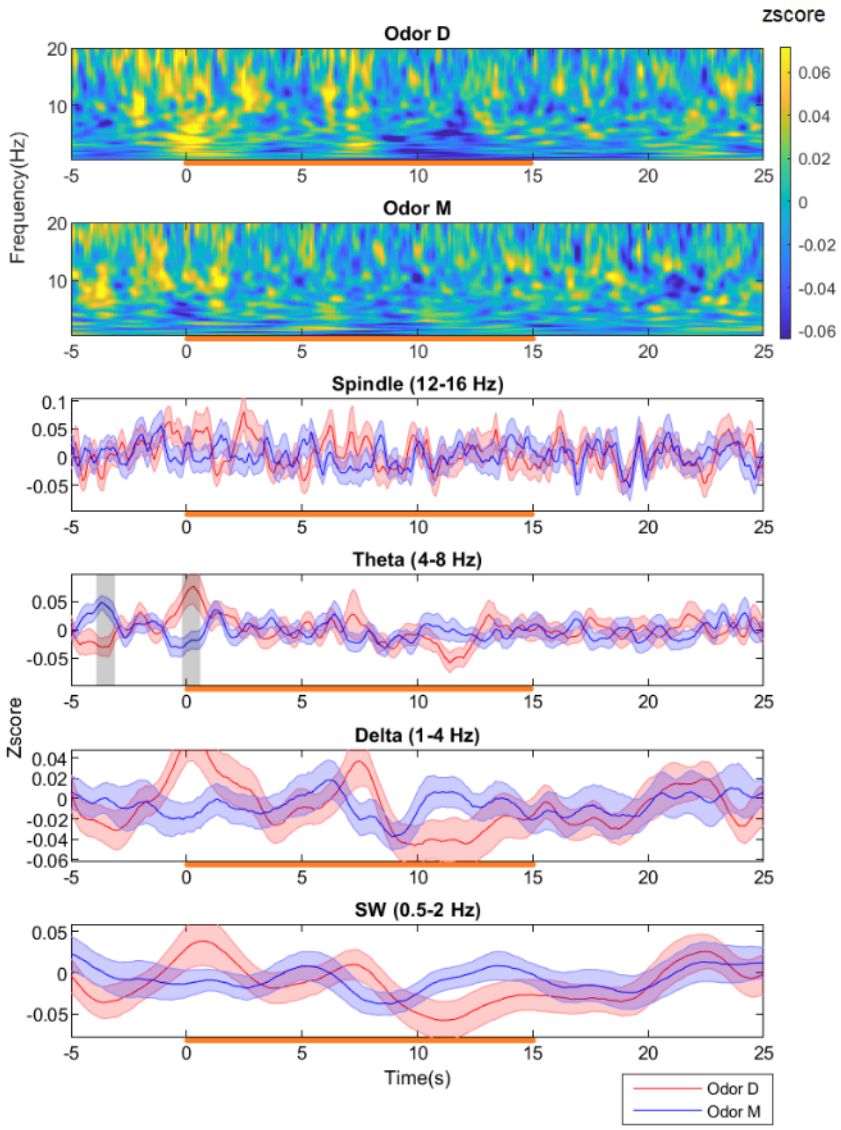

FIGURE 5.13: TF for odor D and Odor M periods are shown on top and z-scored time series of power at selected frequency bands are shown below (red for Odor D, and blue for Odor M), represented by the mean across subjects (continuous line) and SEM (shaded areas). Significant differences after a nonparametric permutation-based test and FDR correction are shown as gray transparent bars. The orange lines in the x-axis, indicate the stimulation period in which the odor is released, outside this area, valves are closed allowing airflow only.

The averaged time-frequency response observed in Figure 5.13 shows that the odor D condition exhibits an increase in the theta frequency band around the odor onset as compared to the odor M condition. This effect is inverted 4 seconds before the odor

onset, in which the odor M condition time series for theta power increase and the odor M one decreases.

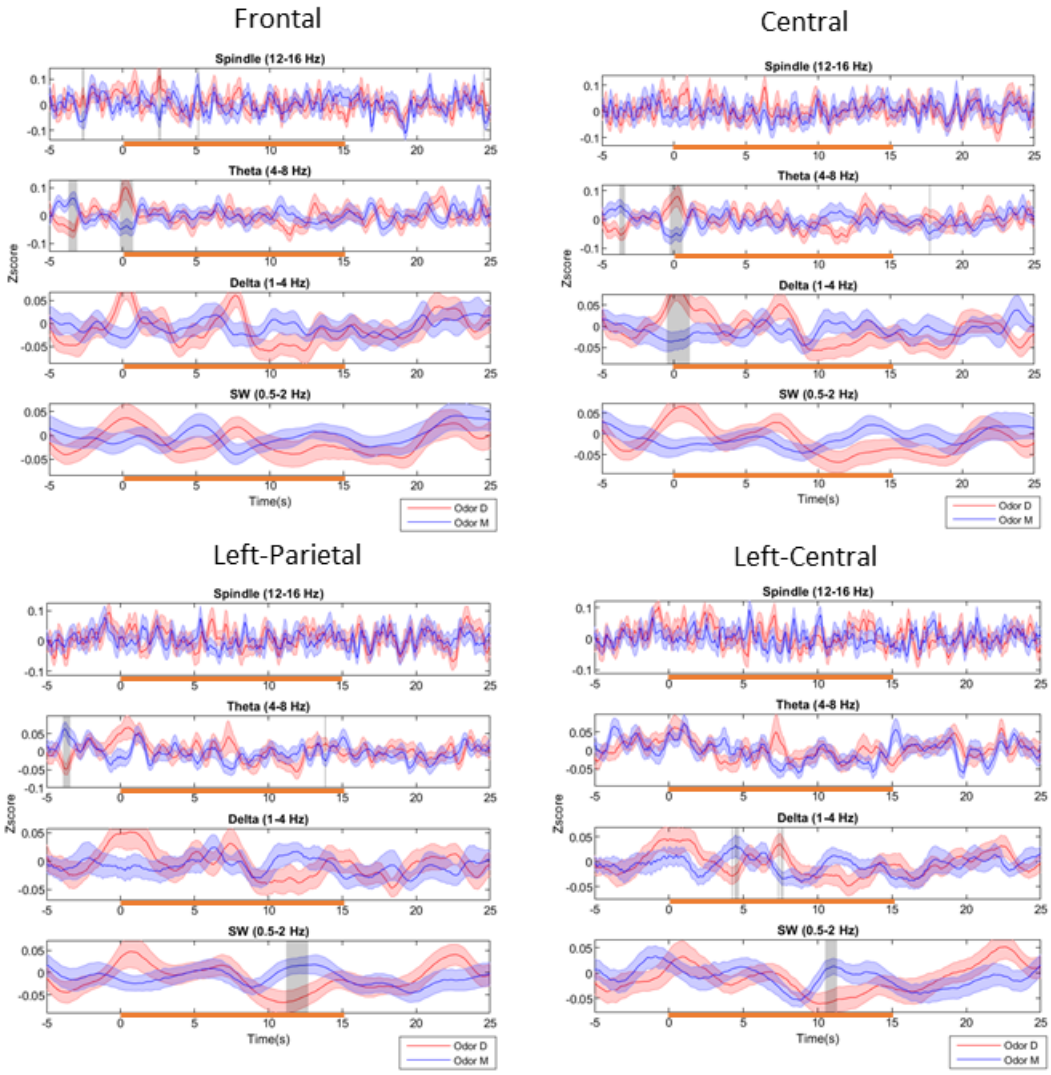

FIGURE 5.14: Time series of z-scored power at selected frequency bands are shown in different regions of interest for Odor D (red), and Odor M (blue). Time series represents the mean across subjects (continuous line) and SEM (shaded areas). Significant differences between odor conditions after a nonparametric permutation-based test and FDR correction are shown as gray transparent bars. The orange lines in the x-axis, indicate the stimulation period in which the odor is released, outside this area, valves are closed allowing airflow only.

5.6.4 *The average time-frequency response by regions of interest shows a significant difference in theta power in frontal and central regions and a significant difference in SW power at left central parietal regions*

When averaging the time-frequency response by clusters of channels, we evidence a significant difference in theta power in frontal and central regions around the odor

onset and a significant difference in SW power at left central parietal regions after 10 seconds from the odor onset. In particular, the significant difference around the odor onset reveals an increase in theta power for the odor D condition as compared to the odor M condition consistent in frontal and central regions. This response is also seen in the delta band for the central cluster of channels. On the other hand, left centroparietal areas reveal a significant difference between odor D and odor M around 11 seconds after odor onset, with a relative decrease in odor D condition and a relative increase in the odor M condition.

5.7 EVOLUTION OF CMR EFFECT OVER TRIALS

5.7.1 *Theta reveals a significant increase in power around the odor onset over trials in the frontal area for CMR*

After calculating the theta power around the odor onset (-1 to 1 seconds), and doing a linear regression to identify the evolution over trials, the slope of the linear regression shows an increase of theta power across trials for the odor D condition in the frontal area. Particularly this increase is stronger in left frontal electrodes when comparing odor D vs vehicle. This increase is even stronger and located prominently in frontal and temporal channels when comparing odor D vs odor M. On another hand, if we compare odor M vs vehicle there is a significant decrease in the slope for occipital areas for odor D vs vehicle.

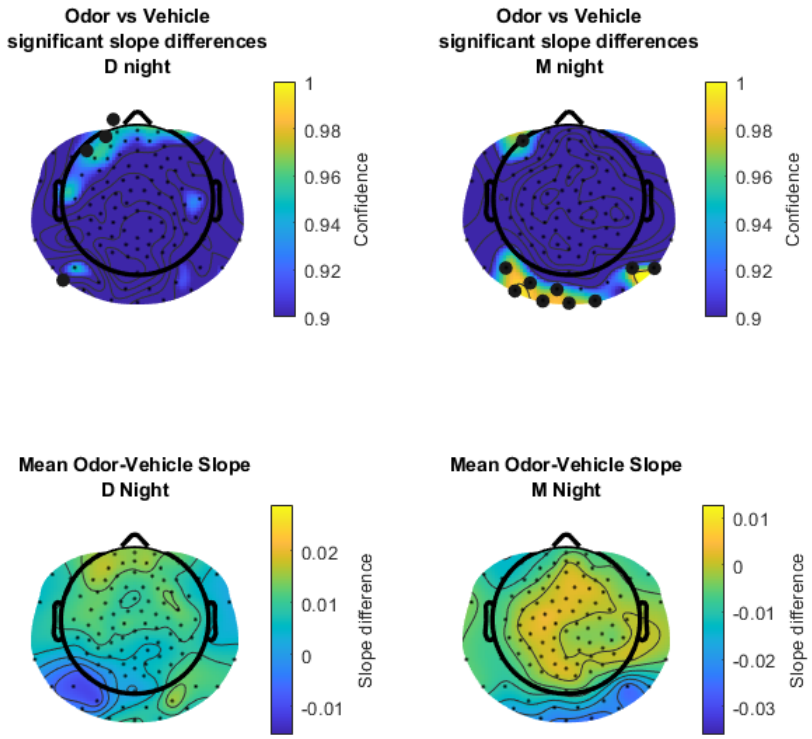

FIGURE 5.15: Topographical maps represent the evolution of theta power at odor onset over the trials for D Night (left) and M Night (right). The bottom figures show the difference in theta power slope across trials between odor and vehicle. The top figures show confidence (1-p) values when calculating significance across subjects above an established threshold of 0.95. Darker dots represent the electrodes that maintain significance after cluster permutation statistics.

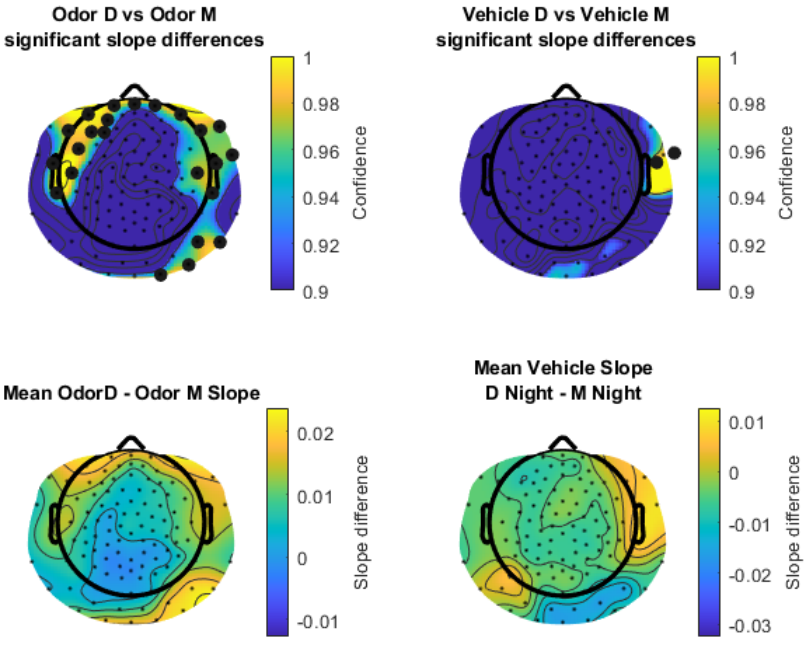

FIGURE 5.16: Topographical maps represent the evolution of theta power at odor onset over the trials for Odor conditions (left) and Vehicle conditions (right). The bottom figures show the difference in theta power slope across trials between conditions. The top figures show confidence (1-p) values when calculating significance across subjects above an established threshold of 0.95. Darker dots represent the electrodes that maintain significance after cluster permutation statistics.

5.7.2 *SO density calculated during the first 5 seconds of odor stimulation increases in power over trials for the parieto-occipital regions*

After calculating the SO density during the first 5 seconds of odor onset, and doing a linear regression to identify the evolution over trials, the slope of the linear regression shows an increase of SO density over parieto-occipital channels when comparing odor D versus vehicle. This significant difference is not observed when comparing odor M versus vehicle.

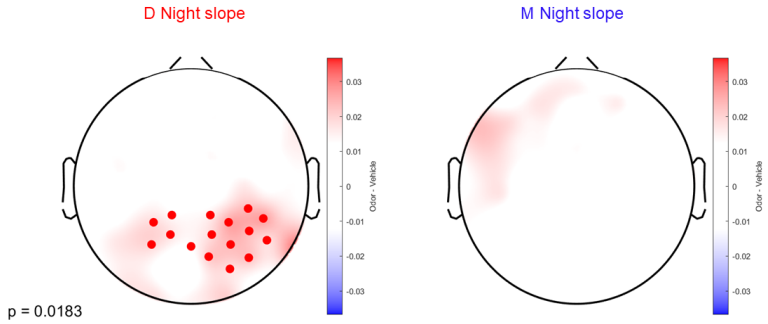

FIGURE 5.17: Topographical maps represent the evolution of SO density during the first 5 seconds of stimulation over the trials for D Night (left) and M Night (right). Figures show the difference in SO density slope calculated across trials between conditions. Red dots represent the electrodes that maintain significance after cluster permutation statistics.

5.8 MACHINE LEARNING CLASSIFICATION RESULTS

5.8.1 *Classification between Odor versus vehicle increases accuracy when selecting the signal around Slow Oscillations, compared to using the entire trial for both classification approaches.*

After performing the classification of Odor versus Vehicle trials, the accuracy is close to the chance (50%) either using subject-dependent or subject-independent classification. However, when the period of interest is changed to the time windows where SO occurs (taking an interval of -1 to 1 s of the SO middle point), the subject-dependent classification accuracy increases for both FBCSP and MVPA-light approaches (see 4). Since the entire trial had 15s in length and the SO minitrials had 2s in length, to control for differences due to the length of the trial, a second analysis was performed using small time windows of 2 seconds in random times within the trial coinciding or not with a SO. The resulting accuracies stayed at the chance level (results not shown).

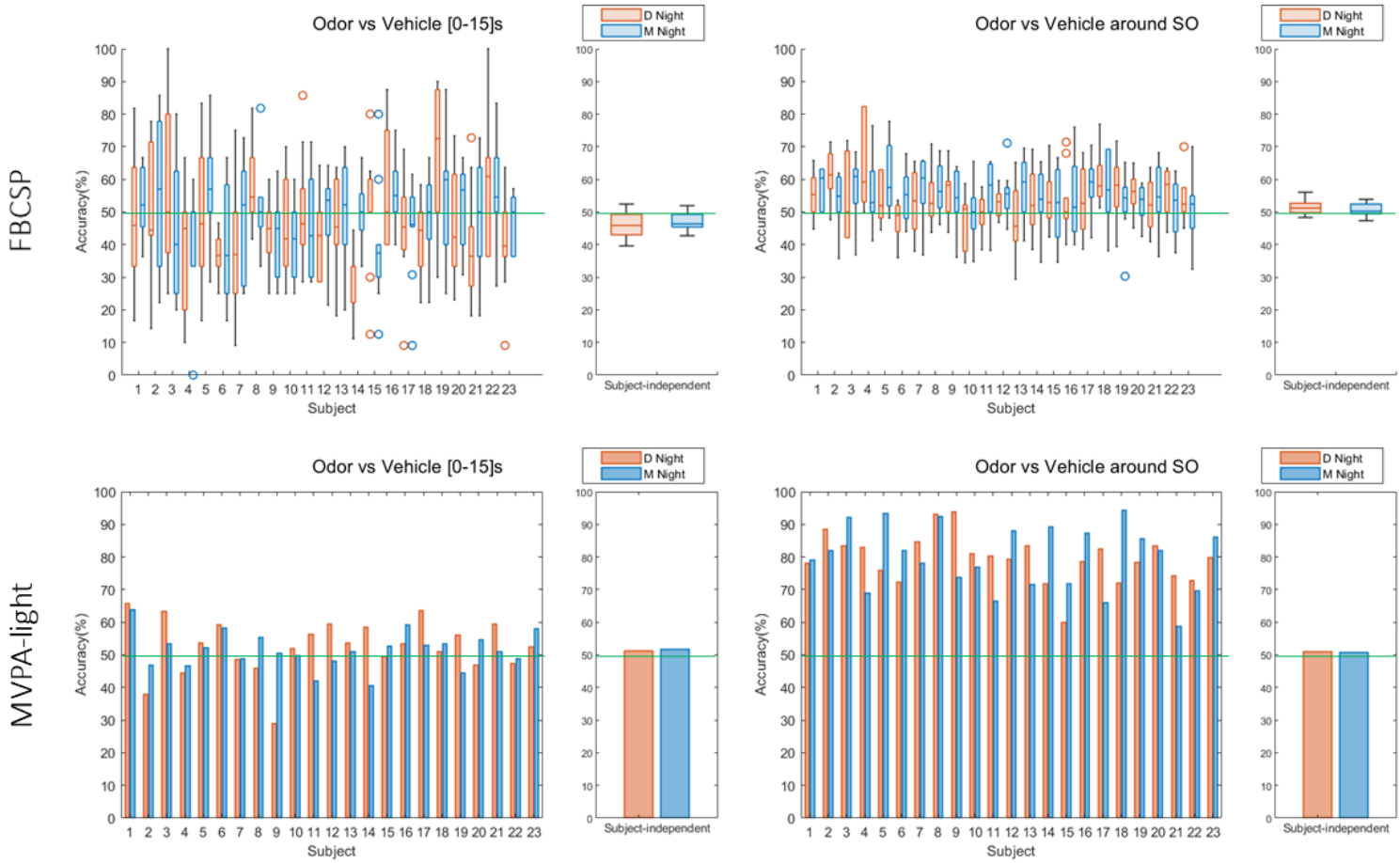

FIGURE 5.18: The top panels show the classification results using the FBCSP approach, and the bottom panels show the classification results using the MVPA-light approach. Panels on the left side show classification results using entire stimulation trials (subject-dependent and subject-independent classification). Panels on the right side show classification results using time windows around the SO (subject-dependent and subject-independent classification).

CHAPTER 6

Discussion

Having no differences in sleep architecture assures that we have similar sleep characteristics across nights making them comparable for the following analyses. The only exception was the S1 sleep stage. However, S1 is the stage of the shortest duration where no CMR occurred. Also, memory consolidation has been reported to be specific to deeper NREM sleep stages as well as to REM sleep assuring that the difference in S1 should not interfere with any brain patterns associated with memory consolidation.

The result in memory performance contradicts our hypothesis that assumes a better memory performance in the Odor D night as compared to the M night as Rihm and colleagues reported in 2014 (Rihm *et al*. (2014)). However, differences exist in the experimental design, as in our study we use an interference learning right after sleep in order to better quantify the consolidation effect through the night. The interference task prevents ceiling effects in the performance and tests for stability against interfering information instead of just memory strength. Further analyses show a correlation between memory performance and the number of stimulations presented for M night, but not for D night. This result may be contradictory if we assume that every odor stimulation causes an equal effect on memory consolidation. However, the number of odor stimulations is similar for both nights, as well as the memory performance, which could make us think that independently of the amount of cue odor D presented, the consolidation effect may be higher for each odor presentation, as compared to the cue odor M. Moreover, when correlating the memory performance if we separate gains, losses, and hithit results, it is possible to see that stimulation with odor D during the night protects memories from being lost, which confirms the role of the CMR in stabilizing memories.

Significant differences for detected SOs and detected spindles between conditions occur during the first 7.5 seconds of odor presentation. This result indicates that the CMR effect is successful for the first seconds of stimulation but after this time window, there is a need for a silent plastic period as suggested in (Farthouat *et al*. (2017)).

These significant differences show, in general, an increase in the SO strength for the CMR, according to the measurements in density, peak to peak amplitude, and slope. This increase is mostly evidenced in posterior regions. For the case of the spindle events, we observe an increase in strength as well induced by CMR, in measurements of density, duration, and peak-to-peak amplitude. The increase in spindle density is observed in posterior regions (probably linked to the SO occurrence), but the increase in spindle duration and peak to peak amplitude happen more anteriorly, in frontal areas. Taken together, these results confirm the role of SOs and spindles in memory reactivation, and position both types of events as a substantial signature of memory consolidation by memory reactivations as previously described in the literature. Moreover, in our results, we observe that spindles are tightly coupled with SOs upstate for the odor D condition reaffirming that the coupling between SOs and spindles is also an important signature in memory reactivation.

Time-frequency response evidence the role of a variety of frequency bands in memory reactivation. On one hand, our results evidence an increase in SW, delta, and theta around the odor onset for the odor D condition, but the significant differences with the odor M appear after 10 seconds of odor presentation where the power drops for lower frequencies. CMR prevents the increase in power after 10 seconds that is observed for vehicle conditions. This effect is stronger between 15 and 20 seconds after odor onset, an effect that is reproduced in (Bar et al., 2020) cued hemisphere versus uncued hemisphere. On another hand, delta power shows a peak around odor onset and a second peak around 7.5 seconds after odor onset, followed by a significant decrease in power in centroparietal regions around 15 to 20 seconds after odor onset. It is surprising to have an effect on low-frequency power after many seconds of odor presentation, and in our case, even when the odor stimulation is interrupted. One explanation for this could be also related to the necessity of a silent plastic period after memory reactivation occurrence, and a necessity for the brain to balance the increase in power produced during the first seconds after the odor onset, a phenomenon that moves from posterior to anterior cortical areas.

The spindle frequency band also pops up in the time-frequency analysis. However, for the case of spindles, the significant difference seems to be particular to the occipital channels with an increase in power after 2.5 seconds of odor onset.

The effect on theta is stronger when comparing time series of power change between odor D and odor M. This effect is particularly prominent around the odor onset and is consistent in anterior cortical regions.

The effect in theta and in low-frequency bands so close to the odor onset might be arguable due to the fact that the odor takes time to reach the subject when the valves are open, and the odor perception may vary as well according to the breathing cycle of the subject. This means that the odor can reach the subject even 3 seconds after the odor is released from the olfactometer. For this reason, we decided to answer the question of whether the brain is able to learn and anticipate the periodicity of the odor presentation and react accordingly inducing a memory reactivation. We then reported the evolution over trials of the power in theta calculated around the odor onset period. Interestingly, results show an increase in power over trials for frontal areas. This increase in power over trials is even stronger when comparing odor D vs odor M involving frontal, but also temporal regions, especially the left-temporal region. Furthermore, we were interested in exploring the evolution over trials in other markers of memory reactivation as the SO density. For this case, we observed an increase in SO density over trials for the first 5 seconds of odor presentation in parieto-occipital regions that is not observed in the control night.

In summary, our results confirm the role of the SO, spindles, and theta in memory reactivations. Moreover, our results provide evidence of the evolution over trials in different memory reactivation markers that can be induced by a periodicity in the cue stimuli presentation.

Finally, the results obtained from the machine learning classification tell us about the relevance of the time window around the SO to decode memory reactivation processes. The fact that classification was better in the subject-dependent classification than the subject-independent classification opens the question of the individuality of the brain patterns associated with memory consolidation that occurs within the SO time window.

Bibliography

Addante R.J. 2015. A critical role of the human hippocampus in an electrophysiological measure of implicit memory. NeuroImage 109:515–528.

Aeschbach D., Cutler A.J., and Ronda J.M. 2008. enA Role for Non-Rapid-Eye-Movement Sleep Homeostasis in Perceptual Learning. The Journal of Neuroscience 28:2766–2772.

Albert N.B., Robertson E.M., Mehta P., and Miall R.C. 2009. Resting state networks and memory consolidation. Communicative & integrative biology 2:530–532.

Anafi R.C., Kayser M.S., and Raizen D.M. 2019. Exploring phylogeny to find the function of sleep. Nature Reviews Neuroscience 20:109–116.

Antony J.W., Gobel E.W., O'Hare J.K., Reber P.J., and Paller K.A. 2012. engCued memory reactivation during sleep influences skill learning. Nature Neuroscience 15:1114–1116.

Antony J.W., Piloto L., Wang M., Pacheco P., Norman K.A., and Paller K.A. 2018. Sleep Spindle Refractoriness Segregates Periods of Memory Reactivation. Current biology: CB 28:1736–1743.e4.

Axmacher N., Elger C.E., and Fell J. 2008a. Ripples in the medial temporal lobe are relevant for human memory consolidation. Brain 131:1806–1817.

Axmacher N., Helmstaedter C., Elger C.E., and Fell J. 2008b. enEnhancement of Neocortical-Medial Temporal EEG Correlations during Non-REM Sleep. Neural Plasticity 2008:1–7.

Badia P., Wesensten N., Lammers W., Culpepper J., and Harsh J. 1990. Responsiveness to olfactory stimuli presented in sleep. Physiology & behavior 48:87–90.

Bar E., Marmelshtein A., Arzi A., Perl O., Livne E., Hizmi E., Paz R., Sobel N., Dudai Y., and Nir Y. 2020. Local targeted memory reactivation in human sleep. Current Biology 30:1435–1446.

Batterink L.J., Creery J.D., and Paller K.A. 2016. engPhase of Spontaneous Slow Oscillations during Sleep Influences Memory-Related Processing of Auditory Cues. The Journal of Neuroscience: The Official Journal of the Society for Neuroscience 36:1401–1409.

Berens P. 2009. en**CircStat** : A *MATLAB* Toolbox for Circular Statistics. Journal of Statistical Software 31.

Bergmann T.O., Mölle M., Diedrichs J., Born J., and Siebner H.R. 2012. Sleep spindle-related reactivation of category-specific cortical regions after learning face-scene associations. Neuroimage 59:2733–2742.

Berry R.B., Brooks R., Gamaldo C., Harding S.M., Lloyd R.M., Quan S.F., Troester M.T., and Vaughn B.V. 2017. Aasm scoring manual updates for 2017 (version 2.4).

Brem A.K., Ran K., and Pascual-Leone A. 2013. Learning and memory. Handbook of clinical neurology 116:693–737.

BuzsÁk G. 1998. Memory consolidation during sleep: a neurophysiological perspective. Journal of sleep research 7:17–23.

Buzsáki G. 1989. Two-stage model of memory trace formation: a role for "noisy" brain states. Neuroscience 31:551–570.

Buzsaki G. 2006. Rhythms of the Brain. Oxford university press.

Buzsáki G., Vanderwolf C.H., *et al*. 1983. Cellular bases of hippocampal eeg in the behaving rat. Brain Research Reviews 6:139–171.

Cairney S.A., El Marj N., Staresina B.P., *et al*. 2018. Memory consolidation is linked to spindle-mediated information processing during sleep. Current Biology 28:948–954.

Cairney S.A., Lindsay S., Sobczak J.M., Paller K.A., and Gaskell M.G. 2016. The benefits of targeted memory reactivation for consolidation in sleep are contingent on memory accuracy and direct cue-memory associations. Sleep 39:1139–1150.

Cairney S.A., Sobczak J.M., Lindsay S., and Gaskell M.G. 2017. Mechanisms of memory retrieval in slow-wave sleep. Sleep 40.

Cantero J.L., Atienza M., Stickgold R., Kahana M.J., Madsen J.R., and Kocsis B. 2003. enSleep-Dependent Oscillations in the Human Hippocampus and Neocortex. The Journal of Neuroscience 23:10897–10903.

Carr M.F., Jadhav S.P., and Frank L.M. 2011. Hippocampal replay in the awake state: a potential substrate for memory consolidation and retrieval. Nature neuroscience 14:147–153.

Carskadon M.A. and Herz R.S. 2004. Minimal olfactory perception during sleep: why odor alarms will not work for humans. Sleep 27:402–405.

Chen Z. and Wilson M.A. 2017. Deciphering neural codes of memory during sleep. Trends in neurosciences 40:260–275.

Clemens Z., Fabo D., and Halasz P. 2005. Overnight verbal memory retention correlates with the number of sleep spindles. Neuroscience 132:529–535.

Clemens Z., Fabó D., and Halász P. 2006. Twenty-four hours retention of visuospatial memory correlates with the number of parietal sleep spindles. Neuroscience letters 403:52–56.

Cousins J.N., El-Deredy W., Parkes L.M., Hennies N., and Lewis P.A. 2014. engCued memory reactivation during slow-wave sleep promotes explicit knowledge of a motor sequence. The Journal of Neuroscience: The Official Journal of the Society for Neuroscience 34:15870–15876.

Cox R., Hofman W.F., de Boer M., and Talamini L.M. 2014. engLocal sleep spindle modulations in relation to specific memory cues. NeuroImage 99:103–110.

Creery J.D., Oudiette D., Antony J.W., and Paller K.A. 2015. enTargeted Memory Reactivation during Sleep Depends on Prior Learning. Sleep 38:755–763.

Csicsvari J., Hirase H., Mamiya A., and Buzsáki G. 2000. Ensemble patterns of hippocampal ca3-ca1 neurons during sharp wave–associated population events. Neuron 28:585–594.

Datta S. 2000. Avoidance task training potentiates phasic pontine-wave density in the rat: a mechanism for sleep-dependent plasticity. Journal of Neuroscience 20:8607–8613.

Datta S., Li G., and Auerbach S. 2008. Activation of phasic pontine-wave generator in the rat: a mechanism for expression of plasticity-related genes and proteins in the dorsal hippocampus and amygdala. European Journal of Neuroscience 27:1876–1892.

De Gennaro L. and Ferrara M. 2003. Sleep spindles: an overview. Sleep medicine reviews 7:423–440.

Diba K. and Buzsáki G. 2007. Forward and reverse hippocampal place-cell sequences during ripples. Nature neuroscience 10:1241–1242.

Diekelmann S., Biggel S., Rasch B., and Born J. 2012. Offline consolidation of memory varies with time in slow wave sleep and can be accelerated by cuing memory reactivations. Neurobiology of learning and memory 98:103–111.

Diekelmann S. and Born J. 2010. The memory function of sleep. Nature Reviews Neuroscience 11:114–126.

Diekelmann S., Born J., and Rasch B. 2016. Increasing explicit sequence knowledge by odor cueing during sleep in men but not women. Frontiers in behavioral neuroscience 10:74.

Diekelmann S., Büchel C., Born J., and Rasch B. 2011. Labile or stable: opposing consequences for memory when reactivated during waking and sleep. Nature neuroscience 14:381–386.

Eichenbaum H. 2000. A cortical–hippocampal system for declarative memory. Nature reviews neuroscience 1:41–50.

Eschenko O., Ramadan W., Mölle M., Born J., and Sara S.J. 2008. Sustained increase in hippocampal sharp-wave ripple activity during slow-wave sleep after learning. Learning & memory 15:222–228.

Farthouat J., Gilson M., and Peigneux P. 2017. enNew evidence for the necessity of a silent plastic period during sleep for a memory benefit of targeted memory reactivation. Sleep Spindles & Cortical Up States 1:14–26.

Favila S.E., Lee H., and Kuhl B.A. 2020a. Transforming the concept of memory reactivation. Trends in neurosciences 43:939–950.

Favila S.E., Lee H., and Kuhl B.A. 2020b. Transforming the concept of memory reactivation. Trends in Neurosciences 43:939–950.

Feld G.B. and Born J. 2017. Sculpting memory during sleep: concurrent consolidation and forgetting. Current Opinion in Neurobiology 44:20–27.

Feld G.B. and Diekelmann S. 2020. Building the bridge: Outlining steps toward an applied sleep-and-memory research program. Current Directions in Psychological Science 29:554–562.

Fogel S., Smith C., and Cote K. 2007. enDissociable learning-dependent changes in REM and non-REM sleep in declarative and procedural memory systems. Behavioural Brain Research 180:48–61.

Folkerts S., Rutishauser U., and Howard M.W. 2018. enHuman Episodic Memory Retrieval Is Accompanied by a Neural Contiguity Effect. The Journal of Neuroscience 38:4200–4211.

Gais S., Albouy G., Boly M., Dang-Vu T.T., Darsaud A., Desseilles M., Rauchs G., Schabus M., Sterpenich V., Vandewalle G., *et al*. 2007. Sleep transforms the cerebral trace of declarative memories. Proceedings of the National Academy of Sciences 104:18778–18783.

Gais S., Lucas B., and Born J. 2006. enSleep after learning aids memory recall. Learning & Memory 13:259–262.

Gais S., Mölle M., Helms K., and Born J. 2002. Learning-dependent increases in sleep spindle density. Journal of Neuroscience 22:6830–6834.

Grandchamp R. and Delorme A. 2011. engSingle-trial normalization for event-related spectral decomposition reduces sensitivity to noisy trials. Frontiers in Psychology 2:236.

Groch S., Schreiner T., Rasch B., Huber R., and Wilhelm I. 2017. Prior knowledge is essential for the beneficial effect of targeted memory reactivation during sleep. Scientific reports 7:1–7.

Göldi M., van Poppel E., Rasch B., and Schreiner T. 2017. enCueing memory during sleep is optimal during slow-oscillatory up-states. preprint, Neuroscience.

Göldi M., van Poppel E.A.M., Rasch B., and Schreiner T. 2019. enIncreased neuronal signatures of targeted memory reactivation during slow-wave up states. Scientific Reports 9:2715.

Hars B., Hennevin E., and Pasques P. 1985a. Improvement of learning by cueing during postlearning paradoxical sleep. Behavioural brain research 18:241–250.

Hars B., Hennevin E., and Pasques P. 1985b. enImprovement of learning by cueing during postlearning paradoxical sleep. Behavioural Brain Research 18:241–250.

Hauner K.K., Howard J.D., Zelano C., and Gottfried J.A. 2013. Stimulus-specific enhancement of fear extinction during slow-wave sleep. Nature neuroscience 16:1553–1555.

Hellman K. and Abel T. 2007. enFear conditioning increases NREM sleep. Behavioral Neuroscience 121:310–323.

Henke K. 2010. A model for memory systems based on processing modes rather than consciousness. Nature Reviews Neuroscience 11:523–532.

Hobson J. 1989. Sleep. Scientific American Library.

Hu X., Antony J.W., Creery J.D., Vargas I.M., Bodenhausen G.V., and Paller K.A. 2015. Unlearning implicit social biases during sleep. Science 348:1013–1015.

Huber R., Felice Ghilardi M., Massimini M., and Tononi G. 2004. enLocal sleep and learning. Nature 430:78–81.

Isomura Y., Sirota A., Özen S., Montgomery S., Mizuseki K., Henze D.A., and Buzsáki G. 2006. Integration and segregation of activity in entorhinal-hippocampal subregions by neocortical slow oscillations. Neuron 52:871–882.

Jafarpour A., Fuentemilla L., Horner A.J., Penny W., and Duzel E. 2014. enReplay of Very Early Encoding Representations during Recollection. Journal of Neuroscience 34:242–248.

Ji D. and Wilson M.A. 2007. Coordinated memory replay in the visual cortex and hippocampus during sleep. Nature neuroscience 10:100–107.

Johnson J.D., Price M.H., and Leiker E.K. 2015. engEpisodic retrieval involves early and sustained effects of reactivating information from encoding. NeuroImage 106:300–310.

Kandel E.R., Schwartz J.H., Jessell T.M., Siegelbaum S.A., and Hudspeth A. 2013. Principles of neural science, fifth editon. *In* Principles of Neural Science, McGraw-Hill Education.

Kerrén C., Linde-Domingo J., Hanslmayr S., and Wimber M. 2018. engAn Optimal Oscillatory Phase for Pattern Reactivation during Memory Retrieval. Current biology: CB 28:3383–3392.e6.

Klinzing J.G. and Diekelmann S. 2019. Cued memory reactivation: a tool to manipulate memory consolidation during sleep. *In* Handbook of behavioral neuroscience, vol. 30, pages 471–488, Elsevier.

Klinzing J.G., Mölle M., Weber F., Supp G., Hipp J.F., Engel A.K., and Born J. 2016. enSpindle activity phase-locked to sleep slow oscillations. NeuroImage 134:607–616.

Knowlton B.J., Ramus S.J., and Squire L.R. 1992. Intact artificial grammar learning in amnesia: Dissociation of classification learning and explicit memory for specific instances. Psychological science 3:172–179.

Kurth-Nelson Z., Economides M., Dolan R.J., and Dayan P. 2016. engFast Sequences of Non-spatial State Representations in Humans. Neuron 91:194–204.

Levy D., Stark C., and Squire L. 2004. Intact conceptual priming in the absence of declarative memory. Psychological Science 15:680–686.

Lewis P.A. and Bendor D. 2019. How targeted memory reactivation promotes the selective strengthening of memories in sleep. Current Biology 29:R906–R912.

Linde-Domingo J., Treder M.S., Kerrén C., and Wimber M. 2019. Evidence that neural information flow is reversed between object perception and object reconstruction from memory. Nature communications 10:1–13.

Liu Y., Dolan R.J., Kurth-Nelson Z., and Behrens T.E.J. 2019. engHuman Replay Spontaneously Reorganizes Experience. Cell 178:640–652.e14.

Louie K. and Wilson M.A. 2001. enTemporally Structured Replay of Awake Hippocampal Ensemble Activity during Rapid Eye Movement Sleep. Neuron 29:145–156.

Manning J.R., Polyn S.M., Baltuch G.H., Litt B., and Kahana M.J. 2011. enOscillatory patterns in temporal lobe reveal context reinstatement during memory search. Proceedings of the National Academy of Sciences 108:12893–12897.

Maquet P. 2000. Sleep on it! Nature neuroscience 3:1235–1236.

Maquet P., Laureys S., Peigneux P., Fuchs S., Petiau C., Phillips C., Aerts J., Del Fiore G., Degueldre C., Meulemans T., *et al*. 2000a. Experience-dependent changes in cerebral activation during human rem sleep. Nature neuroscience 3:831–836.

Maquet P. *et al*. 2000b. Functional neuroimaging of normal human sleep by positron emission tomography. Journal of sleep research 9:207–232.

Marr D. 1971. engSimple memory: a theory for archicortex. Philosophical Transactions of the Royal Society of London. Series B, Biological Sciences 262:23–81.

Marshall L., Helgadóttir H., Mölle M., and Born J. 2006. Boosting slow oscillations during sleep potentiates memory. Nature 444:610–613.

Michelmann S., Bowman H., and Hanslmayr S. 2016. enThe Temporal Signature of Memories: Identification of a General Mechanism for Dynamic Memory Replay in Humans. PLOS Biology 14:e1002528.

Michelmann S., Bowman H., and Hanslmayr S. 2018. engReplay of Stimulus-specific Temporal Patterns during Associative Memory Formation. Journal of Cognitive Neuroscience 30:1577–1589.

Mölle M. and Born J. 2009. Hippocampus whispering in deep sleep to prefrontal cortex—for good memories? Neuron 61:496–498.

Mölle M., Marshall L., Gais S., and Born J. 2002. Grouping of spindle activity during slow oscillations in human non-rapid eye movement sleep. Journal of Neuroscience 22:10941–10947.

Mölle M., Yeshenko O., Marshall L., Sara S.J., and Born J. 2006. Hippocampal sharp wave-ripples linked to slow oscillations in rat slow-wave sleep. Journal of neurophysiology .

Montgomery S.M., Sirota A., and Buzsaki G. 2008. enTheta and Gamma Coordination of Hippocampal Networks during Waking and Rapid Eye Movement Sleep. Journal of Neuroscience 28:6731–6741.

Nádasdy Z., Hirase H., Czurkó A., Csicsvari J., and Buzsáki G. 1999. Replay and time compression of recurring spike sequences in the hippocampus. Journal of Neuroscience 19:9497–9507.

Nishida M., Pearsall J., Buckner R.L., and Walker M.P. 2009. engREM sleep, prefrontal theta, and the consolidation of human emotional memory. Cerebral Cortex (New York, N.Y.: 1991) 19:1158–1166.

Nishida M. and Walker M.P. 2007. Daytime naps, motor memory consolidation and regionally specific sleep spindles. PloS one 2:e341.

Oostenveld R., Fries P., Maris E., and Schoffelen J.M. 2011. engFieldTrip: Open source software for advanced analysis of MEG, EEG, and invasive electrophysiological data. Computational Intelligence and Neuroscience 2011:156869.

Oudiette D., Antony J.W., Creery J.D., and Paller K.A. 2013. The role of memory reactivation during wakefulness and sleep in determining which memories endure. Journal of Neuroscience 33:6672–6678.

Pavlides C. and Winson J. 1989. Influences of hippocampal place cell firing in the awake state on the activity of these cells during subsequent sleep episodes. Journal of neuroscience 9:2907–2918.

Peigneux P., Laureys S., Fuchs S., Collette F., Perrin F., Reggers J., Phillips C., Degueldre C., Del Fiore G., Aerts J., *et al*. 2004. Are spatial memories strengthened in the human hippocampus during slow wave sleep? Neuron 44:535–545.

Penfield W. 1952. Memory mechanisms. AMA Archives of Neurology & Psychiatry 67:178–198.

Pereira S.I.R., Beijamini F., Weber F.D., Vincenzi R.A., da Silva F.A.C., and Louzada F.M. 2017. Tactile stimulation during sleep alters slow oscillation and spindle densities but not motor skill. Physiology & behavior 169:59–68.

Peyrache A., Khamassi M., Benchenane K., Wiener S.I., and Battaglia F.P. 2009. Replay of rule-learning related neural patterns in the prefrontal cortex during sleep. Nature neuroscience 12:919–926.

Plihal W. and Born J. 1997a. enEffects of Early and Late Nocturnal Sleep on Declarative and Procedural Memory. Journal of Cognitive Neuroscience 9:534–547.

Plihal W. and Born J. 1997b. Effects of early and late nocturnal sleep on declarative and procedural memory. Journal of cognitive neuroscience 9:534–547.

Plihal W. and Born J. 1999. engEffects of early and late nocturnal sleep on priming and spatial memory. Psychophysiology 36:571–582.

Poe G.R., Nitz D.A., McNaughton B.L., and Barnes C.A. 2000. enExperience-dependent phase-reversal of hippocampal neuron firing during REM sleep. Brain Research 855:176–180.

Purcell S.M., Manoach D.S., Demanuele C., Cade B.E., Mariani S., Cox R., Panagiotaropoulou G., Saxena R., Pan J.Q., Smoller J.W., Redline S., and Stickgold R. 2017. enCharacterizing sleep spindles in 11,630 individuals from the National Sleep Research Resource. Nature Communications 8:15930.

Purves D. A.G.J.F.D.H.W.C.L.A.S.M.J.O..W.S.M.E. 2004. Neuroscience. (3rd ed.). Sinauer Associates.

Rasch B. and Born J. 2007. Maintaining memories by reactivation. Current opinion in neurobiology 17:698–703.

Rasch B., Buchel C., Gais S., and Born J. 2007. Odor cues during slow-wave sleep prompt declarative memory consolidation. Science 315:1426–1429.

Rauchs G., Bertran F., Guillery-Girard B., Desgranges B., Kerrouche N., Denise P., Foret J., and Eustache F. 2004. enConsolidation of Strictly Episodic Memories Mainly Requires Rapid Eye Movement Sleep. Sleep 27:395–401.

Ray A.M., Sitaram R., Rana M., Pasqualotto E., Buyukturkoglu K., Guan C., Ang K.K., Tejos C., Zamorano F., Aboitiz F., Birbaumer N., and Ruiz S. 2015. A subject-independent pattern-based Brain-Computer Interface. Frontiers in Behavioral Neuroscience 9.

Ribeiro S., Gervasoni D., Soares E.S., Zhou Y., Lin S.C., Pantoja J., Lavine M., Nicolelis M.A.L., and Schultz W. 2004. Long-lasting novelty-induced neuronal reverberation during slow-wave sleep in multiple forebrain areas. PLoS biology 2:e24.

Rihm J.S., Diekelmann S., Born J., and Rasch B. 2014. Reactivating memories during sleep by odors: odor specificity and associated changes in sleep oscillations. Journal of cognitive neuroscience 26:1806–1818.

Ritter S.M., Strick M., Bos M.W., Van Baaren R.B., and Dijksterhuis A. 2012. Good morning creativity: task reactivation during sleep enhances beneficial effect of sleep on creative performance. Journal of sleep research 21:643–647.

Rosanova M. and Ulrich D. 2005. Pattern-specific associative long-term potentiation induced by a sleep spindle-related spike train. Journal of Neuroscience 25:9398–9405.

Rudoy J.D., Voss J.L., Westerberg C.E., and Paller K.A. 2009. Strengthening individual memories by reactivating them during sleep. Science 326:1079–1079.

Schmidt C., Peigneux P., Muto V., Schenkel M., Knoblauch V., Münch M., Dominique J.F., Wirz-Justice A., and Cajochen C. 2006. Encoding difficulty promotes postlearning changes in sleep spindle activity during napping. Journal of Neuroscience 26:8976–8982.

Schreiner T., Doeller C.F., Jensen O., Rasch B., and Staudigl T. 2018. enTheta Phase-Coordinated Memory Reactivation Reoccurs in a Slow-Oscillatory Rhythm during NREM Sleep. Cell Reports 25:296–301.

Schreiner T., Lehmann M., and Rasch B. 2015. Auditory feedback blocks memory benefits of cueing during sleep. Nature communications 6:1–11.

Schreiner T., Petzka M., Staudigl T., and Staresina B.P. 2021. enEndogenous memory reactivation during sleep in humans is clocked by slow oscillation-spindle complexes. Nature Communications 12:3112.

Schreiner T. and Rasch B. 2015a. Boosting vocabulary learning by verbal cueing during sleep. Cerebral Cortex 25:4169–4179.

Schreiner T. and Rasch B. 2015b. Cueing vocabulary in awake subjects during the day has no effect on memory. Somnologie-Schlafforschung und Schlafmedizin 19:133–140.

Schreiner T. and Staudigl T. 2020. Electrophysiological signatures of memory reactivation in humans. Philosophical Transactions of the Royal Society B 375:20190293.

Schönauer M., Alizadeh S., Jamalabadi H., Abraham A., Pawlizki A., and Gais S. 2017. enDecoding material-specific memory reprocessing during sleep in humans. Nature Communications 8:15404.

Scoville W.B. and Milner B. 1957. Loss of recent memory after bilateral hippocampal lesions. Journal of neurology, neurosurgery, and psychiatry 20:11.

Shanahan L.K., Gjorgieva E., Paller K.A., Kahnt T., and Gottfried J.A. 2018. Odor-evoked category reactivation in human ventromedial prefrontal cortex during sleep promotes memory consolidation. Elife 7:e39681.

Shimizu R.E., Connolly P.M., Cellini N., Armstrong D.M., Hernandez L.T., Estrada R., Aguilar M., Weisend M.P., Mednick S.C., and Simons S.B. 2018. Closed-loop targeted memory reactivation during sleep improves spatial navigation. Frontiers in human neuroscience 12:28.

Siapas A.G. and Wilson M.A. 1998. Coordinated interactions between hippocampal ripples and cortical spindles during slow-wave sleep. Neuron 21:1123–1128.

Simon K.C., Gómez R.L., and Nadel L. 2018. Losing memories during sleep after targeted memory reactivation. Neurobiology of Learning and Memory 151:10–17.

Sirota A. and Buzsáki G. 2005. Interaction between neocortical and hippocampal networks via slow oscillations. Thalamus & related systems 3:245–259.

Sirota A., Csicsvari J., Buhl D., and Buzsáki G. 2003. Communication between neocortex and hippocampus during sleep in rodents. Proceedings of the National Academy of Sciences 100:2065–2069.

Skaggs W.E. and McNaughton B.L. 1996. Replay of neuronal firing sequences in rat hippocampus during sleep following spatial experience. Science 271:1870–1873.

Staudigl T. and Hanslmayr S. 2019. engReactivation of neural patterns during memory reinstatement supports encoding specificity. Cognitive Neuroscience 10:175–185.

Steriade M. 2006. Grouping of brain rhythms in corticothalamic systems. Neuroscience 137:1087–1106.

Sterpenich V., Schmidt C., Albouy G., Matarazzo L., Vanhaudenhuyse A., Boveroux P., Degueldre C., Leclercq Y., Balteau E., Collette F., *et al*. 2014. Memory reactivation during rapid eye movement sleep promotes its generalization and integration in cortical stores. Sleep 37:1061–1075.

Treder M.S. 2020. MVPA-Light: A Classification and Regression Toolbox for Multi-Dimensional Data. Frontiers in Neuroscience 14:289.

Tulving E., Hayman C., and Macdonald C.A. 1991. Long-lasting perceptual priming and semantic learning in amnesia: a case experiment. Journal of Experimental Psychology: Learning, Memory, and Cognition 17:595.

Van Dongen E.V., Takashima A., Barth M., Zapp J., Schad L.R., Paller K.A., and Fernández G. 2012. Memory stabilization with targeted reactivation during human slow-wave sleep. Proceedings of the National Academy of Sciences 109:10575–10580.

Vieweg P., Stangl M., Howard L.R., and Wolbers T. 2015. Changes in pattern completion–a key mechanism to explain age-related recognition memory deficits? Cortex 64:343–351.

Wagner U., Gais S., and Born J. 2001. Emotional memory formation is enhanced across sleep intervals with high amounts of rapid eye movement sleep. Learning & memory 8:112–119.

Waldhauser G.T., Braun V., and Hanslmayr S. 2016. enEpisodic Memory Retrieval Functionally Relies on Very Rapid Reactivation of Sensory Information. Journal of Neuroscience 36:251–260.

Wang B., Antony J.W., Lurie S., Brooks P.P., Paller K.A., and Norman K.A. 2019. enTargeted Memory Reactivation during Sleep Elicits Neural Signals Related to Learning Content. The Journal of Neuroscience 39:6728–6736.

Weiskrantz L. and Warrington E.K. 1979. Conditioning in amnesic patients. Neuropsychologia 17:187–194.

Wen H. and Liu Z. 2016. engSeparating Fractal and Oscillatory Components in the Power Spectrum of Neurophysiological Signal. Brain Topography 29:13–26.

Wierzynski C.M., Lubenov E.V., Gu M., and Siapas A.G. 2009. State-dependent spike-timing relationships between hippocampal and prefrontal circuits during sleep. Neuron 61:587–596.

Wilson M.A. and McNaughton B.L. 1994. Reactivation of hippocampal ensemble memories during sleep. Science 265:676–679.

Wimber M., Maaß A., Staudigl T., Richardson-Klavehn A., and Hanslmayr S. 2012. Rapid memory reactivation revealed by oscillatory entrainment. Current Biology 22:1482–1486.

Witkowski S., Schechtman E., and Paller K.A. 2020. Examining sleep's role in memory generalization and specificity through the lens of targeted memory reactivation. Current Opinion in Behavioral Sciences 33:86–91.

Wolpert E.A. 1969. A manual of standardized terminology, techniques and scoring system for sleep stages of human subjects. Archives of General Psychiatry 20:246–247.

Zelano C. and Sobel N. 2005. enHumans as an Animal Model for Systems-Level Organization of Olfaction. Neuron 48:431–454.